LIDIA HILDEBRAND PULZ

Isolation and characterization of Cancer Associated Fibroblasts from canine Mast Cell Tumors and its influence on the malignancy of neoplastic cells: a combined molecular, pathologic and *in vitro* approach

São Paulo
2019

LIDIA HILDEBRAND PULZ

Isolation and characterization of Cancer Associated Fibroblasts from canine Mast Cell Tumors and its influence on the malignancy of neoplastic cells: a combined molecular, pathologic and *in vitro* approach

Thesis submitted to the Postgraduate Program in Experimental and Comparative Pathology of the School of Veterinary Medicine and Animal Science of the University of São Paulo to obtain the Doctor's degree in Sciences.

Department:
Pathology

Area:
Experimental and Comparative Pathology

Advisor:
Prof. Ricardo De Francisco Strefezzi, Ph.D.

São Paulo
2019

DADOS INTERNACIONAIS DE CATALOGAÇÃO NA PUBLICAÇÃO

(Biblioteca Virginie Buff D'Ápice da Faculdade de Medicina Veterinária e Zootecnia da Universidade de São Paulo)

T. 3756
FMVZ

Pulz, Lidia Hildebrand
Isolation and characterization of Cancer Associated Fibroblasts from Canine Mast Cell Tumors and its influence on the malignancy of neoplastic cells: a combined molecular, pathologic and *in vitro* approach / Lidia Hildebrand Pulz. – 2019.
112 f. : il.

Título traduzido: Isolamento e caracterização de Fibroblastos Associados ao Câncer provenientes de Mastocitomas Caninos e sua influência sobre a malignidade de células neoplásicas: uma abordagem molecular, patológica e *in vitro*.

Tese (Doutorado) – Universidade de São Paulo. Faculdade de Medicina Veterinária e Zootecnia. Departamento de Patologia, São Paulo, 2019.

Programa de Pós-Graduação: Patologia Experimental e Comparada.
Área de concentração: Patologia Experimental e Comparada.
Orientador: Prof. Dr. Ricardo De Francisco Strefezzi.

1. RNA-Seq. 2. Cão. 3. Co-cultivo. 4. Miofibroblastos. 5. Matriz extracelular. I. Título.

Ficha catalográfica elaborada pela bibliotecária Maria Aparecida Laet, CRB 5673-8, da FMVZ/USP.

CERTIFICADO

Certificamos que a proposta intitulada "ISOLAMENTO E CARACTERIZAÇÃO DE FIBROBLASTOS ASSOCIADOS AO CÂNCER PROVENIENTES DE MASTOCITOMAS CANINOS E SUA INFLUÊNCIA SOBRE A MALIGNIDADE DE CÉLULAS NEOPLÁSICAS ", protocolada sob o CEUA nº 5637040718 (ID 005827), sob a responsabilidade de **Ricardo de Francisco Strefezzi** *e equipe; Lidia Hildebrand Pulz* - que envolve a produção, manutenção e/ou utilização de animais pertencentes ao filo Chordata, subfilo Vertebrata (exceto o homem), para fins de pesquisa científica ou ensino - está de acordo com os preceitos da Lei 11.794 de 8 de outubro de 2008, com o Decreto 6.899 de 15 de julho de 2009, bem como com as normas editadas pelo Conselho Nacional de Controle da Experimentação Animal (CONCEA), e foi **aprovada** pela Comissão de Ética no Uso de Animais da Faculdade de Medicina Veterinária e Zootecnia da Universidade de São Paulo (CEUA/FMVZ) na reunião de 21/11/2018.

We certify that the proposal "Isolation and Characterization of Cancer Associated Fibroblasts from Canine Mast Cell Tumors and its influence on the malignancy of neoplastic cells", utilizing 20 Dogs (males and females), protocol number CEUA 5637040718 (ID 005827), under the responsibility of **Ricardo de Francisco Strefezzi** *and team; Lidia Hildebrand Pulz* - which involves the production, maintenance and/or use of animals belonging to the phylum Chordata, subphylum Vertebrata (except human beings), for scientific research purposes or teaching - is in accordance with Law 11.794 of October 8, 2008, Decree 6899 of July 15, 2009, as well as with the rules issued by the National Council for Control of Animal Experimentation (CONCEA), and was **approved** by the Ethic Committee on Animal Use of the School of Veterinary Medicine and Animal Science (University of São Paulo) (CEUA/FMVZ) in the meeting of 11/21/2018.

Finalidade da Proposta: Pesquisa

Vigência da Proposta: de 02/2015 a 02/2019 Área: Patologia Experimental E Comparada

Origem:	Animais de proprietários						
Espécie:	Cães	sexo:	Machos e Fêmeas	idade:	0 a 20 anos	N:	20
Linhagem:	não se aplica			Peso:	0 a 60 kg		

Local do experimento: Laboratório de Patologia - Departamento de Medicina Veterinária- Faculdade de Zootecnia e Engenharia de Alimentos - Universidade de São Paulo Laboratório de Oncologia Comparada e Translacional - Departamento de Medicina Veterinária Faculdade de Zootecnia e Engenharia de Alimentos - Universidade de São Paulo

São Paulo, 21 de novembro de 2018

Profa. Dra. Anneliese de Souza Traldi
Presidente da Comissão de Ética no Uso de Animais
Faculdade de Medicina Veterinária e Zootecnia da Universidade de São Paulo

Roseli da Costa Gomes
Secretária
Faculdade de Medicina Veterinária e Zootecnia da Universidade de São Paulo

EVALUATION FORM

Author: PULZ, Lidia Hildebrand

Title: **Isolation and characterization of Cancer Associated Fibroblasts from canine Mast Cell Tumors and its influence on the malignancy of neoplastic cells:** a combined molecular, pathologic and *in vitro* approach

Thesis submitted to the Postgraduate Program in Experimental and Comparative Pathology of the School of Veterinary Medicine and Animal Science of the University of São Paulo to obtain the Doctor's degree in Sciences.

Date: _____/_____/_____

Committee Members

Prof. _____

Institution:_____ Decision: _____

Prof. _____

Institution: _____ Decision: _____

Prof. _____

Institution: _____ Decision: _____

Prof. _____

Institution:_____ Decision: _____

Prof. _____

Institution:_____ Decision: _____

I would like to dedicate this thesis to my family: my Mom Géssia, my Dad Fábio, my brother Otávio and my sisters Luiza and Helena. You are my strength. I give you all my love and gratitude. Your support – and the mental health issues you gave me – made all of this possible.

This thesis is also dedicated to my nieces Gabriela and Isadora. Girls, none of you will read it. However, because of you, I laugh a little harder, cry a little less and smile a lot more.

To my treasured friends: You are the stars in my night sky. You made me unlock the keys to grow deeper. That's it, you bring out the best in me.

And finally for my Tiêta, whose constant warmth and companionship
I could not repay
even with a lifetime of dog treats and bones.
But I'll try anyway.

During this period, there were very painful moments in my life that changed my entire world. I left them make me stronger, smarter and kinder.

For all those who encouraged me to fly toward my dreams: let's soar.

ACKNOWLEDGEMENTS

I would like to thank the special support of my dear teacher, friend and advisor, Prof. Dr. Ricardo De Francisco Strefezzi, for giving me the best's opportunities and advices, who somehow managed to be rigorous but supportive.
You sparked my interest in pathology and I will forever be grateful.
"I walked a mile in your shoes, and now I'm a mile away, and I've got your shoes"♪

My special thanks to the Prof. Dr. Heidge Fukumasu who always support and kept me motivated. Your collaboration was fundamental to the development of my thesis and my personal development. I have great admiration for you. Eternal gratitude.

Thanks to my cousin Martim: however distant you may be, are still close. You basically became my psychiatrist, my dog walker, my support. Thank you forever.

I specially recognize the support of my colleagues from LOCT and Pathology Laboratory. Much appreciation for the years of working together.

I would like to express my gratitude to Nilton P. Santos, Arina L. Rochetti, Linsay Paskoski and Danielle Passarelli for technical support and and pleasant living together

Thanks to my co-workers who loves to teach but hates all the crap that comes with it… You always were understanding and supportive.

I would like to thank Fundação de Apoio à Pesquisa do Estado de São Paulo -FAPESP (grants: #2013/13252-8, #2016-03862-1 and #2014/02493-7), Conselho Nacional de Desenvolvimento Científico e Tecnológico – Cnpq (grant: #141915/2015-3) and Coordenação de Aperfeiçoamento de Pessoal de Nível Superior (CAPES) for financial support.

Finally, I thank to FZEA for opening doors to me.

“The price of success is hard work, dedication to the job, and the determination that whether we win or lose, we have applied the best of ourselves to the task at hand."

Vince Lombardi

RESUMO

PULZ, L. H. **Isolamento e caracterização de Fibroblastos Associados ao Câncer provenientes de Mastocitomas caninos e sua influência sobre a malignidade de células neoplásicas:** uma abordagem molecular, patológica e *in vitro*. 2019. 112 p. Tese (Doutorado em Ciências) – Faculdade de Medicina Veterinária e Zootecnia, Universidade de São Paulo, São Paulo, 2019.

Os mastocitomas cutâneos (MCTs) são neoplasias comuns em cães e são considerados potencialmente malignos. Diversas pesquisas tentaram identificar biomarcadores para melhor predizer o comportamento biológico deste tumor. Além disso, estudos envolvendo o cultivo primário de MCTs caninos podem ser uma ferramenta valiosa para a análise das propriedades funcionais das células. O objetivo deste estudo foi identificar vias moleculares ligadas a características de malignidade histopatológicas, menor tempo de sobrevida e pior prognóstico associados ao MCT. Além disso, objetivamos investigar o comportamento de mastócitos *in vitro* obtidos a partir de MCTs de diferentes graus histopatológicos e determinar o tipo de interação com os fibroblastos estromais. Realizamos análises de expressão gênica em MCTs únicos obtidos de 15 cães e identificamos dois subtipos distintos de tumor – alto risco e baixo risco - associados a diferenças nos graus histológicos, tempos de sobrevida, índices Ki67 e ocorrência de morte devido a doença. Análises comparativas de perfis de sequência de RNA revelaram 71 genes diferencialmente expressos entre MCTs de alto e baixo risco. Ademais, examinamos redes de co-expressão gênica para explorar as funções biológicas dos genes identificados. A construção da rede revelou 63 módulos gênicos, dos quais 4 foram significativamente associados ao grupo mais agressivo. Dois dos módulos gênicos positivamente correlacionados com MCTs de alto risco também foram associados à proliferação celular e à matriz extracelular. No topo do módulo de matriz extracelular, foram identificados genes com funções diretamente relacionadas àqueles de fibroblastos associados ao câncer (CAFs). Análises imuno-histoquímicas também revelaram um maior número de CAFs em MCTs de alto risco. Os experimentos de cultivo foram feitos imediatamente após a ressecção cirúrgica e as células foram cultivadas em DMEM-F12 completo por 4 a 7 passagens. Os mastócitos foram evidenciados por coloração com Romanowsky e azul de toluidina com perda progressiva de seus grânulos em cultivo. A confirmação de fibroblastos como células aderentes foi feita por qRT-PCR para o gene da Proteína Específica de Fibroblastos 1 (FSP1). A caracterização dos fibroblastos cultivados como miofibroblastos foi realizada por imunofluorescência para α-actina de músculo liso (SMA) e vimentina. A percentagem de

células viáveis no sobrenadante foi determinada a cada passagem. Durante as 4-10 semanas de cultivo sem adição de fatores de crescimento ou citocinas, a população de mastócitos vivos diminuiu progressivamente e os fibroblastos e miofibroblastos continuam a crescer até a senescência. Amostras de MCTs de alto grau foram viáveis por períodos mais curtos (P =0.0442) e menor número de passagens (P <0.0001). Examinamos também os efeitos a curto prazo dos fibroblastos estromais na viabilidade dos mastócitos neoplásicos em diferentes condições de culturas. O contato célula-célula foi a melhor condição em que maior proporção de mastócitos neoplásicos permaneceu viável em comparação com todas as outras condições, isto é, utilizando-se de inserto e no cultivo de mastócitos isolados (P<0.05). Verificamos também que os mastócitos neoplásicos não ficam viáveis por mais de 4 dias na ausência de fibroblastos ou de seus fatores solúveis. Estes resultados indicam uma importante interação entre os mastócitos e os fibroblastos, que podem ocorrer no microambiente tumoral.

Palavras-chave: RNA-Seq. Cão. Co-cultivo. Miofibroblastos. Matriz extracelular.

ABSTRACT

PULZ, L. H. **Isolation and characterization of Cancer Associated Fibroblasts from canine Mast Cell Tumors and its influence on the malignancy of neoplastic cells:** a combined molecular, pathologic and *in vitro* approach. 2019. 112 p. Tese (Doutorado em Ciências) – Faculdade de Medicina Veterinária e Zootecnia, Universidade de São Paulo, São Paulo, 2019.

Mast cell tumours (MCTs) are common neoplasms in dogs and are considered potentially malignant. Several researches have attempted to identify biomarkers to better predict biological behavior for this tumor. In addition, studies with primary culture of canine MCTs coud be a valuable tool for the analysis of the cells functional properties. The objetive of this study was to identify molecular pathways connected to histopathological malignancies, shorter survival time and poor prognoses associated with MCTs. Moreover, we aimed to investigate the *in vitro* behavior of mast cells obtained from canine cutaneous MCTs of different histopathological grades and the type of interaction with the stromal fibroblasts. We performed genome-wide gene expression analyses on tissues obtained from 15 dogs with single MCTs, and identified two distinct tumour subtypes - high-risk and low-risk - associated with differences in histological grades, survival times, Ki67 indices, and occurrence of death due the disease. Comparative analyses of RNA sequence profiles revealed 71 genes that were differentially expressed between high and low-risk MCTs. In addition to these analyses, we examined gene co-expression networks to explore the biological functions of the identified genes. The network construction revealed 63 gene modules, 4 of which were significantly associated with the more aggressive tumour group. Two of the gene modules positively correlated with high-risk MCTs were also associated with cell proliferation and extracellular matrix-related terms. At the top of the extracellular matrix module category, genes with functions directly related to those of cancer-associated fibroblasts (CAFs) were identified. Immunohistochemical analyses also revealed a greater number of CAFs in high-risk MCTs. Culture experiments were made immediately after surgical resection and cells were cultured in complete DMEM-F12 for 4 to 7 passages. Mast cells was stained with Romanowsky and toluidine blue and showed progressive loss of their granules in culture. The presence of fibroblasts as adherent cells was confirmed by use of qRT-PCR for Fibroblast-specific Protein 1 (FSP1) gene. The characterization of cultured fibroblasts as myofibroblasts was performed by immunofluorescence for α-smooth muscle-actin (SMA) and vimentin. The percentage of viable cells in the supernatant was determined in each passage. During 4–10 weeks of culture without any addition of growth factors or cytokines, living mast cell population decreased

progressively and adherent fibroblasts and myofibroblasts continue to grow until senescence. High-grade MCTs samples were viable for shorter periods in culture ($P=0.0442$) and lower number of passages ($P<0.0001$). We also have examined the short-term effects of stroma fibroblasts on neoplastic mast cells in different cultures conditions. The cell-cell contact co-culture was the best condition in which canine neoplastic mast cells remained viable in highest proportion during the experiment compared to all other conditions, i.e. with the transwell condition and mast cells isolated cultures ($P<0.05$). We also found that isolated neoplastic mast cells are not viable for more than 4 days in the absence of fibroblasts or their soluble factors. These results indicate an important interaction between mast cells and fibroblasts, which may also occur in the tumor microenvirnomental setting.

Keywords**:** RNA-Seq. Dog. Co-culture. Myofibroblast. Extracellular matrix.

LIST OF ABBREVIATIONS

BMCMC	Bone marrow derived mast cells
CAF	Cancer-associated fibroblast
CCM	Complete conditioned medium
CDMEM-F12	Complete DMEM-F12 medium
cDNA	Complementary DNA
Ct	Cicle threshold
DE	Differentially expressed
DMEM-F12	Dulbecco's modified Eagle medium/Ham's F-12 medium
ECM	Extracellular matrix
FDR	False discovery rate
FFPE	Formalin-fixed paraffin-embedded
FITC	Fluorescein isocyanate
FSP1	Fibroblast-specific Protein 1
GO	Gene Ontology
HE	Haematoxylin and eosin
HIF-1α	Hypoxia inducible factor-1
HMC1	Human mast cell-1
HPF	High power fields
IL-6	Interleukin-6
IL-8	Interleukin 8
LOX	Lysyl oxidase
LOXL2	Lysyl oxidase–like-2
MCT	Mast cell tumour
ME	Module eigengene
mRNA	Messenger RNA
Paj	P value adjusted
PBS	phosphate buffered saline
PCR	Polymerase Chain Reaction
PDGFRa	Platelet derived growth factor receptor-α
PE	Paired end reads
qRT-PCR	Real-time quantitative polymerase chain reaction
RIN	RNA integrity number
RNA-seq	RNA sequencing
rRNA	Ribosomal RNA
SAM	Sequence Alignment/Map
SA-β-Gal	Senescence-associated β-Galactosidase
SCF	Stem Cell Factor
SD	Standard deviation
TGF-β	Transforming growth factor beta
VEGF	Vascular endothelial growth factor
WHO	The World Health Organization
α-SMA	Smooth muscle alpha actin

SUMMARY

1. GENERAL INTRODUCTION

In view of the variable biologic behavior of canine cutaneous mast cell tumors (MCT), development of appropriate prognosis and treatment for individual affected dogs can be very difficult. Advances in human molecular medicine have sought to understand the molecular underpinnings of cancer development, metastatic pattern, and response to treatment. In canine oncology, over the past decades, much evidence has emerged indicating that a substantial part of the variability in tumor behavior is genetically determined, with age, breed, tumor location, environmental conditions, and concurrent therapy playing important contributory roles.

A profile of the gene variations of canine MCTs could guide more precise prognosis, and even allow the selection of drugs or treatment protocols that could minimize harmful side effects or ensure more successful outcomes. Additionally, molecular studies could indicate individual's susceptibility to diseases, allowing veterinarians and owners to design a plan for prevention and early diagnosis.

Another point to consider is the success in the treatment of several human cancers related to the development of targeted therapies. However, in order to develop more effective therapies for canine MCTs, it is necessary to learn about the cells that comprise the tumor, their characteristics, functionality, and interactions with the tumor microenvironment. Little is known about the different mast cell populations in dogs and the requirements for canine neoplastic mast cells culture remain poorly defined.

The objective of this work was to approach the canine cutaneous MCT in several aspects: *in vitro* characteristics, cell interactions and molecular signatures of malignancy. In the present research, we have characterized different RNA expression profiles using high-throughput sequencing (HTS) and compared with survival time and significant prognostic markers for canine cutaneous MCTs, including histologic grading and proliferation activity. In addition, *in vitro* studies have provided information for the understanding of the dynamics of neoplastic mast cell growth, suggesting an important role for cancer-associated fibroblasts in this disease.

2 ARTICLE 1

IDENTIFICATION OF TWO MOLECULAR SUBTYPES IN CANINE MAST CELL TUMOURS THROUGH GENE EXPRESSION PROFILING

2.1 INTRODUCTION AND LITERATURE REVIEW

Canine mast cell tumours (MCTs) are malignant neoplasms composed of atypical mast cells that are characterised by high infiltration capacity and metastatic potential (HOTTENDORF, 1968; BLACKWOOD et al., 2012). It is one of the most commonly diagnosed neoplasms in dogs, accounting for 16–21% of cutaneous tumours (PRIESTER, 1973; COHEN et al., 1974; FINNIE, BOSTOCK, 1979; BOSTOCK, 1986; LONDON, SEGUIN, 2003). Since the biological behaviours of MCTs are highly variable, a better understanding of the development and progression, as well as the identification of new prognostic indicators, can help in treating the diseased animals (SHOOP et al., 2015).

Like most tumours in animals, canine MCTs are classified based on their histological appearances, which presumably reflect degree of cell differentiation. Besides this classification, prediction of biological behaviours in MCTs could be complemented by additional methods based on histochemical and immunohistochemical prognostic markers (WEBSTER et al., 2006; WELLE et al. 2008; VASCELLARI et al., 2013; SABATTINI et al., 2015, PULZ et al., 2016). However, as in human neoplasms, abundant evidence suggests the presence of unrecognised, relevant subclasses of tumours with respect to their underlying molecular phenotypes and prognoses (FREIJE et al., 2004). Clinically, it is also apparent that histologically identical tumours can behave very differently (MISCHEL et al., 2003).

The transcriptomes of canine cancers have been investigated mainly by cDNA microarrays in mammary tumours (UVA et al., 2009; KLOPFLEISCH et al., 2010; KLOPFLEISCH et al., 2011), osteosarcomas (SELVARAJAH et al., 2009; O'DONOGHUE et al., 2010; PANG et al., 2014), hemangiosarcomas (TAMBURINIET al., 2010; THOMAS et al., 2014), lymphomas (FRANTZ et al., 2013; MUDALIAR et al., 2013), histiocytic sarcomas (BOERKAMP et al., 2013), mast cell tumours (GIANTIN et al., 2014; GIANTIN et al., 2016), and melanoma cell lines (FOWLES et al., 2015). Compared to microarrays, next generation RNA sequencing (RNA-seq) is a more powerful technique, allowing the investigation of gene expression data at a whole-transcriptome level with unprecedented sensitivity and accuracy (OZSOLAK, MILOS, 2011). Recent investigations of canine tumours with RNA-seq have been

carried out in B-cell lymphomas (MOONEY et al 2013), mammary carcinomas (LIU et al., 2014), squamous cell carcinomas of the head and neck (LIU et al., 2015), bladder cancers (RAMSEY et al., 2017), and hemangiosarcomas (GORDEN et al., 2014).

In this study, we aimed to identify molecular pathways associated with MCT behaviour using differential expression and co-expression network analyses with RNA-seq-based transcriptomics data from canine MCTs samples. To the best of our knowledge, this is the first study to characterise MCTs using network methods.

2.2 MATERIALS AND METHODS

2.2.1 Canine tissue samples

Since only animals with single lesions were included in this study, a total of 15 cutaneous MCTs from 15 dogs were utilised. Fresh-frozen and formalin-fixed paraffin-embedded (FFPE) tissue sections of spontaneous canine MCTs were obtained from the Veterinary Hospitals of the School of Veterinary Medicine and Animal Science of the University of São Paulo, Methodist University of São Paulo and the Veterinary Clinic Provet. Samples were acquired from routine cases that were treated by wide surgical resectioning. All experiments were approved by "Ethics Committee for the use of animals" of the School of Veterinary Medicine and Animal Science of the University of São Paulo #2893/2013 and consent for the use of foreskin tissue was provided by the legal guardians of all tissue donors in this study.

All tumours were chosen based on the following inclusion criteria: 1) confirmed histological diagnosis of canine cutaneous MCT; 2) treatment with surgical excision without neoadjuvant chemotherapy (no radiation or chemotherapy before or at the time of tumour removal); 3) availability of follow-up data.

Each tumour was evaluated according to a two-tier grading system into low-grade (grade 1) or high-grade (grade 2) of malignancy (KIUPEL et al., 2011) by the same veterinary pathologist (R. F. Strefezzi), who was not supplied with any information about the cases. The choice of this histopathological grading criteria eliminates the ambiguity of intermediate grade MCTs and is more accurate in predicting the biological behaviour of this tumour (KIUPEL et al., 2011; SABATTINI et al., 2015).

Follow-up data collection began from the day of first contact, and continued for at least 180 days post-surgery and included details of age, sex, breed, location of the lesions, time to

relapse, overall survival and *causa mortis*, when applicable. Overall survival was defined as the interval between surgical excision and last follow-up day or death by any cause. At the end of the study, deaths unrelated to MCT were censored. Nine dogs (60%) received adjuvant chemotherapy. The treatment protocols included combinations of vinblastine, prednisone, and lomustine.

2.2.2 Ki67 immunohistochemical staining

FFPE tissues were sectioned into 5 µm-thick sections, deparaffinised in xylene, rehydrated in graded ethanol, and rinsed in distilled water. Endogenous peroxidases were blocked by incubating sections in 3% hydrogen peroxide for 5 m. Antigen retrieval was performed by incubating the sections in citrate buffer (pH 6.0) in a pressure cooker for 2 m and cooled for 20 m. All slides were rinsed with 0.05 M phosphate buffered saline (PBS, pH 7.6) with 0.01% Tween 20. The slides were subsequently incubated with mouse monoclonal anti-Ki67 primary antibodies (MIB1; Dako Cytomation Carpinteria, CA) at a dilution of 1:50, in a moist chamber at 4 ^{o}C for 16 h (overnight). Following this, slides were incubated with secondary antibodies (Code K4068, ADVANCE^{TM} HRP Link, anti-mouse and anti-rabbit secondary antibodies, Dako, Carpinteria, CA) for 25 m and the reaction was amplified with Advance HRP Enzyme Polymer (Code K4068, ADVANCE^{TM} HRP Enzyme, antibodies polymerised with horseradish peroxidase, Dako Cytomation Carpinteria, CA). The reactions were visualised with 3,4-diaminobenzidine (Liquid DAB + Substrate Chromogen System, Dako Cytomation Carpinteria, CA) and counterstained with Mayer's haematoxylin.

For the negative control, the primary antibody was replaced with a normal mouse IgG at the same concentration as the primary antibody. The basal layer of the epidermis served as an internal positive control for Ki67.

2.2.3 Ki67 index

Histological images were evaluated distant from the deep and lateral margins of the tumour mass. For each lesion, a total of five high power fields (HPF) (400x magnification) were selected from areas with the highest percentage of labelled mast cells ("hot spots") at low magnification (100x magnification). To determine the percentage of proliferating cells (Ki67 index), we counted the number of mast cells showing positive and negative immunostaining for Ki67 in the chosen fields per captured image using the ImageJ® software; a minimum of 200

cells for each section were counted. We determined the average percentage of positive mast cells in five fields without prior knowledge of the clinical outcome.

2.2.4 Definition of high-risk and low-risk MCTs

We used four criteria to divide MCT samples into low- or high-risk groups: histological grade, survival time, Ki67 index and death due the disease. The tumours were graded histologically with a two-tier system (low-grade or grade 1 and high-grade or grade 2). Each parameter received a score, which was added to the histological grade to obtain a combined score or score of malignancy.

For survival time, a score of 1 was designated to animals that remained alive for > 365 days; a score of 2, to those surviving for 180 ≥ 365 days; and a score of 3, for animals with survival times of < 180 days.

Scores to evaluate the Ki67 indices of MCT samples were assigned as follows: a score of 1 was assigned to lesions that showed less than 3% immunoreactive cells; a score of 2 was assigned to lesions that showed 3% to 7% immunoreactive cells; and a score of 3 was assigned to lesions that displayed more than 7% of Ki67-positive cells (STREFEZZI et al., 2010)

Finally, one of the most important biological characteristics to be considered in the study of cancers is their capacity to cause death of the patient. A score to quantify occurrence of death in the studied animals was created by assigning a grade of 0 to all animals that remained alive at the end of the study period, as well as to all censored animals, whereas a score of 3 was assigned to dogs that died due the tumour.

Lesions with a total score of 5 or below were classified as “low-risk” MCTs (samples S02, S03, S05, S06, S07, S08, S09, S11, S13) and those with a score of 6 or more were defined as “high-risk” MCTs (samples S01, S04, S10 and S12).

2.2.5 Immunohistochemical staining for αSMA

We evaluated the expression of αSMA in stromal fibroblasts of 44 canine MCTs using immunohistochemistry, with a mouse monoclonal antibody (Clone HHF35; Dako Denmark A/S, Glostrup, Denmark). For negative controls, the primary antibody was replaced with normal rabbit or normal mouse IgG at the same concentration as the primary antibody.

All animals from which lesion samples were obtained for the study met the following criteria: 1) all were treated with extensive surgery; 2) none were subjected to neoadjuvant chemotherapy; and 3) follow-up data for at least 180 days was available.

The same criteria applied for the MCTs analysed by RNA-seq were used to divide the tumours subjected to immunohistochemical analysis into low- and high-risk groups: histological grade, survival time, Ki67 index and death due to disease. The term "low-risk" was attributed to cases with a score lower than 6 and high-risk for tumours with a total score equal to or greater than 6.

The number of positive fibroblasts were counted in five HPFs (400x magnification), using the ImageJ® software . Fields were selected from areas with the highest percentage of labelled cells ("hot spots") at low magnification (100x magnification); the score was calculated from the sum of cells counted in five "hot spots" fields.

2.2.6 Statistical Analysis

Ki67 index values of 44 MCT samples divided into high- and low-risk groups were compared using the Mann-Whitney U test. The number of fibroblasts testing positive for αSMA immunostaining was also compared between the low- and high-risk groups using the Mann-Whitney U test. The data were analysed with GraphPad Prism (version 4.02 for Windows, GraphPad Software, GraphPad Software Inc.) with the significance level set at 5%.

2.2.7 RNA extraction

Total RNA from each of the 15 tissue samples were extracted using the RNeasy Mini Kit (Cat No./ID: 74104, Qiagen, Crawley, West Sussex, UK). Only samples with a nucleic acid 260/280 ratio of approximately 2.0 were subjected to further analyses. RNA quality was assessed using capillary gel electrophoresis on a BioAnalyzer system (Agilent Technologies Inc., Santa Clara, CA) with RNA 6000 Nano Labchips (Agilent Technologies Inc., Santa Clara, CA, EUA) according to the manufacturer's instructions. Only samples exhibiting minimal degradation as evidenced by RNA Integrity Number (RIN) $\geq$ 7.0 were used.

2.2.8 RNA-seq data analysis

Sequencing was conducted using the Illumina platform (Illumina Inc., San Diego, CA), following the protocols provided by the manufacturer. Total RNA from 15 samples were converted into Illumina sequencing libraries using the TruSeq RNA Sample Preparation Kit (Illumina Inc., San Diego, CA). PolyA RNA was enriched from 1 μg of total RNA using oligo dT-coated magnetic beads, following which, the enriched RNA was fragmented and used for cDNA synthesis. The cDNA was fragmented, blunt-ended, ligated to bar-coded adaptors, and amplified using 15 cycles of PCR. Final library size distribution was validated through quantitative polymerase chain reaction (qPCR) using an Agilent 2100 Bioanalyzer with a KAPA Library Quantification kit (KAPA Biosystems, Foster City, USA). Adapter-ligated cDNA fragment libraries were run on Illumina HiSeq 2500 equipment using the TruSeq PE Cluster Kit and the TruSeq SBS Kit (2x100 bp). An average of 28.4 million PE 100-bp reads were sequenced per sample.

Sequencing quality was evaluated using the FastQC software (http://www.bioinformatics.babraham.ac.uk/projects/fastqc/) and due to its high quality, no filter was applied prior to alignment. Read pairs were aligned to the dog reference genome (CanFam3.1) with *TopHat2/Bowtie2* (tophat.cbcb.umd.edu), allowing two mismatches per read. The sequence alignment map (SAM) files were filtered using Samtools (LI et al., 2009) to remove secondary alignments, PCR duplicates, and low-quality alignments. Following this, read counts for each gene was estimated using HTSeq (ANDERS, HUBERT, 2015). Gene expression was estimated as counts per million (CPM) and genes which presented at least 1 CPM in at least 4 samples were retained for DE analysis.

DE analysis was performed using the EdgeR package, which is based on negative binomial distributions, in the R environment (ROBINSON, MCCARTHY, SMYTH, 2010). Only transcripts with adjusted P-values (P_{aj}) ≤ 0.05 e logFC $\geq |2|$ were considered to be differentially expressed. To ensure that the differentially expressed genes were sufficient to differentiate between the 2 groups, a hierarchical clustering analysis was performed. Over-/under-expressed genes in canine MCTs were identified on a heatmap.

2.2.9 Co-expression analysis

Co-expression analysis was used to generate a transcriptional network to investigate associations between gene modules and malignancy grades of MCTs. The analysis was

performed using the WGCNA (Weighted Correlation Network Analysis) package in the R environment (LANGFELDER, HORVATH, 2008). From the total of 13,948 genes which passed quality control, only the 6000 most-connected genes were selected due to computational limitations; furthermore, genes with low connectivity were not considered since they are likely to contribute little to the network (ZHANG, HORVATH, 2005).

Connectivity was calculated as the sum of correlations between one gene and all other genes in the network. To identify modules, a matrix was first generated by calculating Pearson's correlation coefficients between all genes and raising it to a power β (soft threshold) of 11. Following this, a topological overlap measure (TOM) was calculated by assigning values between 0 and 1 to each pair of genes based on the number of shared neighbours; this was then used to generate a clustering tree whose branches were identified for cutting using the dynamic tree-cutting algorithm (LANGFELDER, ZHANG, HORVATH, 2007). Modules containing a minimum of 30 genes were detected and assigned to colour names. Pearson's correlation coefficients were used again to measure correlations between modules' expression profiles (module eigengenes) and the malignancy scores described earlier. Modules with significant correlations ($p < 0.1$) were considered biologically relevant and used for further analysis.

2.2.10 Functional enrichment analysis

A web-server interactive software tool, GOrilla, was used to identify GO terms enriched in both the differentially expressed genes and co-expression modules associated with tumour malignancy; this was done using a hypergeometric distribution with corrections for false positive rate or false discovery rate (FDR). Genes were converted to their human orthologues to obtain the best functional detail available. Only expressed genes were used as background and terms were considered significant only if $P_{aj} \leq 0.05$.

2.3 RESULTS

2.3.1 Clinical and histopathological data and Ki67 index values

A total of 15 dogs diagnosed with MCT were included in this study. The median age at diagnosis was 10 years (mean = 9.7 years, range = 3–15 years) and 41.2% of the patients were male. The most common breeds represented in our sample were Labrador Retrievers (5 dogs), Golden Retrievers (3 dogs) and Pit bulls (2 dogs). The remaining dogs in the sample were a

poodle, dachshund, Cocker Spaniel, pug and mongrel. The most frequent locations of the MCTs were in the extremities (40% in the limbs and tail) and trunk (33.3%), followed by the abdomen and inguinal regions (13.3% each). A summary of the descriptions of the canine population is shown in Table 1.

Histopathological analyses of the MCTs were performed according to the classification system described by Patnaik et al. (1984) and 4 lesions were defined as grade I (26.7%), 10 as grade II (66.7%) and 1 as grade III (6.7%). The tumours were also graded using a two-tier histological system proposed by Kiupel et al. (2011), and 13 (86.7%) MCTs were classified as low-grade while only 2 (13.3%) were classified as having a high grade of malignancy.

Three dogs in our sample died due to MCT aggressiveness, which caused a local recurrence of MCTs with new tumour development after surgical removal or disseminated metastases. The MCTs from all the three animals that died were graded as 'intermediate' according to the criteria of Patnaik et al. (1984), and only one was diagnosed with MCT of high grade of malignancy by the two-tier histological system. One dog died due to unrelated causes and the remaining 12 cases were alive at the end of the study. The minimum follow-up period post-surgery was 190 days (median = 296 days, range = 101–1095 days) (Table 1).

Table 1. Summary of clinical and histopathological data with their respective identification number of RNA-seq.

RNA-seq ID	BREED	AGE years	GENDER	TUMOUR LOCATION	FOLLOW-UP (days)	STATUS	PATNAIK et al. 1984 grade system	TWO-TIER grading system○	KI67 Index
S01	Dachshund	10	Male	Limbs and tail	658	CS	3	2	7.95%
S02	Labrador	11	Female	Trunk	480	LA	1	1	2.92%
S03	Poodle	15	Female	Trunk	466	LA	1	1	2.36%
S04	Golden Retriever	7	Female	Limbs and tail	308	DT	2	1	23.41%
S05	Pug	9	Female	Limbs and tail	587	LA	2	1	5.28%
S06	Pitbull	10	Female	Abdomen	254	LA	2	1	3.65%
S07	Labrador	11	Female	Trunk	364	LA	2	1	4.87%
S08	Cocker	13	Female	Trunk	283	LA	2	1	1.88%
S09	Labrador	9	Male	Limbs and tail	390	LA	2	1	3.8%
S10	Labrador	5	Female	Limbs and tail	101	DT	2	2	15.48%
S11	Golden Retriever	3	Female	Inguinal	232	LA	2	1	0.30%
S12	Labrador	10	Male	Limbs and tail	130	DT	1	1	2.11%
S13	Golden Retriever	9	Male	Trunk	191	LA	2	1	5.21%
S14	Mixed breed	13	Male	Inguinal	1095	LA	2	1	2.89%
S15	Pitbull	11	Male	Abdomen	676	LA	1	1	3.43%

Abbreviations: ID: identification number; LA: live animals; CS: censored (deaths unrelated to MCT); DT: death related to mast cell tumour. ○ Kiupel et al. (2011)
Source: Pulz, L. H. (2019)

The Ki67 index was determined by the percentage of neoplastic mast cells exhibiting a positive nuclear signal to anti-Ki67 antibodies. Ki67 scores ranged from 0.30–23.41% (mean = 5.7 ± 5.84%). The Ki67 scores for MCTs from the dogs that died due to tumour aggressiveness were 23.4%, 15.5% and 2.11%. (Table 1).

2.3.2 Classification of samples as high- or low-risk MCTs

The categorisation of malignancy in the MCTs was based on clinical and histopathological features. We established individual scores for measures of survival time, proliferation index, and death due the disease. Each of these scores was added to the histological grade assigned to obtain a score of malignancy (Table 2). This numerical scale allowed us to divide all MCT cases into two groups: higher scores indicated high risk of malignancy in tumours (samples S01, S04, S10 and S12), whereas lower scores indicated low risk of malignancy (samples S02, S03, S05, S06, S07, S08, S09, S11, S13).

Table 2. Scoring of mast cell tumours. Assignment of a score for each characteristic considered: histological grade, survival time, Ki67 index and death due the disease. The mixed score (malignancy score) method was determined from these four characteristics, which together gave a numeric value for each tumour.

RNA-seq ID	TWO-TIER grading system °	FOLLOW-UP SCORE	STATUS SCORE	KI67 SCORE	MALIGNANCY SCORE
S01	2	1	0	3	6*
S02	1	1	0	1	3
S03	1	1	0	1	3
S04	1	2	3	3	9*
S05	1	1	0	2	4
S06	1	2	0	2	5
S07	1	2	0	2	5
S08	1	2	0	1	4
S09	1	1	0	2	4
S10	2	3	3	3	11*
S11	1	2	0	1	4
S12	1	3	3	1	8*
S13	1	2	0	2	5
S14	1	1	0	1	3
S15	1	1	0	2	4

Abbreviations: ID: identification number; ° Kiupel et al. (2011)
* Malignancy Score ≥ 6 = high-risk MCT
Source: Pulz, L. H. (2019)

2.3.4 Canine mast cell tumour transcriptome

The number of paired end (PE) reads sequenced per sample ranged from 22,885,802 to 32,305,518 (an average of 28,404,278 PE reads were generated per sample). These sequences were mapped to the canine reference genome (canFam3.1) with a mean alignment rate of 83%, with a minimum alignment of 77.7% and maximum alignment of 86.4%. On average, the analyses revealed multiple alignments in 11% of multiple and discordant alignments in 2% of the reads. The remaining 79% of the reads were concordant alignments. Data per sample can be seen in S1 Table in Supporting Information (Apendix A).

2.3.5 Differentially expressed genes in high- and low-risk MCTs

Comparisons of transcriptome profiles between high- and low-risk MCTs revealed 71 differentially expressed (DE) genes ($P_{aj} \leq 0.05$) (Figure 1). Of these, 68 were upregulated in the high-risk group while 3 genes were downregulated (Figure 1). A list of the differentially expressed genes with their respective descriptions is available in Table 3.

Table 3: List of Differentially expressed (DE) genes between the high-risk MCTs and low-risk MCTs.

GENE NAME	DESCRIPTION	PValue	P_{aj}
MMP3	matrix metallopeptidase 3 (stromelysin 1, progelatinase)	1.17E-20	1.63E-16
CXCL8	IL8 or C-X-C Motif Chemokine Ligand 8	3.26E-17	2.27E-13
IL1B	Interleukin 1 beta	5.95E-16	2.76E-12
FMO1	flavin containing monooxygenase 1	4.96E-11	1.73E-07
CSF3R	colony stimulating factor 3 receptor	2.02E-09	5.62E-06
MAB21L1	mab-21 like 1	3.41E-09	7.93E-06
CDO1	cysteine dioxygenase type 1	7.94E-09	1.58E-05
ensembl code	-	1.01E-08	1.77E-05
GTSF1	gametocyte specific factor 1	1.19E-08	1.85E-05
WNT5A	Wnt family member 5[a]	1.39E-08	1.94E-05
NCAM2	neural cell adhesion molecule 2	2.62E-08	3.33E-05
IL18BP	interleukin 18 binding protein	1.86E-07	0.0002
LOC483397	interferon-induced transmembrane protein 1	2.89E-07	0.0003
IL11	interleukin 11	5.97E-07	0.0006
IL18RAP	interleukin 18 receptor accessory protein	6.50E-07	0.0006
WIF1	WNT inhibitory factor 1	7.73E-07	0.0006
MFSD2B	major facilitator superfamily domain containing 2B	7.75E-07	0.0006
EXO1	exonuclease 1	1.54E-06	0.0012
PI15	peptidase inhibitor 15	3.13E-06	0.0023
KMO	kynurenine 3-monooxygenase	4.09E-06	0.0029
COL21A1	collagen type XXI alpha 1 chain	4.45E-06	0.0030
LOC102155886/ SAA1(human)	serum amyloid A protein-like	5.79E-06	0.0037
MYRIP	myosin VIIA and Rab interacting protein	6.09E-06	0.0037
LOC476879/ SAA1 (human)	serum amyloid A protein-like	9.23E-06	0.0054
SMPDL3A	sphingomyelin phosphodiesterase acid like 3[a]	1.20E-05	0.0067
ensembl code	-	1.38E-05	0.0074
EDNRB	endothelin receptor type B	1.61E-05	0.0082
HTR7	5-hydroxytryptamine receptor 7	1.74E-05	0.0082
GNAZ	G protein subunit alpha z	1.76E-05	0.0082
CHGA	chromogranin A	1.73E-05	0.0082
LOC106557449	alveolar macrophage chemotactic factor-like	2.04E-05	0.0092
PGF	placental growth fator	2.25E-05	0.0098
LOC484867	docosahexaenoic acid omega-hydroxylase CYP4F3	2.82E-05	0.0119
DNM3	dynamin 3	3.10E-05	0.0127
KLHL41	kelch like family member 41	3.30E-05	0.0128
GAB3	GRB2 associated binding protein 3	3.31E-05	0.0128
FRMPD4	FERM and PDZ domain containing 4	3.62E-05	0.0136
SAMSN1	SAM domain, SH3 domain and nuclear localization signals 1	4.05E-05	0.0149
S100A9 (human)	S100 calcium binding protein A9	4.40E-05	0.0157
TNFRSF4	TNF receptor superfamily member 4	4.53E-05	0.0158

GRIK4	glutamate ionotropic receptor kainate type subunit 4	4.76E-05	0.0162
IGKV2-24 (human)	immunoglobulin kappa variable 2-24	6.52E-05	0.0216
PNMT	phenylethanolamine N-methyltransferase	6.86E-05	0.0218
SIRPA (human)	signal regulatory protein alpha	6.77E-05	0.0218
CLEC4E	C-type lectin domain family 4 member E	8.64E-05	0.0268
CSF2RA	colony stimulating factor 2 receptor alpha subunit	9.24E-05	0.0280
MUC4 (human)	mucin 4, cell surface associated	9.47E-05	0.0281
PLAUR	plasminogen activator, urokinase receptor	0.0001	0.0289
SPP2	secreted phosphoprotein 2	0.0001	0.0289
SLAMF1	signaling lymphocytic activation molecule family member 1	0.0001	0.0289
SOCS1	suppressor of cytokine signaling 1	0.0001	0.0306
COL11A2	collagen type XI alpha 2 chain	0.0001	0.0321
CLEC5A	C-type lectin domain family 5 member A	0.0001	0.0327
IL1RN	interleukin 1 receptor antagonist	0.0001	0.0327
CTSE	cathepsin E	0.0001	0.0334
IL2RB	interleukin 2 receptor subunit beta	0.0001	0.0356
ANOS1	anosmin 1	0.0001	0.0356
CYP27B1	cytochrome P450, family 27, subfamily B, polypeptide 1	0.0002	0.0359
IDO1	indoleamine 2,3-dioxygenase 1	0.0002	0.0364
SLC4A8	solute carrier family 4 member 8	0.0002	0.0365
HJURP	Holliday junction recognition protein	0.0002	0.0365
SOD2	superoxide dismutase 2, mitochondrial	0.0002	0.0380
UCHL1	ubiquitin C-terminal hydrolase L1	0.0002	0.0380
C20orf96	chromosome 24 open reading frame, human C20orf96	0.0002	0.0404
COL27A1 (human)	collagen type XXVII alpha 1 chain	0.0002	0.0425
IL22RA2	interleukin 22 receptor subunit alpha 2	0.0002	0.0426
DDC	dopa decarboxylase	0.0002	0.0470
GPR35	G-protein coupled receptor 35-like	0.0002	0.0486
S100A8	S100 calcium binding protein A8	0.0002	0.0489
RFX8	RFX family member 8, lacking RFX DNA binding domain	0.0003	0.0498
PCSK1N	proprotein convertase subtilisin/kexin type 1 inhibitor	0.0003	0.0498

Human orthologues were used in ensembl gene ID that not found a respective gene name in canine transcriptome.
Source: Pulz, L. H. (2019)

Figure 1. Hierarchical clustering of 15 dog samples based on a subset of 71 differentially expressed genes. A total of 13,948 genes are represented in a heat map. Colour intensity was normalised to log10 (fragments per kilobase of transcript per million mapped reads + 1). Increasing red intensity indicates increased gene expression and increasing blue intensity indicates decreased gene expression, as shown in the scale bar. Statistically significant differences in gene expression ($p < 0.05$) define two molecular subtypes of canine MCTs— high-risk (n = 4) and low-risk MCTs (n = 11). According to the differential gene expression profile, samples were clustered separately and arranged from the low-risk group (left/light grey bar) to the high-risk group (right/ dark grey bar)

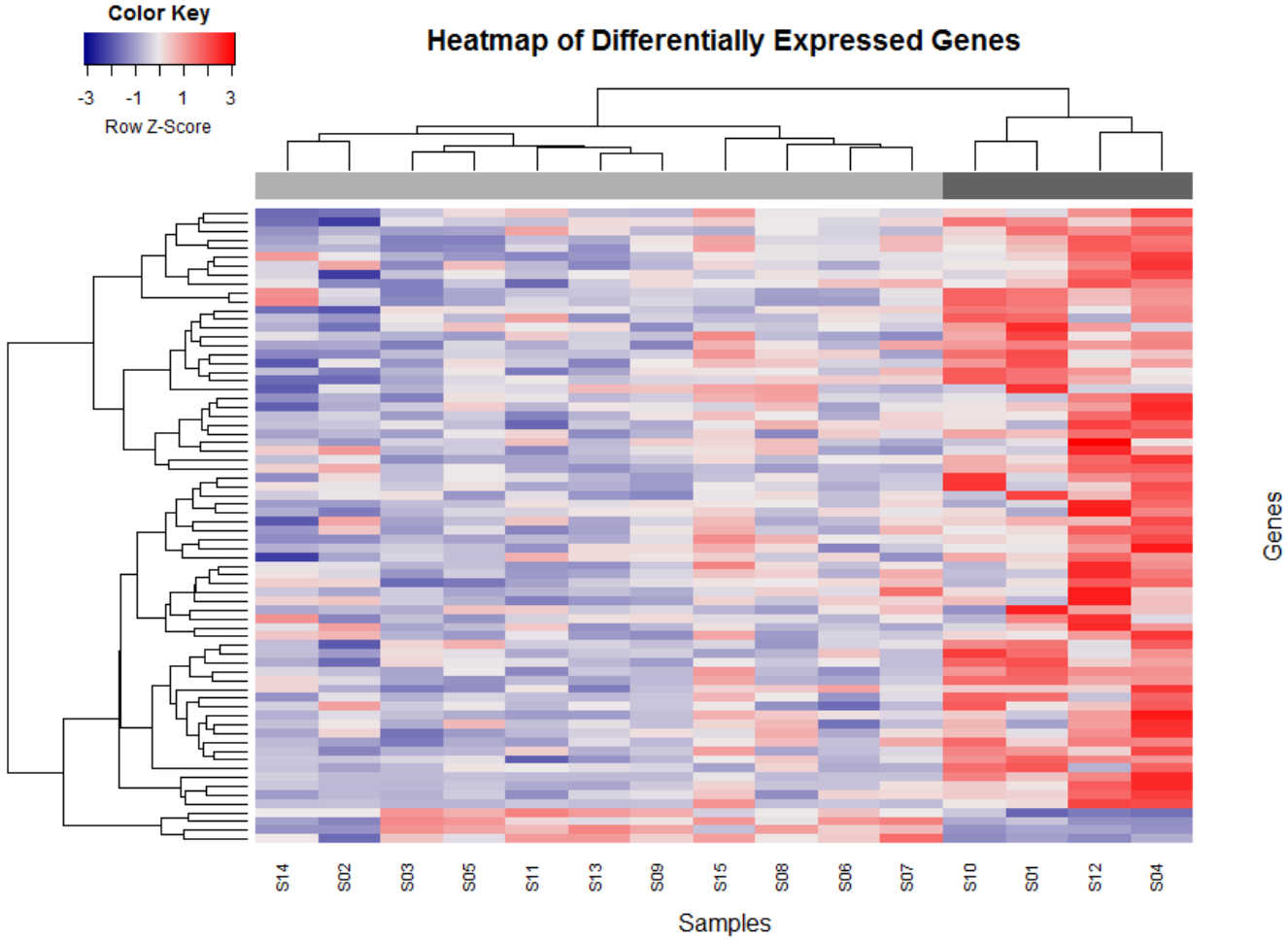

Source: Pulz, L. H. (2019)

2.3.6 Co-expression analysis

A total of 63 modules were identified when the 6000 most-connected genes from the 15 samples were used for the analysis. Genes that are highly interconnected within the network (modules) are expected to be involved in the same pathways or in roles with related biological functions. The correlation analysis between module eigengene values and malignancy scores resulted in the identification of four significant modules ($P < 0.1$) (Figure 2).

Two modules, *Palevioletred3* ($r = -0.46$, $P = 0.09$) and *Floralwhite* ($r = -0.45$, $P = 0.09$), are negatively correlated with malignancy scores, whereas the other two modules, *Darkorange2* ($r = 0.51$, $P = 0.05$) and *Darkorange* ($r = 0.45$, $P = 0.09$), were positively correlated with malignancy scores (Figure 2). The *Palevioletred3* module included 43 unique genes (S2A Table in Supporting Information- Appendix B) and the *Floralwhite* module included 54 genes (S2B Table in Supporting Information – Appendix C). The *Darkorange* module included 85 unique genes (S2C Table in Supporting Information – Appendix D) and the *Darkorange2* module with 53 genes (S2D Table in Supporting Information- Appendix E).

Figure 2. Correlations between module eigengene (ME) values and malignancy scores. Highly connected genes were identified in 63 modules with respective colours considering the 6000 most connected genes in all samples. The level of red intensity indicates degree of positive correlation between module expression and malignancy scores. The level of green intensity indicates the degree of negative correlation of module expression and malignancy scores. The *p*-values for correlation analyses are provided in brackets

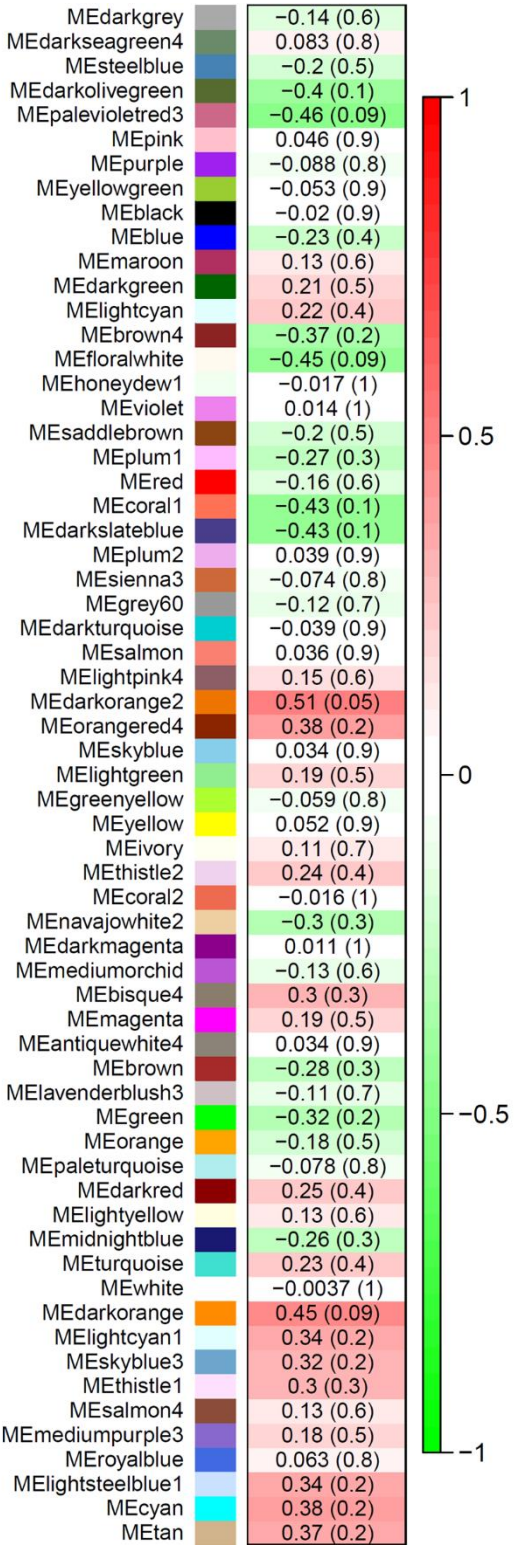

Source: Pulz, L. H. (2019)

2.3.7 Functional enrichment analysis

The functional enrichment analysis of all 71 DE genes indicated that these genes were connected to immune/inflammatory responses, mitochondrial activity, and extracellular region ($P_{aj} \leq 0.05$); most of them were found to be up-regulated in the high-risk group. Considering biological processes, there was an enrichment related to response to biotic stimulus (P=1.28 x 10^{-10}, 17/71), chemotaxis (P=1.37 10^{-9}, 12/71), response to lipopolysaccharide (P=6.77 x 10^{-9}, 11/71), immune response (P=7.33 x 10^{-9}, 16/71) and cytokine-mediated signaling pathway (P=8.32 x 10^{-9}, 13/71). When molecular functions were analysed, the enriched gene ontology (GO) terms included oxido-reductase activity (P = 5.97^{-11}, 7/71), mono-oxygenase activity (P = 8.26^{-9}, 7/71) and G-protein coupled receptor binding (P = 9.61^{-7}, 8/71). Interestingly, when cellular components were included in the analysis, genes related to the extracellular region were also enriched (P = 9.65^{-10}, 22/71).

A new functional enrichment analysis to test for co-expression was carried out for each significant module. This analysis showed that only those modules positively correlated with MCT risk scores (*Darkorange2* and *Darkorange*) presented significant enrichment in GO ($P_{aj} \leq 0.05$).

The *Darkorange2* module (53 genes) is involved mostly in biological processes related to positive regulation of cell proliferation. The most representative terms in this module included ‘cell cycle process’ (P = 3.08 x 10^{-17}), ‘mitotic cell cycle process’ (P = 9.16 x 10^{-13}), ‘regulation of chromosome segregation’ (P = 1.18 x 10^{-11}) and ‘regulation of cell cycle’ (P = 1.55 x 10^{-10}) (Figure 3A). Corroborating this result, the enriched GO terms also included ‘chromosomal part’ (8.1 x 10^{-9}), and ‘chromosome, centromeric region’ (5.11 x 10^{-8}) (Figure 3B) when cellular components were included in the analysis.

Figure 3. Enriched gene ontology (GO) terms from the *Darkorange2* module associated with cell proliferation. Colour-coded graphical representation reflecting the degree of enrichment of each (A) biological process and (B) cellular components. The higher intensity of red colour represents more significant terms

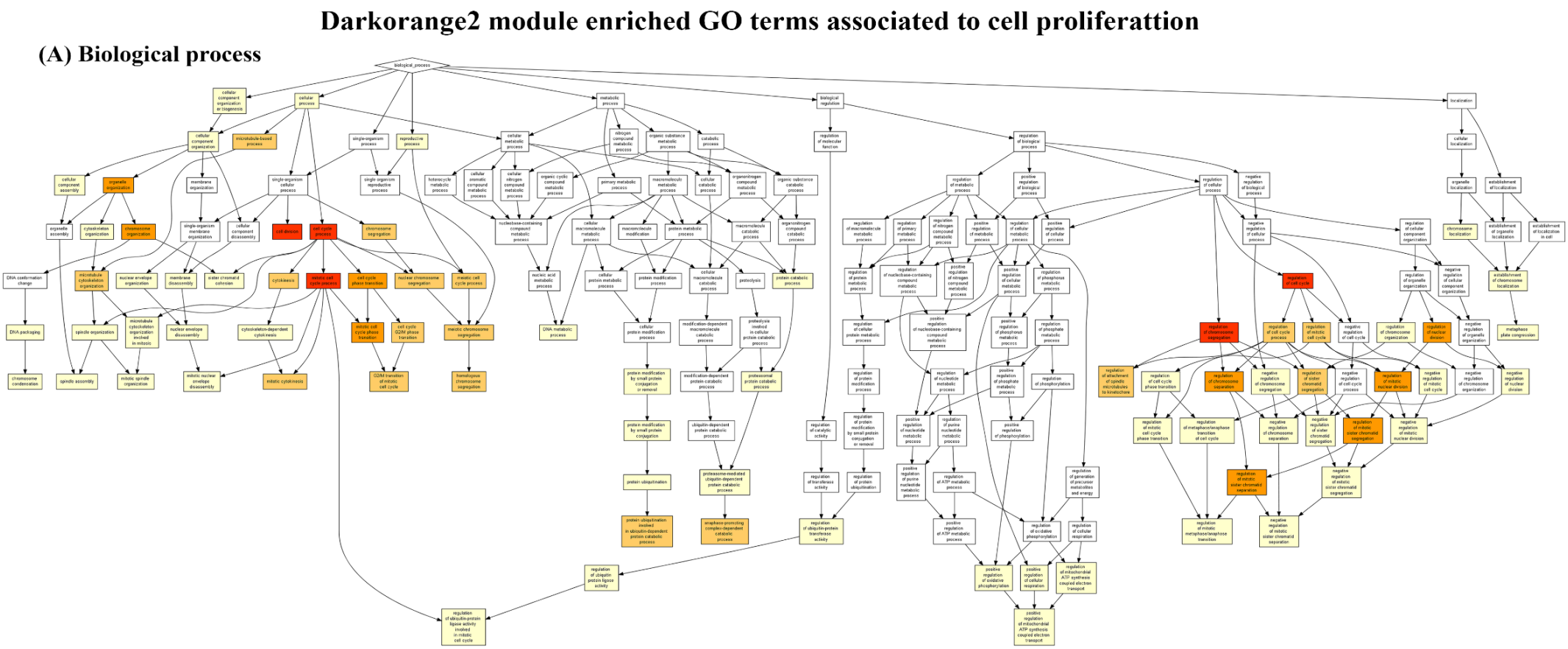

Source: Pulz, L. H. (2019)

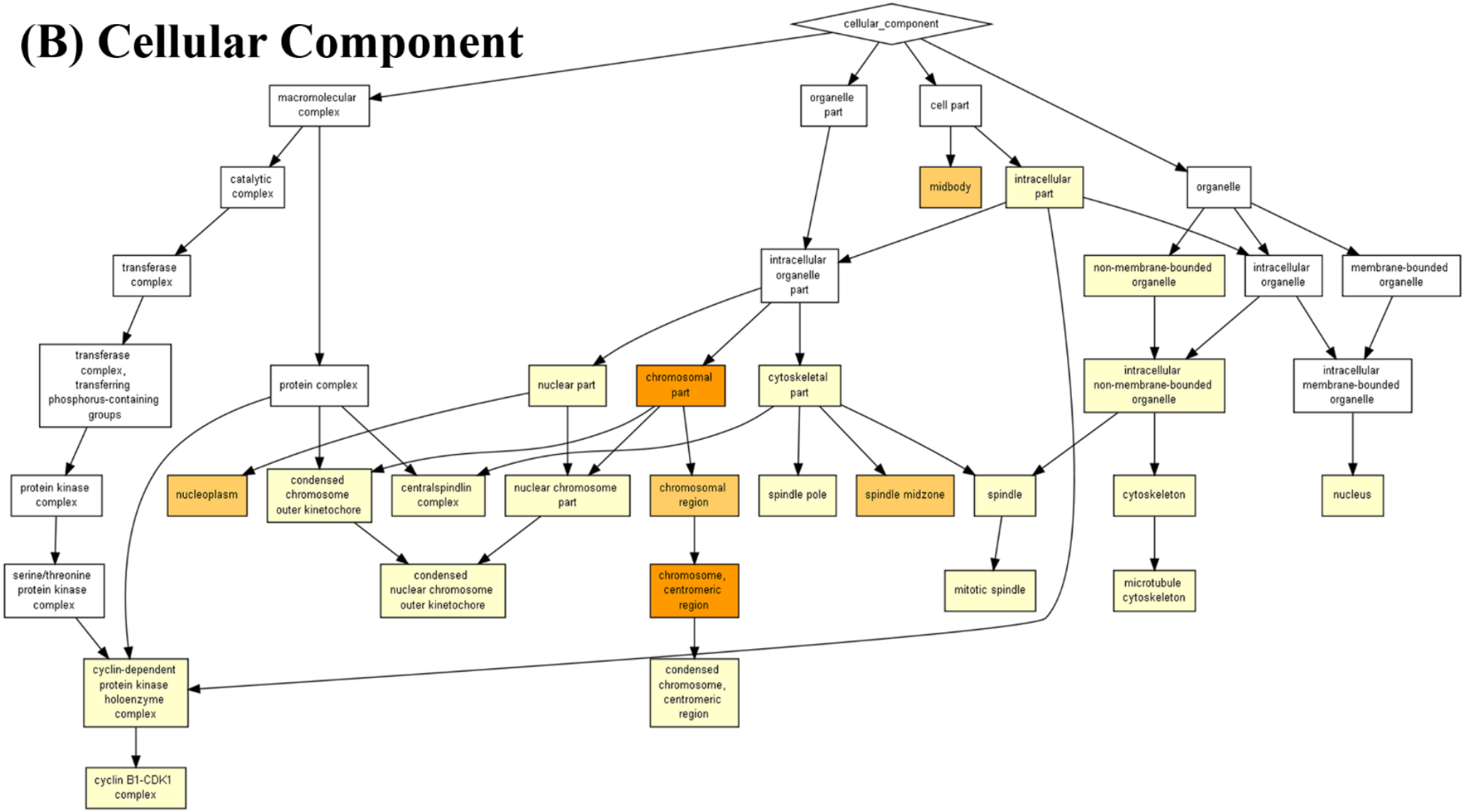

Source: Pulz, L. H. (2019)

The second module, *Darkorange* (P = 0.09), showed functional enrichment in genes associated with the extracellular matrix (ECM). The enriched terms were ‘extracellular matrix organisation’ ($P = 1.41 \times 10^{-19}$), ‘extracellular structure organisation’ ($P = 1.55 \times 10^{-19}$), ‘collagen metabolic process’ ($P = 2.28 \times 10^{-14}$), ‘multicellular organismal macromolecule metabolic process’ ($P = 4.32 \times 10^{-14}$), and ‘collagen catabolic process’ ($P = 1.12 \times 10^{-13}$) (Figure 4A). When cellular components were included in the analysis, enrichment in terms related to ‘extracellular matrix’ ($P = 2.59 \times 10^{-15}$), ‘endoplasmic reticulum lumen’ ($P = 5.75 \times 10^{-15}$), ‘collagen trimer’ ($P = 2.91 \times 10^{-13}$), and ‘extracellular matrix component’ ($P = 7.3 \times 10^{-12}$) were also included in the results (Figure 4B). When molecular functions were analysed, the enriched GO terms included ‘platelet-derived growth factor binding’ ($P = 5.04 \times 10^{-8}$) and ‘extracellular matrix structural constituent’ ($P = 1.02 \times 10^{-7}$) (Figure 4C).

Figure 4. Enriched gene ontology (GO) terms from the *Darkorange* module associated with the extracellular matrix (ECM). Colour-coded graphical representation reflecting the degree of enrichment of (A) biological processes, (B) cellular components and (C) molecular functions. The higher intensity of red colour represents more significant terms

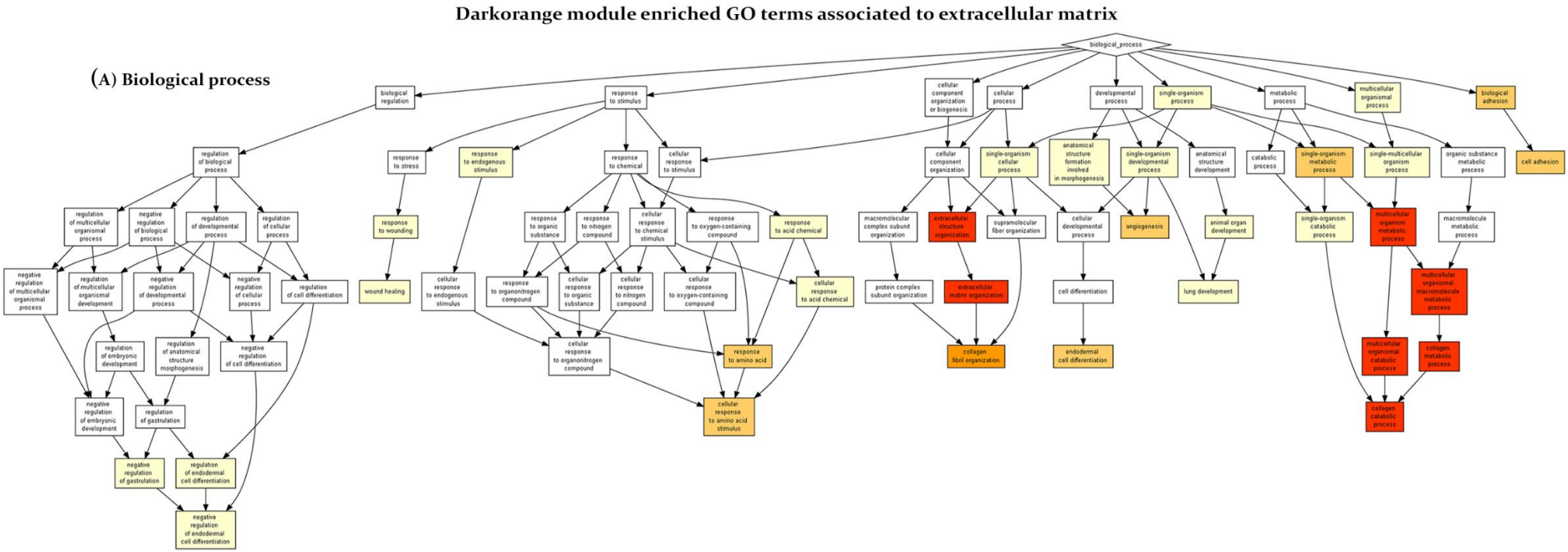

Source: Pulz, L. H. (2019)

(B) Cellular component

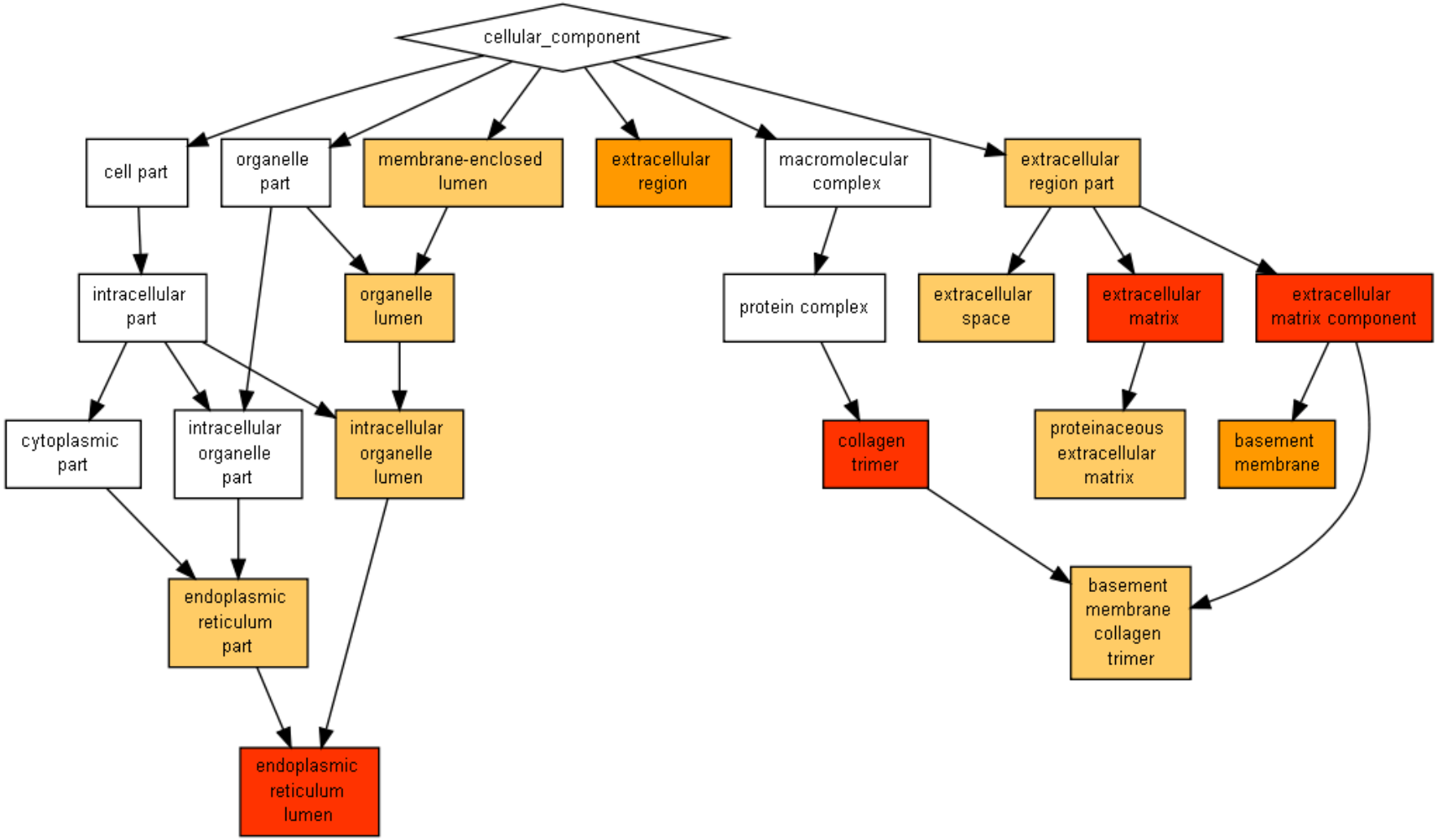

Source: Pulz, L. H. (2019)

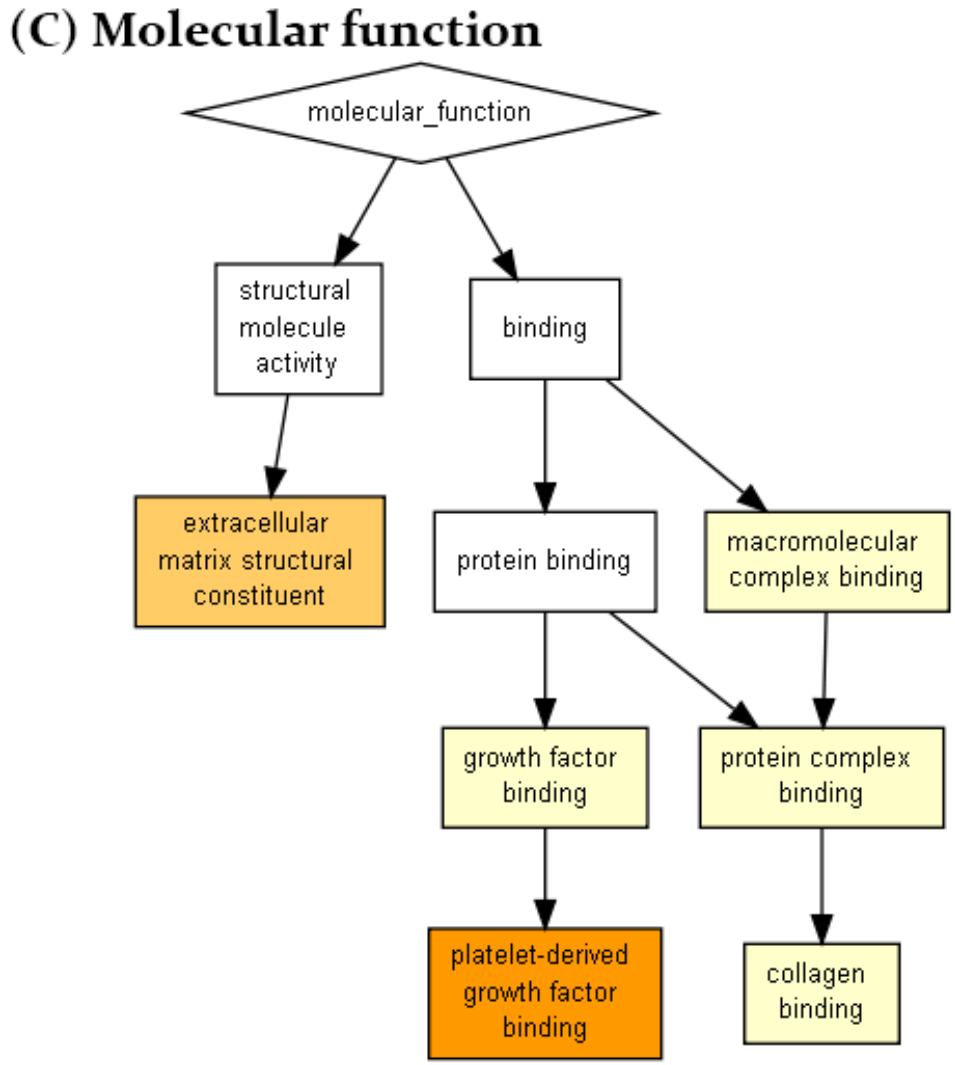

Source: Pulz, L. H. (2019)

2.3.8 Biological validation of significant modules

Since the *Darkorange2* module expression profile yielded robust results related to cell proliferation, we proceeded to analyse the Ki67 indices of another set of 44 MCT samples (Table S6 – Appendix F). Comparison of Ki67 indices between low-risk MCTs (samples 01–22, mean = 4.16% ± 0.03%) and high-risk (samples 23–44; mean = 8.91% ± 0.05%) revealed that the percentage of proliferating cells was significantly higher in high-risk MCTs (P = 0.0044) (Graphic S1 – Appendix G).

Since the 'extracellular matrix module' (*Darkorange* module) was significantly associated with high-risk MCTs, we further analysed samples to detect the presence of fibroblasts, one of the main components of the stroma that influences the ECM. Fibroblasts within the tumour stroma with a modified phenotype are termed 'cancer-associated fibroblasts' (CAFs) and are mostly defined based on the expression of markers such as α-smooth-muscle actin (αSMA). Immunohistochemical analyses to identify and quantify CAFs in 44 canine MCT samples revealed diffuse cytoplasmic immunostaining patterns in fibroblasts (Graphic 1).

Figure 5. Photomicrographs showing positive immunostaining for α-smooth-muscle actin (αSMA) in canine mast cell tumours (MCTs). (A) Evident stromal fibroblasts immunoexpression (400x magnification). (B) Immunostaining with anti-αSMA antibodies specifically stains the cytoplasm of cancer-associated fibroblasts (CAFs) (1000x magnification). All sections were counterstained with Harris's haematoxylin

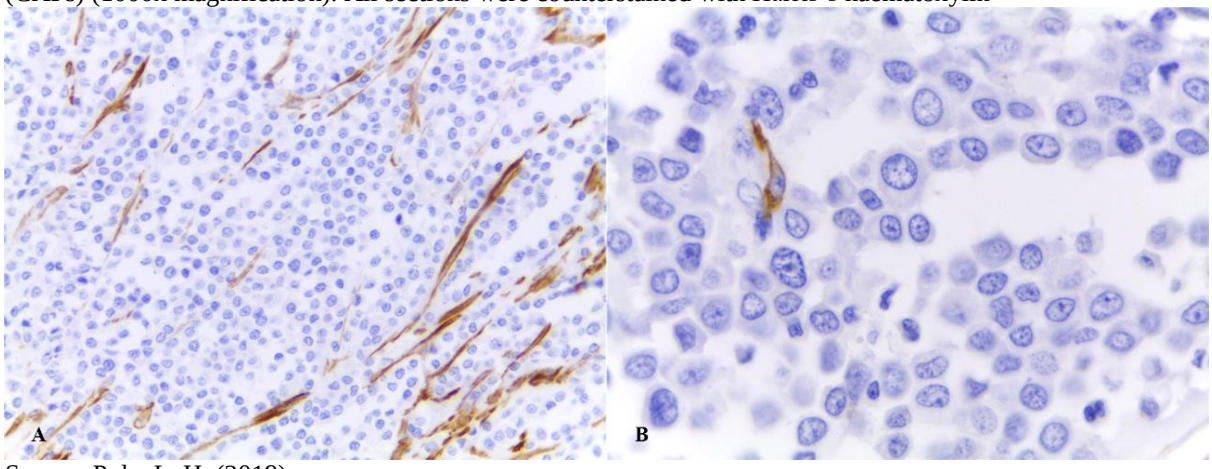

Source: Pulz, L. H. (2019)

Graphic 1. Number of cancer-associated fibroblasts (CAFs) in mast cell tumour (MCT) stroma of low-risk vs. high-risk canine MCTs. The number of CAFs in high-risk tumours (P = 0.0021, Mann-Whitney U test) was significantly higher than in low-risk tumours

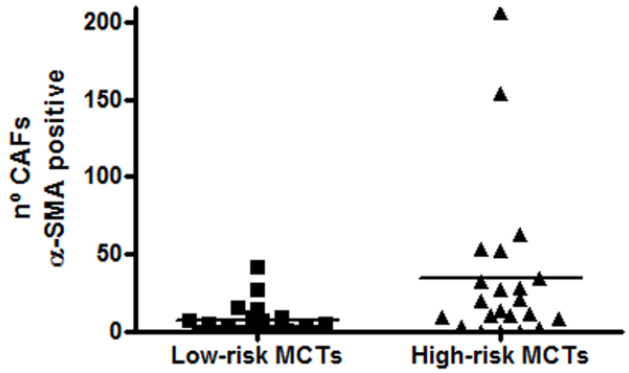

Source: Pulz, L. H. (2019)

2.4 DISCUSSION

In this study, we aimed to identify the mechanisms involved in MCT progression using a transcriptomic approach. Our integrative approach, involving datasets on global gene expression profiles, co-expression analyses, functional enrichment analyses, and validation by immunohistochemistry, revealed that high-risk MCTs are associated with genes that promote increased cellular proliferation and stimuli from the tumour stroma.

First, in a typical genome-wide expression analysis experiment, we used mRNA expression profiles to generate a large number of genes ordered in a ranked list, according to their DE in the high-risk and low-risk MCT groups. The challenge with these data was to extract biological meaning from the list obtained, since single-gene analyses may miss important roles played by whole pathways (SUBRAMANIAN et al., 2005). Alternatively, we performed co-expression analyses to examine our data at the level of gene sets to obtain information on significant pathways or on ontology.

Since we used proliferation index as a criterion for categorising MCT samples into high- and low-risk groups, our bioinformatics analyses show that a significant number of genes involved in providing proliferation stimuli are upregulated in high-risk MCTs. This result suggests that the molecular pathways identified in our study are biologically relevant to the phenotypes observed. Our results partially corroborate those obtained by Giantin et al. (2014), who demonstrated that a different set of up-regulated genes in undifferentiated MCTs are involved in pathways regulating mitosis. More importantly, these results also confirm earlier

results that demonstrate the importance of the Ki67 index as a prognostic indicator for MCT, independent of the histopathological grade of the disease (ABADIE, AMARDEILH, DELVERDIER 1999; STREFEZZI et al., 2010) and that dogs with high scores of Ki67 expression have shorter survival times (SCASE et al., 2006; WEBSTER et al., 2007).

However, the key finding of our study was obtained from the functional enrichment analyses of transcriptomic networks involving the ECM. We must consider that RNA is extracted from the whole MCT tissue. In addition to simply anchoring cells, it is now known that the ECM is an active and complex tissue component (DVORAK, 1986; ALBERTS et al., 2002). Since fibroblasts are the most abundant cells in connective tissues and are intimately linked to the ECM, both as builders and residents, the modulatory properties of the local ECM are most apparent in fibroblast functions (SCHULTZ et al., 2009).

GO terms associated with the ECM were the most over-represented in the *Darkorange* module, and their expression levels were also positively correlated with malignancy scores. Thus, this module appears to integrate multiple ECM signatures and is likely to play an important role in the progression of MCTs. The *Darkorange* module contains 10 over-expressed collagen genes (S2D Table); as of now, it is not possible to dissociate the role of these molecules from those of the fibroblasts' matrix microenvironment. In addition, the *Darkorange* module also includes the mRNAs of Lysyl oxidase (LOX) and lysyl oxidase-like-2 (LOXL2), which are matrix enzymes that promote cross-linking of fibrillar collagen and are synthesised by fibroblasts (KAGAN, 2003). Stromal LOX expression has been implicated in the development of the metastatic niche (ERLER et al., 2006) and LOXL2 expression is also thought to play a role in promoting invasion (AKIRI et al., 2003; FONG et al., 2007; PAYNE, HENDRIX, KIRSCHMANN, 2007; HOLLOSI et al., 2009; KIRSCHMANN et al., 2009).

Interestingly, another gene that is included in the *"*extracellular matrix module*"* is the platelet derived growth factor receptor-α (PDGFRA), a tyrosine-kinase receptor. Notably, PDGFRA expression on the cell surface is restricted to the stromal compartment in skin and tumour cells (EREZ et al., 2010) and the molecule is reportedly expressed by up to 90% of stromal fibroblasts in solid tumours (MICKE, OSTMAN, 2004). Local fibroblasts or fibroblast precursors stimulated by members of the PDGF or transforming growth factor beta (TGF-β) family have generally been considered to be the major source of CAFs (KALLURI; ZEISBERG, 2006). These cells within the tumour stroma contribute structurally and functionally to the progression, growth, and spread of cancers (BARSKY et al., 1984; DURNIN, SCHOR, 1984; SCHOR et al., 1988; KALLURI, ZEISBERG, 2006;). CAFs in the tumour stroma acquire a modified phenotype, similar to wound healing fibroblasts, and are also

known as myofibroblasts, reactive stromal fibroblasts, tumour-associated fibroblasts, or activated fibroblasts (BARSKY et al., 1984; MUELLER, FUSENIG, 2004; KALLURI; ZEISBERG, 2006;). Several studies highlight αSMA as an important marker for these cells (TSUKADA et al., 1987; RONNOV-JESSEN, PETERSEN, BISSELL, 1996; GABBIANI, 2003).

Based on these findings, we hypothesised that high-risk tumours have an altered microenvironment influenced by CAFs. To confirm this possibility, we demonstrated by immunohistochemistry, that high-risk MCTs have higher number of CAFs in their stroma than low-risk MCTs. The importance of this subpopulation of cells in the tumour microenvironment is emphasised when taken in conjunction with the results of functional enrichment analysis of the *Darkorange* module for angiogenesis. CAFs have been shown to support tumorigenesis by stimulating angiogenesis, cancer cell proliferation, and invasion (ALLINEN et al., 2004; BHOWMICK, NEILSON, MOSES, 2004; ORIMO et al., 2005; EREZ et al., 2010).

In accordance with our results, several studies have demonstrated that higher expression levels of αSMA in tumour stromal fibroblasts is an independent prognostic marker for several human cancer types (TSUJINO et al., 2007; ERKAN et al., 2008; Yamashita et al., 2012) and animal neoplasms (KLOBUKOWSKA, MUNDAY, 2016). In addition, it is interesting to note that there is an association between LOXL2 protein expression and α-SMA-positive stromal fibroblasts in diverse types of solid tumours and that LOXL2 inhibition was efficacious in inhibiting cancer growth in both primary and metastatic xenograft models (BARRY-HAMILTON et al., 2010).

2.5 CONCLUSIONS

In summary, our study indicates a set of specific genes in MCT samples that have different expression levels in high-risk and low-risk groups. An integrative analytic approach revealed that these genes are related to cellular proliferation and ECM components, mainly from stromal CAFs. While our study provides some insight into the emergent properties of CAFs, more efforts are required to validate and extend our findings.

Availability of data and material

The datasets supporting the conclusions of this article are included within the article and its additional files. The data sets supporting the results of this article are available in the ArrayExpress database (https://www.ncbi.nlm.nih.gov/assembly/GCF_000002285.3/).

2.6 REFERENCES

ABADIE, J. J.; AMARDEILH, M. A.; DELVERDIER, M. E. Immunohistochemical detection of proliferating cell nuclear antigen and Ki-67 in mast cell tumors from dogs. **Journal of the American Veterinary Medical Association**, v. 215, n. 11, p. 1629-1634, 1999.

AKIRI, G.; SABO, E.; DAFNI, H.; VADASZ, Z.; KARTVELISHVILY, Y.; GAN, N.; KESSLER, O.; COHEN, T.; RESNICK, M.; NEEMAN, M.; NEUFELD, G. Lysyl oxidase-related protein-1 promotes tumor fibrosis and tumor progression in vivo. **Cancer Research**, v. 63, n. 7, p. 1657-1666, 2003.

ALBERTS, J.; JOHNSON, B.; LEWIS, A. et al. The Extracellular Matrix of Animals. In: ALBERTS, B.; JOHNSON, A.; LEWIS, J.; RAFF, M.; ROBERTS, K.; WALTER, P. **Molecular Biology of the Cell**. 4th edition. New York: Garland Science; 2002; Bookshelf ID: NBK26810.

ALLINEN, M.; BEROUKHIM, R.; CAI, L.; BRENNAN, C.; LAHTI-DOMENICI, J.; HUANG, H.; PORTER, D.; HU, M.; CHIN, L.; RICHARDSON, A.; SCHNITT, S.; SELLERS, W. R.; POLYAK, K. Molecular characterization of the tumor microenvironment in breast cancer. **Cancer Cell**, v. 6, n. 1, p. 17-32, 2004.

ANDERS, S.; PYL, P. T.; HUBER, W. HTSeq—a Python framework to work with high-throughput sequencing data. **Bioinformatics**, v. 31, n. 2, p. 166-169, 2015.

BARRY-HAMILTON, V.; SPANGLER, R.; MARSHALL, D.; MCCAULEY, S.; RODRIGUEZ, H. M.; OYASU, M. et al. Allosteric inhibition of lysyl oxidase–like-2 impedes the development of a pathologic microenvironment. **Nature Medicine**, v. 16, n. 9, p. 1009, 2010.

BARSKY, S. H.; GREEN, W. R.; GROTENDORST, G. R.; LIOTTA, L. A. Desmoplastic breast carcinoma as a source of human myofibroblasts. **The American Journal of Pathology**, v. 115, n. 3, p. 329, 1984.

BHOWMICK, N. A.; NEILSON, E. G.; MOSES, H. L. Stromal fibroblasts in cancer initiation and progression. **Nature**, v. 432, n. 7015, p. 332, 2004.

BLACKWOOD, L.; MURPHY, S.; BURACCO, P.; DE VOS, J. P.; DE FORNEL-THIBAUD, P.; HIRSCHBERGER J. et al. European consensus document on mast cell tumours in dogs and cats. **Veterinary and Comparative Oncology**, v. 10, n. 3, p. e1-e29, 2012.

BOERKAMP, K. M.; VAN DER KOOIJ, M.; VAN STEENBEEK, F. G.; VAN WOLFEREN, M. E.; GROOT KOERKAMP, M. J. A.; VAN LEENEN, D. et al. Gene expression profiling of histiocytic sarcomas in a canine model: the predisposed flatcoated retriever dog. **PLoS One**, v. 8, n. 8, p. e71094, 2013.

BOSTOCK, D. E. Neoplasms of the skin and subcutaneous tissues in dogs and cats. **British Veterinary Journal**, v. 142, n. 1, p. 1-19, 1986.

COHEN, D.; REIF J. S.; BRODEY R. S.; KEISER H. Epidemiological analysis of the most prevalent sites and types of canine neoplasia observed in a veterinary hospital. **Cancer Research**, v. 34, n. 11, p. 2859-2868, 1974.

DURNING, P.; SCHOR, S. L. Fibroblasts from patients with breast cancer show abnormal migratory behaviour in vitro. **The Lancet**, v. 324, n. 8408, p. 890-892, 1984.

DVORAK, H. F. Tumors: wounds that do not heal. Similarities between tumor stroma generation and wound healing. New England Journal of Medicine. V. 315, p. 1650–59, 1986.

EREZ, N.; TRUITT, M.; OLSON, P.; HANAHAN, D. Cancer-associated fibroblasts are activated in incipient neoplasia to orchestrate tumor-promoting inflammation in an NF-κB-dependent manner. **Cancer Cell**, v. 17, n. 2, p. 135-147, 2010.

ERKAN, M.; MICHALSKI, C. W.; RIEDER, S.; REISER-ERKAN, C.; ABIATARI, I.; KOLB, A.; GIESE, N. A.; ESPOSITO, I.; FRIESS, H.; KLEEF, J. The activated stroma index is a novel and independent prognostic marker in pancreatic ductal adenocarcinoma. **Clinical Gastroenterology and Hepatology**, v. 6, n. 10, p. 1155-1161, 2008.

ERLER, J. T.; BENNEWITH, K. L.; NICOLAU, M.; DORNHÖFER, N.; KONG, C.; LE, Q. T.; CHI, J. T.; JEFFREY, S. S.; GIACCIA, A. J. Lysyl oxidase is essential for hypoxia-induced metastasis. **Nature.** v. 27, n.440 (7088), p. 1222-6, 2006

FINNIE, J. W.; BOSTOCK, D. E. Skin neoplasia in dogs. **Australian Veterinary Journal**, v. 55, n. 12, p. 602-604, 1979.

FONG, S. F.; DIETZSCH, E.; FONG, K. S.; HOLLOSI, P.; ASUNCION, L.; HE, Q.; PARKER, M. I.; CSISZAR, K. Lysyl oxidase-like 2 expression is increased in colon and esophageal tumors and associated with less differentiated colon tumors. **Genes, Chromosomes and Cancer**, v. 46, n. 7, p. 644-655, 2007.

FOWLES, J. S.; DENTON, C. L.; GUSTAFSON, D. L. Comparative analysis of MAPK and PI3K/AKT pathway activation and inhibition in human and canine melanoma. **Veterinary and Comparative Oncology**, v. 13, n. 3, p. 288-304, 2015.

FRANTZ, A. M.; SARVER, A. L.; ITO, D.; PHANG, T. L.; KARIMPOUR-FARD, A.; SCOTT, M. C. et al. Molecular profiling reveals prognostically significant subtypes of canine lymphoma. **Veterinary Pathology**, v. 50, n. 4, p. 693-703, 2013.

FREIJE, W. A.; CASTRO-VARGAS, F. E.; FANG, Z.; HORVATH, S.; CLOUGHESY, T.; LIAU, L. M.; MISCHEL, O. S.; NELSON, S. F. Gene expression profiling of gliomas strongly predicts survival. **Cancer Research**, v. 64, n. 18, p. 6503-6510, 2004.

GABBIANI G. The myofibroblast in wound healing and fibrocontractive diseases. **The Journal of Pathology: A Journal of the Pathological Society of Great Britain and Ireland**, v. 200, n. 4, p. 500-503, 2003.

GIANTIN, M.; GRANATO, A.; BARATTO, C.; MARCONATO, L.; VASCELLARI, M.; MORELLO, E. M.; VERCELLI, A.; MUTINELLI, F.; DACASTO, M. Global gene expression analysis of canine cutaneous mast cell tumor: could molecular profiling be useful for subtype classification and prognostication?. **PloS One**, v. 9, n. 4, p. e95481, 2014.

GIANTIN, M.; BARATTO, C.; MARCONATO, L.; VASCELLARI, M.; MUTINELLI, F.; DACASTO, M. et al. Transcriptomic analysis identified up-regulation of a solute carrier transporter and UDP glucuronosyltransferases in dogs with aggressive cutaneous mast cell tumours. **The Veterinary Journal**, v. 212, p. 36-43, 2016.

GORDEN, B. H.; KIM, J. H.; SARVER, A. L.; FRANTZ, A. M.; BREEN, M.; LINDBLAD-TOH, K. et al. Identification of three molecular and functional subtypes in canine hemangiosarcoma through gene expression profiling and progenitor cell characterization. **The American Journal of Pathology**, v. 184, n. 4, p. 985-995, 2014.

HOLLOSI, P.; YAKUSHIJI, J. K.; FONG, K. S.; CSISZAR, K.; FONG, S. F. Lysyl oxidase-like 2 promotes migration in noninvasive breast cancer cells but not in normal breast epithelial cells. **International Journal of Cancer**, v. 125, n. 2, p. 318-327, 2009.

HOTTENDORF, G. H.; NIELSEN, S. W. Pathologic report of 29 necropsies on dogs with mastocytoma. **Pathologia Veterinaria**, v. 5, n. 2, p. 102-121, 1968.

KAGAN, H. M.; LI, W. Lysyl oxidase: properties, specificity, and biological roles inside and outside of the cell. **Journal of Cellular Biochemistry**, v. 88, n. 4, p. 660-672, 2003.

KALLURI, R.; ZEISBERG M. Fibroblasts in cancer. **Nature Reviews Cancer**, v. 6, n. 5, p. 392, 2006.

KIRSCHMANN, D. A.; SEFTOR, E. A.; FONG, S. F.; NIEVA, D. R. C.; SULLIVAN, C. M.; EDWARDS, E. M.; SOMMER, P.; CSISZAR, K.; HENDRIX, M. J. C. A molecular role for lysyl oxidase in breast cancer invasion. **Cancer Research**, v. 62, n. 15, p. 4478-4483, 2002.

KIUPEL, M.; WEBSTER, J. D.; BAILEY, K. L.; BEST, S.; DELAY, J.; DETRISAC, C. J. et al. Proposal of a 2-tier histologic grading system for canine cutaneous mast cell tumors to more accurately predict biological behavior. **Veterinary pathology**, v. 48, n. 1, p. 147-155, 2011.

KLOBUKOWSKA, H. J.; MUNDAY, J. S. High numbers of stromal cancer-associated fibroblasts are associated with a shorter survival time in cats with oral squamous cell carcinoma. **Veterinary Pathology**, v. 53, n. 6, p. 1124-1130, 2016.

KLOPFLEISCH, R.; LENZE, D.; HUMMEL, M.; GRUBER A. D. Metastatic canine mammary carcinomas can be identified by a gene expression profile that partly overlaps with human breast cancer profiles. **BMC Cancer**, v. 10, n. 1, p. 618, 2010.

KLOPFLEISCH, R.; VON EULER, H.; SARLI, G.; PINHO, S. S.; GÄRTNER, F.; GRUBER, A. D. Molecular carcinogenesis of canine mammary tumors: news from an old disease. **Veterinary Pathology**, v. 48, n. 1, p. 98-116, 2011.

LANGFELDER, P.; ZHANG, B.; HORVATH, S. Defining clusters from a hierarchical cluster tree: the Dynamic Tree Cut package for R. **Bioinformatics**, v. 24, n. 5, p. 719-720, 2007.

LANGFELDER, P.; HORVATH, S. WGCNA: an R package for weighted correlation network analysis. **BMC Bioinformatics**, v. 9, n. 1, p. 559, 2008.

LI, H.; HANDSAKER, B.; WYSOKER, A.; FENNELL, T.; RUAN, J.; HOMER, N.; ABECASIS, G.; DURBIN, R. The sequence alignment/map format and SAMtools. **Bioinformatics**, v. 25, n. 16, p. 2078-2079, 2009.

LIU, D.; XIONG, H.; ELLIS, A. E.; NORTHRUP, N. C.; RODRIGUEZ, C. O.; O'REGAN, R. M. et al. Molecular homology and difference between spontaneous canine mammary cancer and human breast cancer. **Cancer Research**, 2014.

LIU, D.; XIONG, H.; ELLIS, A. E.; NORTHRUP, N. C.; DOBBIN, K. K.; SHIN, D. M. et al. Canine spontaneous head and neck squamous cell carcinomas represent their human counterparts at the molecular level. **PLoS Genetics**, v. 11, n. 6, p. e1005277, 2015.

LONDON, C. A.; SEGUIN, B. Mast cell tumors in the dog. **The Veterinary clinics of North America. Small animal practice**, v. 33, n. 3, p. 473-89, v, 2003.
MICKE, P.; OSTMAN, A. Tumour-stroma interaction: cancer-associated fibroblasts as novel targets in anti-cancer therapy?. **Lung Cancer**, v. 45, p. S163-S175, 2004.

MISCHEL, P. S.; NELSON, S. F.; CLOUGHESY, T. F. Molecular analysis of glioblastoma: pathway profiling and its implications for patient therapy. **Cancer Biology & Therapy**, v. 2, n. 3, p. 242-247, 2003.

MOONEY, M.; BOND, J.; MONKS, N.; EUGSTER, E.; CHERBA, D.; BERLINSKI, P. et al. Comparative RNA-Seq and microarray analysis of gene expression changes in B-cell lymphomas of Canis familiaris. **PloS One**, v. 8, n. 4, p. e61088, 2013.

MUDALIAR, M. A. V.; HAGGART, R. D.; MIELE, G.; SELLAR, G.; TAN, K. A. L.; GOODLAD, J. R. et al. Comparative gene expression profiling identifies common molecular signatures of NF-κB activation in canine and human diffuse large B cell lymphoma (DLBCL). **PloS One**, v. 8, n. 9, p. e72591, 2013.

MUELLER, M. M.; FUSENIG, N. E. Friends or foes—bipolar effects of the tumour stroma in cancer. **Nature Reviews Cancer**, v. 4, n. 11, p. 839, 2004.

O'DONOGHUE, L. E.; PTITSYN, A A.; KAMSTOCK, D. A.; SIEBERT, J.; THOMAS, R. S.; DUVAL, D. L. Expression profiling in canine osteosarcoma: identification of biomarkers and pathways associated with outcome. **BMC Cancer**, v. 10, n. 1, p. 506, 2010.

ORIMO, A.; GUPTA, P. B.; SGROI, D. C.; ARENZANA-SEISDEDOS, F.; DELAUNAY, T.; NAEEM, R.; CAREY, V. J.; RICHARDSON, A. L.; WEINBERG, R. A. Stromal fibroblasts present in invasive human breast carcinomas promote tumor growth and angiogenesis through elevated SDF-1/CXCL12 secretion. **Cell**, v. 121, n. 3, p. 335-348, 2005.

OZSOLAK, F.; MILOS, P. M. RNA sequencing: advances, challenges and opportunities. **Nature Reviews Genetics**, v. 12, n. 2, p. 87, 2011.

PANG, L. Y.; GATENBY, E. L.; KAMIDA, A.; WHITELAW, B. A.; HUPP, T. R.; ARGYLE, D. J. Global gene expression analysis of canine osteosarcoma stem cells reveals a novel role for COX-2 in tumour initiation. **PLoS One**, v. 9, n. 1, p. e83144, 2014.

PATNAIK, A. K., EHLER, W. J., MACEWEN, E. G. Canine cutaneous mast cell tumor: morphologic grading and survival time in 83 dogs. **Veterinary pathology**, v. 21, n. 5, p. 469-474, 1984.

PAYNE, S. L.; HENDRIX, M. J.; KIRSCHMANN, D. A. Paradoxical roles for lysyl oxidases in cancer—a prospect. **Journal of Cellular Biochemistry**, v. 101, n. 6, p. 1338-1354, 2007.

PENG, L.; RAN, Y. L.; HU, H.; YU, L.; LIU, Q.; ZHOU, Z.; SUN, Y. M.; SUN, L. C.; PAN, J.; SUN, L. X.; ZHAO, P.; YANG, Z. H. Secreted LOXL2 is a novel therapeutic target that promotes gastric cancer metastasis via the Src/FAK pathway. **Carcinogenesis**, v. 30, n. 10, p. 1660-1669, 2009.

PRIESTER, W. A. Skin tumors in domestic animals. Data from 12 United States and Canadian colleges of veterinary medicine. **Journal of the National Cancer Institute**, v. 50, n. 2, p. 457-466, 1973.

PULZ, L. H.; BARRA, C. N.; KLEEB, S. R.; XAVIER, J. G.; CATÃO-DIAS, J. L.; SOBRAL, R. A.; FUKUMASU, H.; STREFEZZI, R. F. Increased expression of Tissue Inhibitor of Metalloproteinase-1 correlates with improved outcome in canine cutaneous mast cell tumours. **Veterinary And Comparative Oncology**, v. 15, n. 2, p. 606-614, 2017.

RAMSEY, S. A.; XU, T.; GOODALL, C.; RHODES, A. C.; KASHYAP, A.; HE, J. et al. Cross-species analysis of the canine and human bladder cancer transcriptome and exome. **Genes, Chromosomes and Cancer**, v. 56, n. 4, p. 328-343, 2017.

ROBINSON, M. D.; MCCARTHY, D. J.; SMYTH, G. K. edgeR: a Bioconductor package for differential expression analysis of digital gene expression data. **Bioinformatics**, v. 26, n. 1, p. 139-140, 2010.

RONNOV-JESSEN, L.; PETERSEN, O. W.; BISSELL, M. J. Cellular changes involved in conversion of normal to malignant breast: importance of the stromal reaction. **Physiological reviews**, v. 76, n. 1, p. 69-125, 1996.

SABATTINI, S.; SCARPA, F.; BERLATO, D.; BETTINI, G. Histologic grading of canine mast cell tumor: is 2 better than 3?. **Veterinary Pathology**, v. 52, n. 1, p. 70-73, 2015.

SCASE, T. J.; EDWARDS, D.; MILLER, J.; HENLEY, W.; SMITH, K.; BLUNDEN, A. et al. Canine mast cell tumors: correlation of apoptosis and proliferation markers with prognosis. **Journal of Veterinary Internal Medicine**, v. 20, n. 1, p. 151-158, 2006.

SCHOR, S. L.; SCHOR, A. M.; GREY, A. M.; RUSHTON, G. Foetal and cancer patient fibroblasts produce an autocrine migration-stimulating factor not made by normal adult cells**. Journal of Cell Science**, v. 90, n. 3, p. 391-399, 1988.

SCHULTZ, G. S.; WYSOCKI, A. Interactions between extracellular matrix and growth factors in wound healing. **Wound Repair and Regeneration**, v. 17, n. 2, p. 153-162, 2009.

SELVARAJAH, G. T.; KIRPENSTEIJN, J.; VAN WOLFEREN, M. E.; RAO, N. A. S.; FIETEN, H.; MOL, J. A.Gene expression profiling of canine osteosarcoma reveals genes associated with short and long survival times. **Molecular Cancer**, v. 8, n. 1, p. 72, 2009.

SHOOP, S. J.; MARLOW, S.; CHURCH, D. B.; ENGLISH, K.; MCGREEVY, P. D.; STELL, A. J. et al. Prevalence and risk factors for mast cell tumours in dogs in England. **Canine Genetics and Epidemiology**, v. 2,

n. 1, p. 1, 2015.

STREFEZZI, R. D. F.; KLEEB, S. R.; XAVIER, J. G.; DIAS, J. L. C. Avaliação da proliferação celular como indicador prognóstico para mastocitomas cutâneos caninos. **Pesquisa Veterinária Brasileira**, v. 30, n. 7, p. 559-565, 2010.

SUBRAMANIAN, A.; TAMAYO, P.; MOOTHA, V. K.; MUKHERJEE, S.; EBERT, B. L.; GILLETTE, M. A.; PAULOVICH, A.; POMEROY, S. L.; GOLUB, T. R.; LANDER, E. S.; MESIROV, J. P. Gene set enrichment analysis: a knowledge-based approach for interpreting genome-wide expression profiles. **Proceedings of the National Academy of Sciences**, v. 102, n. 43, p. 15545-15550, 2005.

TAMBURINI, B. A.; PHANG, T. L.; FOSMIRE, S. P.; SCOTT, M. C.; TRAPP, S. C.; DUCKETT, M. M. et al. Gene expression profiling identifies inflammation and angiogenesis as distinguishing features of canine hemangiosarcoma. **BMC Cancer**, v. 10, n. 1, p. 619, 2010.

THOMAS, R.; BORST, L.; ROTROFF, D.; MOTSINGER-REIF, A.; LINDBLAD-TOH, K.; MODIANO, J. F. et al. Genomic profiling reveals extensive heterogeneity in somatic DNA copy number aberrations of canine hemangiosarcoma. **Chromosome Research**, v. 22, n. 3, p. 305-319, 2014.

TSUJINO, T.; SESHIMO, I.; YAMAMOTO, H.; NGAN, C. Y.; EZUMI, K.; TAKEMASA, I.; IKEDA, M.; SEKIMOTO, M.; MATSUURA, N.; MONDEN, M. Stromal myofibroblasts predict disease recurrence for colorectal cancer. **Clinical Cancer Research**, v. 13, n. 7, p. 2082-2090, 2007.

TSUKADA, T.; MCNUTT, M. A.; ROSS, R.; GOWN, A. M. HHF35, a muscle actin-specific monoclonal antibody. II. Reactivity in normal, reactive, and neoplastic human tissues. **The American Journal of Pathology**, v. 127, n. 2, p. 389, 1987.

UVA, P.; AURISICCHIO, L.; WATTERS, J.; LOBODA, A.; KULKARNI, A.; CASTLE J. et al. Comparative expression pathway analysis of human and canine mammary tumors. **BMC Genomics**, v. 10, n. 1, p. 135, 2009
.
VASCELLARI, M.; GIANTIN, M.; CAPELLO, K.; CARMINATO, A.; MORELLO, E. M.; VERCELLI, A. et al. Expression of Ki67, BCL-2, and COX-2 in canine cutaneous mast cell tumors: association with grading and prognosis. **Veterinary Pathology**, v. 50, n. 1, p. 110-121, 2013.

WEBSTER, J. D.; YUZBASIYAN-GURKAN, V.; KANEENE, J. B.; MILLER, R.; RESAU, J. H.; KIUPEL, M. The role of c-KIT in tumorigenesis: evaluation in canine cutaneous mast cell tumors. **Neoplasia**, v. 8, n. 2, p. 104-111, 2006.

WEBSTER, J. D.; YUZBASIYAN-GURKAN, V.; MILLER, R. A.; KANEENE, J. B.; KIUPEL, M. Cellular proliferation in canine cutaneous mast cell tumors: associations with c-KIT and its role in prognostication. **Veterinary Pathology**, v. 44, n. 3, p. 298-308, 2007.

WELLE, M. M.; BLEY, C. R.; HOWARD, J.; RÜFENACHT, S. Canine mast cell tumours: a review of the pathogenesis, clinical features, pathology and treatment. **Veterinary Dermatology**, v. 19, n. 6, p. 321-339, 2008.

YAMASHITA, M.; OGAWA, T.; ZHANG, X.; HANAMURA, N.; KASHIKURA, Y.; TAKAMURA, M.; YONEDA, M.; SHIRAISHI, T. Role of stromal myofibroblasts in invasive breast cancer: stromal expression of alpha-smooth muscle actin correlates with worse clinical outcome. **Breast Cancer**, v. 19, n. 2, p. 170-176, 2012.

ZHANG, B.; HORVATH, S. A general framework for weighted gene co-expression network analysis. **Statistical Applications in Genetics and Molecular Biology**, v. 4, n. 1, 2005.

APPENDICES

APPENDIX A – Supporting information: RNA-seq data

S1 Table. RNA-seq data**.** RNA-seq data analyses with the description of each lesion detailing the percentages of alignment to the dog reference genome

Samples	**PE *reads* sequenced**	**Pairs Aligned**	**% Alignment**	**Multiple alignments**	**% Multiple alignments**	**Discordant alignments**	**% Discordant alignments**	**% Concordant alignments**
S01	29190352	22914898	80.5	2829154	12.3	441541	1.9	77.0
S02	27666655	21618809	80.2	2890863	13.4	395265	1.8	76.7
S03	30672031	23212150	77.7	2732208	11.8	340275	1.5	74.6
S04	28642711	22381680	81.8	2351917	10.5	533191	2.4	76.3
S05	29264458	24663416	86.4	2207626	9.0	497104	2.0	82.6
S06	32305518	24637223	78.1	4861085	19.7	483150	2.0	74.8
S07	28226076	23485552	85.3	2991151	12.7	589289	2.5	81.1
S08	29706470	23740961	82.3	3542897	14.9	560530	2.4	78.0
S09	28799480	23616367	84.2	2359155	10.0	549727	2.3	80.1
S10	25683836	21163186	84.7	2146377	10.1	563797	2.7	80.2
S11	29340694	23210833	81.4	2522283	10.9	596017	2.6	77.1
S12	26148434	21603608	85.0	1988881	9.2	584255	2.7	80.4
S13	28758356	23669181	84.8	2388535	10.1	806580	3.4	79.5
S14	22885802	19213272	86.4	1936646	10.1	525150	2.7	81.7
S15	31081917	25783024	85.1	2458563	9.5	551114	2.1	81.2
Mean	28404278	22973137	83.3	2560321	11.1	538073	2.4	79.1

APPENDIX B – Supporting information: S2A Table. Gene co-expression networks.

S2A Table. Genes in Palevioletred3 module

Ensembl ID	Gene Name	GS score	GS score P-value	MM	MM P-value	Kw
ENSCAFG00000000017	ZNF236	-0.411538592	0.12748843	0.946902447	8.93E-08	8.578074485
ENSCAFG00000000241	HNRNPAB	0.490464529	0.063424926	-0.794954446	0.000397216	1.539756768
ENSCAFG00000001785	-	-0.320132778	0.244731509	0.963607429	7.98E-09	10.24431597
ENSCAFG00000002667	-	0.485779659	0.066384323	-0.84580201	7.10E-05	2.774338312
ENSCAFG00000004698	ABCB8	-0.440744026	0.100100462	0.954177256	3.49E-08	9.492674052
ENSCAFG00000005415	ARRB1	-0.727392872	0.002117531	0.720340231	0.002453291	1.077207718
ENSCAFG00000005436	-	0.182285646	0.515547018	-0.892977297	7.44E-06	5.881385996
ENSCAFG00000005877	ALYREF	0.342926125	0.21082595	-0.920374479	1.17E-06	6.933803553
ENSCAFG00000006203	FCHSD1	-0.313798478	0.25471679	0.906150193	3.27E-06	6.482429028
ENSCAFG00000006878	KMT2B	0.272432217	0.325933009	-0.912899426	2.05E-06	6.967672054
ENSCAFG00000007160	ZC3H6	-0.379683094	0.162754599	0.91976599	1.22E-06	6.718610654
ENSCAFG00000007555	PDCD5	0.63844636	0.010420783	-0.819152625	0.00018691	2.445117824
ENSCAFG00000007664	ZBTB38	-0.320496553	0.244165504	0.93407844	3.53E-07	8.34302219
ENSCAFG00000008700	FNIP2	-0.506637889	0.053941936	0.9023265	4.20E-06	5.785796136
ENSCAFG00000009699	CHD9	-0.275619181	0.320078486	0.913915628	1.90E-06	7.56138908
ENSCAFG00000010340	PHC2	0.430949734	0.108776981	-0.887655058	1.01E-05	4.370595985
ENSCAFG00000010572	U2AF1L5	0.450690652	0.091797082	-0.947736615	8.07E-08	8.703044568
ENSCAFG00000012027	YBEY	0.415073911	0.123927514	-0.901597394	4.41E-06	5.769769469
ENSCAFG00000012420	MTMR3	-0.382814224	0.159029785	0.913755917	1.93E-06	6.587271277
ENSCAFG00000012733	PFDN2	0.288304314	0.297380886	-0.893831547	7.08E-06	5.913503324
ENSCAFG00000012961	DCAF7	0.607701078	0.016256084	-0.864855202	3.16E-05	3.445049761
ENSCAFG00000014115	CCDC43	-0.354864106	0.194326586	0.879014931	1.59E-05	4.431829254
ENSCAFG00000014269	ATXN7L3	-0.143896378	0.60890605	0.912283644	2.14E-06	6.363775672
ENSCAFG00000014592	NBR1	-0.300754504	0.276050987	0.946128206	9.79E-08	9.363061149
ENSCAFG00000014816	CNOT9	0.420431064	0.11866246	-0.899939603	4.89E-06	4.712779864

ENSCAFG00000016025	SMARCE1	0.513662843	0.050164504	-0.872383734	2.22E-05	3.707333826
ENSCAFG00000016374	tcap	0.567409485	0.027377137	-0.865427441	3.08E-05	3.421208831
ENSCAFG00000016901	ALDH6A1	-0.370476815	0.174039552	0.950722031	5.55E-08	10.35572835
ENSCAFG00000016941	DAP3	0.516355018	0.048769758	-0.957673864	2.10E-08	9.606257799
ENSCAFG00000017626	FAXDC2	-0.63378811	0.011179527	0.877104384	1.76E-05	3.619000004
ENSCAFG00000018523	USP22	-0.376624983	0.166447907	0.953701682	3.72E-08	10.18467819
ENSCAFG00000018668	TMEM199	-0.424074133	0.115171302	0.807432624	0.000272771	2.074473088
ENSCAFG00000018701	-	0.496372576	0.059830753	-0.888077894	9.84E-06	4.435622431
ENSCAFG00000019101	VPS53	-0.393411822	0.146844956	0.956468649	2.51E-08	10.13917976
ENSCAFG00000019928	GSE1	-0.460824111	0.083849969	0.903841519	3.81E-06	5.630498662
ENSCAFG00000019939	ZDHHC7	-0.607868261	0.016218725	0.851859008	5.56E-05	2.764849319
ENSCAFG00000020037	TBC1D13	-0.34322423	0.210403451	0.935624147	3.04E-07	8.504716456
ENSCAFG00000020050	GLE1	-0.414862506	0.124138511	0.899343301	5.08E-06	5.066589298
ENSCAFG00000020072	-	-0.400256631	0.13931772	0.951376121	5.09E-08	9.241933712
ENSCAFG00000020335	PSKH1	-0.417012079	0.12200453	0.957900818	2.03E-08	9.728728867
ENSCAFG00000023406	-	-0.573236921	0.025487845	0.829595788	0.000130418	2.486518966
ENSCAFG00000030556	-	0.255040652	0.358945598	-0.92629241	7.16E-07	8.483552526
ENSCAFG00000031010	-	-0.231908765	0.405586012	0.915551486	1.69E-06	7.395730135

GS – gene significance; MM – module membership; Kw - Connectivity within the module; - Data no available

APPENDIX C – Supporting information: **S2B Table. Gene co-expression networks.**

S2B Table. Genes in Floralwhite module

Ensembl ID	Gene Name	GS score	GS score P-value	MM	MM P-value	Kw
ENSCAFG00000000261	RPA3	0.477789973	0.071659661	-0.932843551	3.97E-07	6.249545586
ENSCAFG00000000612	-	-0.130097573	0.643991055	0.813174509	0.000227388	2.655741527
ENSCAFG00000001442	MICALL1	-0.120749991	0.66816669	0.866448039	2.94E-05	4.125376612
ENSCAFG00000002305	LRRC1	-0.201083209	0.47237485	0.859490713	4.02E-05	3.338489376
ENSCAFG00000002533	SEC61B	0.20570714	0.46203157	-0.873936207	2.06E-05	4.132117283
ENSCAFG00000003105	ANKRD6	-0.2293039	0.411028847	0.806581015	0.000280092	2.119969315
ENSCAFG00000003751	CC2D1B	-0.621642626	0.013360814	0.866740657	2.90E-05	3.636058267
ENSCAFG00000003759	ZFYVE9	-0.254181382	0.360622871	0.917032576	1.51E-06	6.415206814
ENSCAFG00000004646	UROD	0.07154769	0.799969168	-0.802493662	0.000317505	2.312945279
ENSCAFG00000005139	JMJD6	0.333034968	0.225150524	-0.830002909	0.00012854	2.45818587
ENSCAFG00000005327	TGDS	0.267569123	0.33498355	-0.811537562	0.000239643	2.514341847
ENSCAFG00000006115	EXOSC8	0.456624216	0.087081942	-0.89186961	7.94E-06	4.607319974
ENSCAFG00000006124	ALG5	0.635457815	0.010902778	-0.872446968	2.21E-05	3.497909035
ENSCAFG00000006699	CALCOCO1	-0.371546872	0.172702232	0.912405583	2.12E-06	5.981545395
ENSCAFG00000007163	NDUFAF2	0.63023369	0.01178686	-0.847705869	6.58E-05	3.309556997
ENSCAFG00000007489	RILPL2	0.488017164	0.064958715	-0.874028059	2.05E-05	3.857983119
ENSCAFG00000007812	-	0.32998467	0.229688136	-0.864104648	3.27E-05	4.273987099
ENSCAFG00000007875	TMSB10	0.255655339	0.357748393	-0.817604848	0.000196773	1.917708196
ENSCAFG00000008363	P2RX4	0.346155047	0.206278324	-0.836041869	0.000103187	2.811876025
ENSCAFG00000009142	LPIN3	-0.217165638	0.436887512	0.809176042	0.000258271	1.869980478
ENSCAFG00000010567	BSDC1	-0.590014243	0.020598238	0.819130676	0.000187047	2.583992006
ENSCAFG00000010582	BOC	-0.344811423	0.208163018	0.771401117	0.000757412	1.946244381
ENSCAFG00000010870	UBE3B	-0.493413617	0.0616118	0.949854025	6.20E-08	8.107448223
ENSCAFG00000011101	GPR137B	0.286426589	0.300679471	-0.831312459	0.000122648	3.034789993
ENSCAFG00000011273	SUN1	-0.290459603	0.293621027	0.912581366	2.10E-06	5.930390999

ENSCAFG00000011279	ZNF639	0.196790916	0.482075519	-0.820193188	0.000180511	3.251321732
ENSCAFG00000011513	ABLIM1	-0.285987097	0.301454605	0.937477506	2.52E-07	6.906769365
ENSCAFG00000011659	ATP9A	-0.220278446	0.430179008	0.921066924	1.10E-06	6.166656035
ENSCAFG00000012307	NF2	-0.589974871	0.020608801	0.876704266	1.79E-05	4.339900856
ENSCAFG00000012851	TRIM41	-0.318646342	0.247052687	0.884129975	1.22E-05	3.541263887
ENSCAFG00000013830	CAPN1	-0.5060288	0.054278991	0.873871925	2.06E-05	3.296393658
ENSCAFG00000015081	ARPC1B	0.528263697	0.042940719	-0.883603606	1.25E-05	4.420736981
ENSCAFG00000015089	RETREG2	-0.624746327	0.012774479	0.837606459	9.73E-05	2.760031665
ENSCAFG00000015422	KIAA0753	-0.524280922	0.044829358	0.796949755	0.000374686	2.494190619
ENSCAFG00000015727	ARHGEF10L	-0.072013303	0.79869198	0.797245386	0.000371439	2.440078953
ENSCAFG00000016305	GPHN	-0.251717507	0.365456194	0.908343509	2.82E-06	5.417451056
ENSCAFG00000018349	CCL2	0.482880939	0.06826468	-0.819722096	0.000183385	1.960538751
ENSCAFG00000018424	TOM1L2	-0.506474176	0.05403238	0.91050975	2.43E-06	5.70518952
ENSCAFG00000018436	SREBF1	-0.78211552	0.000570134	0.797894101	0.000364393	2.170823825
ENSCAFG00000019134	PPL	-0.368240927	0.17685577	0.866389951	2.95E-05	3.42343043
ENSCAFG00000019275	DVL1	-0.509143821	0.052571328	0.884924975	1.17E-05	4.391452729
ENSCAFG00000019838	RXRA	-0.348516764	0.202992025	0.883065493	1.29E-05	4.833617816
ENSCAFG00000019991	PTPA	-0.52432487	0.044808188	0.898385565	5.38E-06	5.201902366
ENSCAFG00000020131	FAM129B	-0.364025024	0.182246673	0.903159471	3.99E-06	5.050519651
ENSCAFG00000020247	WWP2	-0.463957502	0.081494909	0.941820545	1.60E-07	7.038012002
ENSCAFG00000023602	ECSCR	0.432230366	0.107613833	-0.836967057	9.97E-05	2.35403828
ENSCAFG00000023730	BCL7B	0.52804657	0.043042133	-0.902449284	4.17E-06	5.581914077
ENSCAFG00000024324	-	0.165553801	0.555422338	-0.813772277	0.000223043	2.321027309
ENSCAFG00000029284	SAT1	0.525264587	0.044357293	-0.947434275	8.37E-08	7.770504982
ENSCAFG00000030112	DDIT3	0.259286242	0.350721801	-0.855760767	4.72E-05	3.213627179
ENSCAFG00000030662	-	-0.231189531	0.407085044	0.908973676	2.70E-06	5.341685381
ENSCAFG00000031195	TMEM189	0.537418537	0.038823838	-0.756416476	0.001100193	1.417027658
ENSCAFG00000032483	LY96	0.572314671	0.025780053	-0.871429935	2.32E-05	4.620919493
ENSCAFG00000032663	SPCS2	0.596601855	0.018888391	-0.890817578	8.43E-06	3.921329885

GS – gene significance; MM – module membership; Kw - Connectivity within the module; - Data no available

APPENDIX D – Supporting information: S2C Table. Gene co-expression networks

S2C Table. Genes in Darkorange2 module

Ensembl ID	Gene Name	GS score	GS score P-value	MM	MM P-value	Kw
ENSCAFG00000000244	MTFR2	0.534836085	0.03995402	0.851079449	5.74E-05	5.182751535
ENSCAFG00000000887	SAMM50	-0.527992971	0.043067195	-0.899139855	5.14E-06	6.225564007
ENSCAFG00000000936	PACSIN2	-0.435103555	0.105035759	-0.908309077	2.83E-06	7.090653453
ENSCAFG00000001557	CCDC171	-0.522803923	0.045545143	-0.844110968	7.59E-05	3.671199011
ENSCAFG00000002126	CENPQ	0.51572577	0.049093165	0.870219954	2.46E-05	5.020096667
ENSCAFG00000002334	MELK	0.52579629	0.044103665	0.870872526	2.39E-05	5.317275701
ENSCAFG00000003001	JAZF1	-0.313857802	0.254622136	-0.878057553	1.67E-05	5.051805576
ENSCAFG00000003243	ANLN	0.432992766	0.106925498	0.928085564	6.12E-07	8.994817156
ENSCAFG00000003278	CDCA8	0.415540996	0.1234622	0.911407424	2.28E-06	10.28883531
ENSCAFG00000003886	PLEKHA4	-0.598031634	0.018532112	-0.823454671	0.000161607	3.114188772
ENSCAFG00000004672	HECTD3	0.418266964	0.12077046	0.908233023	2.84E-06	7.347696257
ENSCAFG00000005548	RAD18	0.383059433	0.158740498	0.876710102	1.79E-05	5.509184782
ENSCAFG00000005898	CKAP2	0.357257082	0.191122609	0.913984143	1.89E-06	8.352664602
ENSCAFG00000005945	RRM1	0.407177495	0.131976592	0.915648076	1.68E-06	7.977168388
ENSCAFG00000006215	POLE	0.604901398	0.016891617	0.89873776	5.27E-06	6.656532692
ENSCAFG00000006383	BRCA2	0.576465334	0.024484706	0.860160198	3.90E-05	4.359405994
ENSCAFG00000007075	TPX2	0.36019161	0.187240428	0.916083689	1.62E-06	8.446927736
ENSCAFG00000007614	CCNE1	0.483342789	0.067962541	0.971236288	1.76E-09	13.04640362
ENSCAFG00000007705	-	0.511761569	0.051167029	0.963049959	8.80E-09	14.00958561
ENSCAFG00000008236	-	0.55907316	0.030261692	0.969138894	2.77E-09	14.50851342
ENSCAFG00000008340	RACGAP1	0.502885936	0.05604273	0.976595629	4.67E-10	16.1648353
ENSCAFG00000009336	MYBL2	0.582554229	0.022674716	0.95054063	5.68E-08	11.54029121
ENSCAFG00000009674	CHAF1B	0.413518242	0.125485944	0.91020877	2.48E-06	8.075694783
ENSCAFG00000009745	UBE2C	0.496262261	0.059896472	0.92974834	5.28E-07	11.70477374
ENSCAFG00000009903	MYLIP	-0.381924092	0.160082872	-0.845307338	7.24E-05	3.466551892

ENSCAFG00000010509	UBE2T	0.391170374	0.14936808	0.940025717	1.94E-07	11.01913342
ENSCAFG00000010719	SEMA3B	-0.359736204	0.187839518	-0.848518924	6.37E-05	4.081628034
ENSCAFG00000010836	CENPE	0.421821376	0.117321637	0.909874992	2.54E-06	8.097834804
ENSCAFG00000011403	ASPM	0.415175049	0.123826657	0.95097509	5.37E-08	11.69454786
ENSCAFG00000011522	IRF2BP2	-0.501476104	0.056847371	-0.836360223	0.000101974	3.425881232
ENSCAFG00000011598	-	0.650230958	0.008679814	0.84257705	8.05E-05	4.287409593
ENSCAFG00000011757	RCC1	0.315376937	0.252205601	0.903679353	3.85E-06	7.563094612
ENSCAFG00000011768	STK39	0.347320286	0.204652695	0.906893923	3.12E-06	7.396427251
ENSCAFG00000011769	ANK2	-0.286126921	0.30120787	-0.845747297	7.11E-05	4.457996775
ENSCAFG00000012904	CDK1	0.558052566	0.030629978	0.96343095	8.23E-09	14.23973441
ENSCAFG00000012941	TFRC	0.472310672	0.075447492	0.85630335	4.61E-05	4.336045626
ENSCAFG00000014529	CENPL	0.61507225	0.014670731	0.9440947	1.24E-07	11.27647237
ENSCAFG00000014650	CDCA3	0.512248714	0.050908771	0.917562496	1.45E-06	10.74345904
ENSCAFG00000015455	ECT2	0.479213026	0.070698709	0.971548222	1.64E-09	13.55363896
ENSCAFG00000016090	TOP2A	0.4786786	0.071058499	0.942537521	1.48E-07	11.88816751
ENSCAFG00000016530	PLXDC1	-0.203921469	0.466012703	-0.896787699	5.94E-06	6.786422391
ENSCAFG00000016600	-	0.471261686	0.076188696	0.963187844	8.59E-09	14.68276657
ENSCAFG00000016677	NCAPG	0.567467463	0.027357834	0.894483389	6.81E-06	6.627599064
ENSCAFG00000017264	-	0.484761453	0.067040498	0.896349585	6.10E-06	8.425458547
ENSCAFG00000017455	GAS7	-0.414988127	0.124013103	-0.850565019	5.86E-05	3.935245029
ENSCAFG00000017658	PLK1	0.503991368	0.055417668	0.942999501	1.40E-07	12.55826782
ENSCAFG00000019666	PER3	-0.559618952	0.030066116	-0.938109531	2.37E-07	11.31694936
ENSCAFG00000029848	TGIF2-C20orf24	0.561344532	0.029454045	0.856553853	4.56E-05	4.160203252
ENSCAFG00000030889	ZBTB47	-0.242796618	0.383250617	-0.798474868	0.000358179	3.043096517
ENSCAFG00000031302	-	-0.415826634	0.123178238	-0.90260544	4.13E-06	6.893411769
ENSCAFG00000031326	CEBPB	0.523037768	0.045431258	0.876938025	1.77E-05	4.880274365
ENSCAFG00000031673	-	-0.19137846	0.494441926	-0.815490948	0.000210928	2.524547923
ENSCAFG00000032746	MXD1	0.461645341	0.083228111	0.933760062	3.64E-07	9.68402791

GS – gene significance; MM – module membership; Kw - Connectivity within the module; - Data no available

APPENDIX E – Supporting information: S2D Table. Gene co-expression networks

S2D Table. Genes in Darkorange module

Ensembl ID	Gene Name	GS score	GS score P-value	MM	MM P-value	Kw
ENSCAFG00000000094	LMAN1	0.387088656	0.154037025	0.971535487	1.65E-09	18.983549
ENSCAFG00000000253	PEX7	-0.312403767	0.25694832	-0.893594673	7.18E-06	8.70603204
ENSCAFG00000000334	ADAMTS2	0.424920282	0.114370703	0.891646028	8.04E-06	8.90470701
ENSCAFG00000000603	NCAPH2	-0.401873025	0.137579019	-0.886496011	1.07E-05	8.32399615
ENSCAFG00000000745	TBC1D22A	-0.491760857	0.062623229	-0.933146047	3.86E-07	12.8990893
ENSCAFG00000000774	RNF5	-0.543084131	0.036428016	-0.909250391	2.65E-06	10.5858399
ENSCAFG00000000874	THBS2	0.551273917	0.033162409	0.871308844	2.34E-05	7.78371141
ENSCAFG00000001420	TMEM184B	0.329705428	0.230106369	0.948647263	7.22E-08	16.4555869
ENSCAFG00000001443	EIF3L	-0.507372422	0.053537506	-0.939877244	1.97E-07	14.0203222
ENSCAFG00000001640	CALU	0.471579022	0.075963922	0.965575328	5.59E-09	17.9647031
ENSCAFG00000001875	CKAP4	0.480033274	0.07014905	0.864509808	3.21E-05	6.53635029
ENSCAFG00000002057	PDGFRA	0.396269555	0.143669838	0.947810805	8.00E-08	17.3846898
ENSCAFG00000002163	ROR2	0.37091157	0.173495393	0.873969855	2.05E-05	7.91815063
ENSCAFG00000002525	COL15A1	0.243880016	0.381065086	0.933260966	3.82E-07	14.5554169
ENSCAFG00000003228	PXDN	0.435340796	0.104824828	0.954189757	3.48E-08	16.1598669
ENSCAFG00000003620	RCN3	0.458193318	0.085864305	0.950320793	5.84E-08	17.3887881
ENSCAFG00000003895	HSD17B14	-0.371117777	0.173237687	-0.848618882	6.34E-05	6.0477449
ENSCAFG00000004295	RNASEH2B	0.436416279	0.10387232	0.843451853	7.78E-05	6.05764371
ENSCAFG00000005334	GPR180	0.601114792	0.017781396	0.864602102	3.20E-05	6.59359423
ENSCAFG00000005386	SERPINH1	0.247281939	0.374246302	0.949615627	6.39E-08	16.0916554
ENSCAFG00000005984	KDELC1	0.421541469	0.117590737	0.886587956	1.07E-05	9.186411
ENSCAFG00000006062	COL4A1	0.282424283	0.307781436	0.865093242	3.13E-05	7.85755194
ENSCAFG00000006069	COL4A2	0.298430014	0.279961782	0.889905466	8.88E-06	9.73419584

ENSCAFG00000006454	ELK3	0.623516043	0.013004459	0.886946749	1.05E-05	8.29540171
ENSCAFG00000006540	TF	0.112565009	0.689587907	0.862609459	3.50E-05	6.42380098
ENSCAFG00000006598	MCM4	0.638182794	0.010462611	0.885979237	1.10E-05	7.93298802
ENSCAFG00000007117	EIF4B	-0.445876696	0.095752657	-0.913119489	2.02E-06	10.8877988
ENSCAFG00000007598	GGT7	0.450666773	0.091816414	0.853295095	5.23E-05	6.11792691
ENSCAFG00000007986	ZNF366	0.331938213	0.226775526	0.828672125	0.000134764	4.31738578
ENSCAFG00000008101	PLOD2	0.336348404	0.220285685	0.923749088	8.87E-07	11.8569733
ENSCAFG00000008351	TLR2	0.484636531	0.067121324	0.907373225	3.02E-06	10.6192428
ENSCAFG00000009187	LOXL2	0.38644275	0.154784678	0.89491098	6.64E-06	9.10426261
ENSCAFG00000009282	CREB3L1	0.35574823	0.193138818	0.938584679	2.25E-07	14.6370309
ENSCAFG00000009587	BMP1	0.506281319	0.054139067	0.92494751	8.02E-07	12.2505162
ENSCAFG00000009810	JAM3	0.453844261	0.089269167	0.948997602	6.91E-08	16.4262281
ENSCAFG00000009822	HTATIP2	-0.238404197	0.392180231	-0.900025874	4.86E-06	10.6558265
ENSCAFG00000010913	C11orf24	0.349316755	0.201886491	0.874520298	2.00E-05	8.88872553
ENSCAFG00000010930	COL16A1	0.598919455	0.01831349	0.878833857	1.61E-05	8.05170175
ENSCAFG00000011196	NID1	0.290597203	0.293381942	0.896794381	5.93E-06	10.2595266
ENSCAFG00000011197	MMP14	0.542199212	0.036794742	0.87747079	1.73E-05	7.97513918
ENSCAFG00000011401	KIRREL	0.418539731	0.120503357	0.827639145	0.000139764	5.07465877
ENSCAFG00000011751	CD86	0.413334736	0.125670655	0.938111509	2.37E-07	15.3021348
ENSCAFG00000011911	COL6A1	0.321021447	0.243350236	0.888123821	9.81E-06	10.6409248
ENSCAFG00000012051	PDIA5	0.225069445	0.41995743	0.895376944	6.46E-06	10.5591042
ENSCAFG00000012054	ENSA	-0.311440243	0.258496894	-0.954846009	3.17E-08	16.3058608
ENSCAFG00000012226	COL6A3	0.382418074	0.159497888	0.906463219	3.21E-06	12.8477685
ENSCAFG00000012364	FLVCR1	0.336310224	0.220341361	0.874365665	2.01E-05	7.33899166
ENSCAFG00000013010	TBL2	0.148060196	0.598468317	0.809628748	0.000254611	4.27538904
ENSCAFG00000013079	OLFML2B	0.529347978	0.04243693	0.808088219	0.000267242	4.19890453
ENSCAFG00000014345	FN1	0.435677028	0.10452639	0.881940622	1.37E-05	8.12273892
ENSCAFG00000014617	ECD	-0.377374396	0.165537761	-0.858010798	4.28E-05	6.82017136
ENSCAFG00000014670	-	0.454566937	0.08869688	0.867826197	2.76E-05	7.22078408
ENSCAFG00000014812	COL3A1	0.438354735	0.102170796	0.925760263	7.49E-07	14.2160731

ENSCAFG00000014837	COL5A2	0.502422006	0.056306587	0.96143079	1.16E-08	18.5065453
ENSCAFG00000015105	BIRC3	0.668988427	0.006386918	0.861703336	3.64E-05	6.31036964
ENSCAFG00000015337	PLVAP	0.149146653	0.595756619	0.753893103	0.001168619	2.9337528
ENSCAFG00000015746	KDELR2	0.29353228	0.288309522	0.864684924	3.19E-05	7.92369062
ENSCAFG00000015885	FKBP10	0.443362245	0.097865688	0.927368942	6.52E-07	14.8586537
ENSCAFG00000015978	UGDH	0.360225567	0.187195808	0.926419664	7.08E-07	12.560804
ENSCAFG00000016023	COQ8A	-0.493394377	0.061623505	-0.917913152	1.41E-06	10.8096296
ENSCAFG00000016064	MAGED1	0.415557976	0.123445308	0.94571809	1.03E-07	16.2929227
ENSCAFG00000016115	ACBD3	0.160138311	0.568604992	0.816676331	0.000202891	4.08054645
ENSCAFG00000016769	NES	0.207426583	0.458213928	0.89678938	5.94E-06	9.83541734
ENSCAFG00000016935	RANBP17	0.499657767	0.057897575	0.803889674	0.000304294	3.990344
ENSCAFG00000016992	SPDL1	0.445309174	0.096226749	0.83980053	8.96E-05	5.57102527
ENSCAFG00000017018	COL1A1	0.420245178	0.118842526	0.896659502	5.98E-06	11.4334934
ENSCAFG00000017165	PMVK	-0.558741958	0.03038084	-0.888381432	9.67E-06	8.89995103
ENSCAFG00000017266	C1orf43	-0.506432068	0.054055661	-0.810024123	0.00025145	3.53017749
ENSCAFG00000017855	SPARC	0.378578579	0.164082209	0.924240021	8.51E-07	12.2770445
ENSCAFG00000017892	-	0.333880729	0.223902412	0.868808688	2.63E-05	6.3451478
ENSCAFG00000018234	MCOLN1	-0.430152733	0.109505258	-0.874381641	2.01E-05	8.32090557
ENSCAFG00000018802	RAD1	0.275690098	0.319948901	0.808144607	0.000266771	4.09841002
ENSCAFG00000019808	TCF25	-0.65213692	0.008421085	-0.802675567	0.000315757	4.12537663
ENSCAFG00000019848	COL5A1	0.450718463	0.091774571	0.928154823	6.09E-07	14.1519639
ENSCAFG00000020069	KARS	-0.622148263	0.013263897	-0.800626593	0.000335903	3.59514907
ENSCAFG00000020106	ENG	0.21614973	0.43908832	0.930222013	5.06E-07	13.3451321
ENSCAFG00000025390	SLC22A17	0.139377181	0.620314347	0.839743134	8.98E-05	5.02771064
ENSCAFG00000028461	LOX	0.474444623	0.073955633	0.900059425	4.85E-06	10.6018059
ENSCAFG00000028571	ZBED8	0.570886957	0.026237416	0.824128115	0.000157914	4.31073612
ENSCAFG00000029022	-	0.254467068	0.36006474	0.883849083	1.24E-05	10.2979383
ENSCAFG00000030285	CDR2L	0.479938038	0.070212711	0.938227611	2.34E-07	14.908705
ENSCAFG00000030944	-	-0.367831658	0.177374476	-0.881931051	1.37E-05	8.14708944
ENSCAFG00000031841	-	0.14549409	0.604892531	0.761551218	0.000970946	2.80549959

ENSCAFG00000031865	-	0.326589754	0.23480511	0.907400897	3.01E-06	10.0685268
ENSCAFG00000032281	XKR8	0.574991637	0.024938823	0.889596385	9.03E-06	9.01941576

GS – gene significance; MM – module membership; Kw - Connectivity within the module; - Data no available

APPENDIX F – Supporting information: Table S6- Summary of Clinical, Histopathological and Immunohistochemical data in dogs with MCTs

Table S6. Breed, age, gender, location of the lesions, follow-up time, survival data, histopathological grades, Ki67 score, quantitative analisys of CAFs with their respective malignancy score.

ID	BREED	AGE (years)	GENDER	TUMOR LOCATION	FOLLOW-UP (days)	STATUS	TWO-TIER GRADING SYSTEM•	Ki67 Index	KI67 SCORE	MALIGNANCY SCORE	CAFs α-SMA POSITIVE (nº)
1	Great Dane	6	male	limbs and tail	840	CS	1	2.13%	1	3	42
2	mixed breed	7	female	limbs and tail	1035	LA	1	1.27%	1	3	0
3	Poodle	7	male	limbs and tail	1450	LA	1	2.66%	1	3	7
4	Boxer	4	female	limbs and tail	1242	CS	1	2.00%	1	3	4
5	Pinscher	7	female	limbs and tail	991	CS	1	0.00%	1	3	5
6	poodle	15	female	trunk	466	LA	1	2.36%	1	3	9
7	mixed breed	13	male	inguinal	454	LA	1	2.30%	1	3	0
8	Fila	9	male	trunk	1443	CS	1	2.09%	1	3	0
9	Boxer	9	female	trunk	379	CS	1	2.27%	1	3	5
10	mixed breed	9	female	limbs and tail	1286	LA	1	0.00%	1	3	9
11	Poodle	4	female	limbs and tail	2670	LA	1	1.80%	1	3	2
12	mixed breed	5	female	trunk	1500	CS	1	3.09%	2	4	0
13	mixed breed	n.d.	male	inguinal	1800	CS	1	3.97%	2	4	7
14	Fila	9	male	trunk	692	CS	1	6.19%	2	4	27
15	Labrador	9	male	limbs and tail	395	LA	1	3.80%	2	4	0
16	Poodle	7	male	limbs and tail	1898	LA	1	3.93%	2	4	15
17	Poodle	4	female	trunk	2670	LA	1	3.88%	2	4	0
18	Pit bull	12	female	inguinal	303	LA	1	4.80%	2	5	0
19	mixed breed	13	male	limbs and tail	292	LA	1	6.22%	2	5	1
20	mixed breed	5	female	limbs and tail	392	LA	1	8.92%	3	5	0
21	Labrador	3	male	limbs and tail	920	LA	1	15.18%	3	5	14
22	Fila	10	male	trunk	1067	CS	1	12.73%	3	5	0
23	mixed breed	13	female	trunk	224	LA	1	8.07%	3	6	13
24	Boxer	10	male	limbs and tail	551	CS	2	21.87%	3	6	52
25	Golden retriever	9	female	limbs and tail	289	LA	1	8.75%	3	6	8
26	mixed breed	14	female	head and neck	200	DT	1	2.66%	1	7	9
27	Boxer	8	female	limbs and tail	248	DT	1	2.86%	1	7	10
28	Dachshund	12	male	abdomen	751	DT	2	2.27%	1	7	0
29	Boxer	12	male	trunk	1119	DT	2	4.59%	2	8	3
30	Labrador	10	male	limbs and tail	130	DT	1	2.11%	1	8	28
31	Boxer	14	male	trunk	68	DT	1	1.84%	1	8	34

32	Dachshund	12	male	trunk	131	LA	2	13.00%	3	8	21
33	mixed breed	13	female	limbs and tail	407	DT	2	7.67%	3	9	63
34	Boxer	9	female	abdomen	3	DT	2	1.84%	1	9	53
35	Pug	9	female	trunk	308	DT	2	13.76%	3	10	20
36	mixed breed	13	male	inguinal	207	DT	2	12.89%	3	10	27
37	Doberman	9	male	limbs and tail	112	DT	2	6.59%	2	10	32
38	Dachshund	10	male	limbs and tail	222	DT	2	18.78%	3	10	11
39	Poodle	11	male	trunk	228	DT	2	16.04%	3	10	207
40	Boxer	9	female	abdomen	3	DT	2	7.09%	3	11	154
41	Pit Bull	7	female	trunk	51	DT	2	13.12%	3	11	10
42	Labrador	8	female	trunk	120	DT	2	7.25%	3	11	0
43	Labrador	8	female	trunk	120	DT	2	10.05%	3	11	2
44	Labrador	8	female	trunk	120	DT	2	12.98%	3	11	0

Abbreviations: ID: identification number; CAF: cancer-associated fibroblasts; LA: live animals; CS: censored (deaths unrelated to MCT); DT: death related to mast cell; n.d.: no data. • Kiupel et al. (2011)

APPENDIX G – Supporting information: Graphic S1. Ki67 index. Comparison of Ki67 indices between low-risk and high-risk MCTs

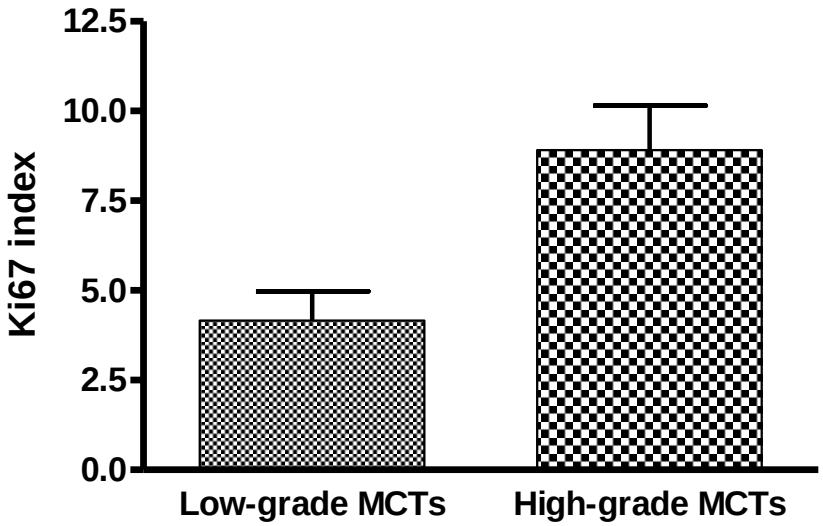

Source: Pulz, L. H., 2019

3 ARTICLE 2

CULTIVATION AND CHARACTERIZATION OF CANINE CUTANEOUS MAST CELLS TUMOR-DERIVED CELLS

3.1 INTRODUCTION AND LITERATURE REVIEW

Canine mast cells are highly reactive cells that and play important role not only in the pathogenesis of inflammatory and allergic reactions, but also in neoplastic processes (GALLI, 1997). Canine mast cell tumor (MCT) is a common skin cancer in dogs, representing 11–27% of all malignant skin tumors (VAIL, 1996), thus neoplastic mast cell lines should provide an important tool for research in the area of veterinary oncology.

Previous studies with canine normal mast cells involved short-term cultures of canine gastric and hepatic mast cells with IgE receptors activating histamine release (SOLL, LEWIN, BEAVEN, 1979; SOLL et al., 1988). Others used the dog skin as the source of normal mast cells (DEMORA et al., 1996), but low number of cells and low purity of cell culture were reported as limiting factors. Bone marrow derived mast cells (BMCMCs) were purified and cultured from CD34+ precursors with phenotypic and functional properties similar to mast cells found *in vivo* (LIN, RUSH, LONDON, 2006). However, normal mast cell lines may not reflect the molecular properties of their malignant counterparts.

Cultivation of canine MCTs could give rise to permanent cell lines representing the original cell population. Several groups have focused on isolation and purification of neoplastic canine mast cells using propagation of this cells in nude mice (LAZARUS et al., 1986; CAUGHEY et al., 1988; DEVINNEY, GOLD, 1990; ISHIGURO et al., 2001; NAGAMINE et al., 2011). These cell lines were obtained with freshly disaggregated cells from MCTs which were inoculated in athymic (nude) mice (LAZARUS et al., 1986; CAUGHEY et al., 1988; DEVINNEY, GOLD, 1990; NAGAMINE et al., 2011) or severe combined immunodeficiency (SCID) mice (ISHIGURO et al., 2001). Lazarus et al. (1986) developed 4 mast cell lines (C2, C1, G, and BR) derived from malignant MCT and propagated subcutaneously in athymic mice. Subsequently, DeVinney & Gold (1990) established the C1 and C2 cell lines in permanent culture *in vitro*, and both shared the characteristic of releasing histamine after non-immunological stimulation as well as common morphological features (DEVINNEY, GOLD, 1990; BRAZIS et al., 2002). Mast cells from G cell line were shown to release higher chymase:tryptase proportion (CAUGHEY et al., 1988) while mast cells from BR cell line did

not express the cell surface receptor FcεRI and expressed KIT with a point mutation in the juxtamembrane domain, showing stimulatory similarities with the canine mast cell lines C1 and C2 (CAUGHEY et al., 1988; GARCIA et al., 1998). Morphologically, cells from all four cell lines resembled mature mast cells. Another canine MCT cell line established with *in vivo* passage in mice was named CoMS and showed few functional IgE receptors and significant IgE-independent histamine release. CoMS was originated from a canine oral mucosal MCT and showed similar features to those of gastric mucosa and airway lumen mast cells, but not to the skin-derived mast cells (ISHIGURO et al., 2001), thus showing less importance in the study of this cutaneous tumor.

Some authors suggested that neoplastic mast cells have adapted to the mouse and grown with no significant morphological or functional changes (LAZARUS et al., 1986; DEVINNEY, GOLD, 1990; GUECK, SEIDEL, FUHRMANN, 2003). Although a great amount of useful data has been generated from this cell lines, the limitations are obvious: mast cells are influenced by the microenvironment. In addition, there are differences between wild-type neoplastic mast cells and those from nude mice to suggest that these studies may be of limited value.

Several attempts to establish direct primary culture of canine MCTs have been made, but some of them do not describe the survival time of neoplastic mast cells *in vitro (*GOETZL, PHILLIPS, GOLD, 1983; CALONICO et al., 1985; TAKAHASHI et al., 2001) or report that the neoplastic mast cells have a lifetime of 30 days without extra supplement factors (PINELLO et al., 2009). The main reports on the establishment of cell lines isolated from canine MCTs in continuous culture and with no previous passage in mice are: HRMC (OHMORI et al., 2008), CM-MC, VI-MC, CoMS (TAKAHASHI et al., 2001, TAKAHASHI et al., 2007), MPT-1 (AMAGAI, et al., 2008), MPT-2 (MATSUDA et al., 2011) and MPT-1.2 cells (AMAGAI et al., 2013).

HRMC cells are similar to immature canine neoplastic mast cells, present surface IgE that bound to IgE receptors, and express wild-type KIT on cell surface (OHMORI et al., 2008). CM-MC cells were obtained from a dog with cutaneous MCT and VI-MC from a dog with visceral MCT tumor. Both cell populations were characterized morphologically by the presence of typical mast cell cytoplasmic granules and released histamine in response to various secretagogues (TAKAHASHI et al., 2001). CoMS was derived from an oral MCT and cells were capable of binding to the extracellular matrix (TAKAHASHI et al., 2007). MPT-1 cell line derived from a connective tissue-type MCT and showed larger amount of histamine and the expression of wild-type KIT receptors and FcεRI (AMAGAI et al., 2008). MPT-2 derived from an aggressive recurrent MCT and their cells expressed the same proteins on the cell

surface as MPT-1, but KIT had an internal tandem duplication in the juxtamembrane domain (MATSUDA et al., 2011). MPT-1.2 cells, a subline of MPT-1 cells, expressed KIT with a N508I point mutation in the extracellular domain (AMAGAI et al., 2013). However, in these studies, important characteristics were not sufficiently described, such as the number of passages with viable cells, the culture purification method, culture conditions, and presence of fibroblasts or other cells.

Human mast cell lines are also used in the study of canine MCTs (MATSUDA et al., 2011), such as a cell line established from a patient with mast cell leukemia referred as human mast cell-1 (HMC1) (BUTTERFIELD et al., 1988). HMC1 cells rarely express FceRI (BUTTERFIELD et al., 1988) and have mutated KIT receptors that are constitutively activated (FURITSU et al., 1993), similarly to some canine MCTs. Nevertheless, the process of generating mast cells *in vitro* is fairly species-specific (LIN, RUSH, LONDON, 2006), suggesting that certain aspects of canine mast cell biology cannot be established with human mast cells.

Given the prevalence of cutaneous MCTs in dogs, the culture of a large number of tumor samples would be extremely useful, not only for dissecting the *in vitro* behavior of these neoplastic cells, but also for the identification of molecular mechanisms that promote malignant transformation or could influence the prognosis. In the present study, we demonstrate that the primary culture of MCT represent a heterogeneous population of cells composed by three major phenotypes: mast cells, fibroblasts and myofibroblasts. As such, the purpose of this work is to demonstrate the limited viability of neoplastic mast cells under *in vitro* conditions. Our data show that the primary culture of canine MCTs without extra supplement factors or nude mice passages could not be maintained for a prolonged time.

3.2 MATERIALS AND METHODS

3.2.1Tumour samples

Mast cell tumor samples were obtained from dogs that underwent surgery at the Veterinary Hospital of the School of Animal Science and Food Engineering of University of Sao Paulo, Veterinary Hospital Dr. Vicente Borelli, from the Octávio Bastos Foundation University (UNIFEOB) and private veterinary clinics, which agreed to participate in the present study. All surgical procedures were performed as part of the treatment, aiming the cure. Inclusion criteria for enrolment were histopathological diagnosis of cutaneous MCT, no

previous antineoplastic treatment (radio or chemotherapy) and availability of complete medical records. The protocols were approved by the local Ethic Committee on Animal Use, University of Sao Paulo, protocol number CEUA/5637040718.

Immediately after surgical excision, tumor fragments were washed in sterile phosphate buffer solution (PBS) and placed in sterile transport medium consisting of Dulbecco's modified Eagle medium/Ham's F-12 medium - DMEM-F12 (Thermo Fisher, Fremont, California, USA) with 2% penicillin/streptomycin (PenStrep, Thermo Fisher, Fremont, California, USA) at 4°C until arrival at the laboratory. Part of surgically resected tumor tissues were placed in 10% neutral buffered formalin and all excisional sample were processed routinely and embedded in paraffin. Four-µm sections were stained with haematoxylin and eosin (HE) and MCTs were graded following the criteria described by Patnaik et al. (1986) and Kiupel et al. (2011).

3.2.2 Dissociation and cell culture technicque

The tumor tissue isolated from dogs with MCT was minced finely and treated with Collagenase type I (Sigma– Aldrich, St. Louis, MO) 200 U/mL and Hyaluronidase (Sigma Aldrich, St. Louis, Missouri, USA) 100 U/mL for 3 hours, at 37°C. Then, suspension was filtered through a 100-µm filter followed by filtration through a 40-µm mesh.

After washing with phosphate-buffered saline (PBS), tumor cells were cultured in DMEM-F12 (Gibco-BRL, Gaithersburg, MD) supplemented with 15% fetal bovine serum (FBS) and 1% antibiotic antimycotic solution (100 U/mL penicillin G, 100 ng/mL streptomycin sulfate; Sigma-Aldrich) at 37°C in a humidified atmosphere with 5% CO_2. Cells were plated in 75-mm cell culture bottle (Corning Incorporated, Corning, NY) with 10 mL of complete DMEM-F12 medium. To maintain the culture condition, the medium was changed every 4–6 days. When cells adherent to the flask reached confluence (approximately 70% confluency), all bottles were subjected to 0.25% trypsin/EDTA activity (Gibco, Life Technologies®), and then passed to sterile new bottles for maintenance of the neoplastic cells. Confluent fibroblasts were detached from culture flasks and seeded into a 75-mm cell culture bottle at a density of 10^5 cells per mL in DMEM-F12 medium containing 15% SFB. Before removing the adherent fibroblasts, the supernatant containing the neoplastic mast cells was take out from the bottle and separated into falcon tube. The cell suspension was centrifuged at 1500 rpm for 5 min, the supernatant was discarded and the mast cells were quantified and resuspended in complete DMEM-F12 medium. Culture evolution was evaluated daily by Eclipse-TS100 microscope equipped with a Nikon camera (Nikon, Tokyo, Japan).

3.2.3 Mast cell staining

At each passage, an aliquot of 100 μL of the supernatant was withdrawn from the medium, centrifuged at 1500 rpm for 5 min and placed on a glass slide. Neoplastic mast cells harvested from the supernatant were fixed in methanol and stained with 0.05% toluidine blue (SigmaAldrich Corporation). Additionally, an aliquot of the cytocentrifuged preparations were air-dried in glass slides and stained with Romanowsky stain (*Diff-Quik* solution, Dade Behring Inc**.,** Düdingen, Switzerland) according to the manufacturer's instructions. The slides were analyzed with optical microscopy (Eclipse TS100, Nikon, Japan).

3.2.4 Cell viability

To determine the cell viability of canine MCT cell, each tumor subjected to Trypan Blue Exclusion Test according to Strober, 1997. Briefly, an aliquot of mast cells suspension was harvested and centrifuged fot 5 min at 100 g. The cell pellet was resuspended in PBS and mixed with 0.4% trypan blue (GIBCO/BRL), for 3 min in the proportion of 1 part of 0.4% trypan blue and one part of cell suspension. The cell counting was done in a hemocytometer on the stage of a binocular microscope. Unstained cells were considered as viable and stained cells as nonviable.

3.2.5 Quantitative real-time polymerase chain reaction analysis for Fibroblast-specific Protein 1 (FSP 1)

Adherent cells derived from canine cutaneous MCT were grown to 70-80% confluence and then trypsinized at the initial (P0) and first passage (P1). Total RNA was extracted using TRIzol reagent (Thermo) according to the manufacturer's instructions. NanoDrop2000 (Thermo Scientific, USA) and RNA integrity number (RIN) were used to verify the amount and integrity of the extracted RNA following manufacturer's protocol (RNA 6000 Nano kit, 2100 Bioanalyzer, Agilent Technologies, USA). Samples with A260/A280 ratio between 1.8 and 2.1 and RIN superior than 8 were considered appropriate for use.

Subsequently, reverse transcription into cDNA was made using the commercial kit “High Capacity cDNA Reverse Transcription Kit” (Thermo) at 37°C for 120 min and 75°C for

5 min in a PCR thermal cycler. Specific primers for Fibroblast-specific Protein 1 (FSP1) gene were designed with Primer-BLAST (YE et al., 2012).

Real-time quantitative polymerase chain reaction (qRT-PCR) was performed with Fast SYBR Green Master Mix in a final volume of 10 μL in the presence of primers for canine FSP1 gene: 5′-TCCTCATCTCTTCTCCTTCTTGGT-3′ (forward) and 5′-TGAACTTGTCACCCTCCTTGC-3′ (reverse). Conditions for quantitative PCR were as follows: a pre-denaturation step at 95°C for 20 seconds, followed by 40 cycles at 95°C for 3 seconds for denaturation, and 60°C for 30 seconds for anneal/extend. Gene expression analysis were performed by qRT-PCR using a StepOne System (Thermo Fisher Scientific).

Relative expression levels of the target gene were normalized to the housekeeping gene (18S ribosomal RNA) and calculated with the 2-ΔΔCt method (LIVAK, SCHMITTGEN, 2001). The experiment was performed twice and in biological triplicates.

3.2.6 *In vitro* characterization of stromal fibroblasts: immunofluorescence for α-SMA - smooth muscle alpha actin and vimentin

Fibroblasts derived from the MCT stroma were grown on glass coverslips in complete DMEM-F12 medium concomitant with the primary culture. Adherent cells were washed three times with PBS and then fixed in 4% paraformaldehyde solution (in PBS) for 10 min at room temperature. After washing with PBS, unspecific antigens were blocked for 45 min with a 5% fat-free skim milk solution at room temperature. Coverslips containing fixed cells were first incubated at 4°C in in humid chamber with the primary anti-vimentin antibody conjugated to fluorophore Alexa Fluor® 647 (clone V9, cod. ab195878, Abcam, USA) diluted 1:100, for 16 hours (overnight), washed and incubated for 60 min in a 1:500 dilution of monoclonal anti-alpha smooth muscle actin antibody conjugated to fluorescein isocyanate (FITC) (clone 1A4, Sigma-Aldrich, St Louis, MO, USA) at room temperature. After rinsing in PBS, nuclei were stained with DAPI. For the negative control, the antibodies were replaced with PBS. Coverslips were mounted on glass slides using ProLong ™ solution (Thermo Scientific, USA) and observed immediately with an inverted fluorescence microscope (ZEISS—Axio Vert A1) and photographed with a coupled camera Axio Can 503 attached using 540 nm wavelength filter for the observation of smooth muscle actin filaments (FITC) and 670-695 wavelength filter for visualization of vimentin (Alexa Fluor® 647) and 358 nm for observation of the DAPI-labeled nuclei. Photomicrographs were taken using a ZEISS ZEN 2 Microscope Software (Carl Zeiss,

Jena, Germany). All double immunofluorescence results were verified by single labeling techniques using direct (vimentin and alpha-actinin) fluorescence.

3.2.7 Tumor fibroblasts senescence assay

Canine fibroblasts were obtained from the mast cell tumor primary culture produced by serial passages until the cells stopped dividing for a period of approximately 2 months. Cells were grown in a 5% CO_2 incubator in DMEM-F12 medium supplemented with 15% fetal bovine serum and 100 U/mL penicillin G sodium, 100 ng/mL streptomycin sulfate. Senescent cells were maintained without further passage by changing the media every 4–6 days until their use in the experiments 7–10 days after cessation of growth. The senescent fibroblasts used in these studies were between passages 5 and 7.

The cells were washed in PBS, fixed in 4% paraformaldehyde solution for 5 min at room temperature and incubated overnight at 37 °C with X-gal chromogenic substrate at pH 6.0 following the conventional protocol for SA-β-gal staining (DIMRI et al., 1995). The X-gal staining solution contains 1 mg/ mL 5-bromo-4-chloro-3-indolyl β-galactoside (X-Gal-Sigma), 40 mM citric sodium phosphate (pH 6.0), 5 mM potassium ferrocyanide, 5 mM potassium ferrocyanide, 150 mM NaCl and 2 mM Magnesium Chloride. At pH 6.0, only senescent cells stained. The proportion of cells positive for β-gal activity can be easily determined by counting the number of blue cells in the total population.

To evaluate the cytochemical staining activity of lysosomal β-galactosidase in senescent fibroblasts, cells were observed by iverted ZEISS—Axio Vert A1 microscope and photographed with a coupled camera Axio Can 503 attached.

3.2.8 Statistical analysis

The number of cells obtained for the primary culture for the samples were presented as the mean ± standard deviation (SD). MCT grading using the 2-tier grading system (KIUPEL et al., 2011) was compared with total time in cell culture, cell viability and number of passages with a 2-way ANOVA test, using GraphPad Prism software (GraphPad Software, Inc., La Jolla, CA). The level of significance was set at 5%.

3.3 RESULTS

3.3.1 Population

Thirteen MCT samples were collected from eleven dogs immediately after the excisional biopsy from January 2016 to August 2018 (Table 1). All fragments were submitted to concomitant histopathological processing. The age of the dogs ranged from 3 to 14 years (mean = 7.5 years) and females (63.6%) were more frequently affected than males (36.4%). Considering the racial distribution, 45.5% of the MCTs cases were crossbred and 54.5% were purebred dogs. Based on the Patnaik et al. (1984) grading system, one lesion (7.7%) was diagnosed as grade I MCT, nine (69.2%) as grade II, and three (23.1%) as grade III. Using the 2-tier grading system (KIUPEL et al., 2011), 6 tumors (46.2%) were high-grade MCTs and 7 (53.8%) were low-grade. The characteristics of the dog population and histological classifications of these lesions are described in Table 1.

Table 1. Summary of Clinical and Histopathological data in dogs with MCTs submitted to the cell culture. Breed, age, gender, location of the lesions and histopathological grades, with their respective identification number.

ID	BREED	AGE (years)	GENDER	TUMOR LOCATION	PATNAIK et al. [26] GRADING SYSTEM	TWO-TIER GRADING SYSTEM [27]
5-16	mixed breed	8	male	trunk	II	Low grade
6-16	mixed breed	8	male	limbs and tail	II	Low grade
232-16	mixed breed	4	female	abdomen	III	High grade
334-16	mixed breed	10	male	inguinal	II	High grade
346-16	Labrador	5	female	trunk	II	Low grade
395-17	mixed breed	7	male	limbs and tail	III	High grade
550-17	Boxer	10	female	abdomen	III	High grade
603-17	Brazilian Terrier	14	female	limbs and tail	II	High grade
19-18	Labrador	6	male	limbs and tail	II	Low grade
816-18	Boxer	6	female	limbs and tail	II	High grade
1171-18	mixed breed	9	female	trunk	II	Low grade
1172-18	mixed breed	9	female	trunk	II	Low grade
1249-18	Australian Cattle Dog	3	female	head	I	Low grade

Abbreviations: ID: identification number
Source: Pulz, L. H., 2019

3.3.2 General characteristics of canine MCT primary cultures

During all the passages of the primary culture, neoplastic mast cells were nonadherent cells, and fibroblasts attached to the glass surface of the culture flask. After 72h in culture, the cells in suspension were round-shaped and presented oval nuclei, typical of cultured mast cells. They also formed floating aggregates, and were readily morphologically distinguishable from

other cell types (Figure 1). Initially, small quantities of flat fibroblastic cells were present (Figure 1). As the culture was maintained in complete DMEM-F12 medium, the flat cells rapidly multiplied to form a confluent monolayer under the neoplastic mast cells (Figure 1). In all cultures, mast cells grew in clumps in continuity with the adherent layer with fibroblastic characteristics.

Figure 1. Microscopic features of canine MCT culture sample H334-16. (a) and (b) Early passage (P0) 4 days after initiation of culture, showing small clumps as well as individual neoplastic mast cells in the supernatant in association with the adherent layer. (c) and (d) 14 days of cultivation (P1 passage), with primary mast cells overlaying fibroblasts. (e) and (f) 34 days of cultivation, showing low number of viable mast cells in the supernatant and the fibroblasts tending to confluence. Phase contrast microscope.

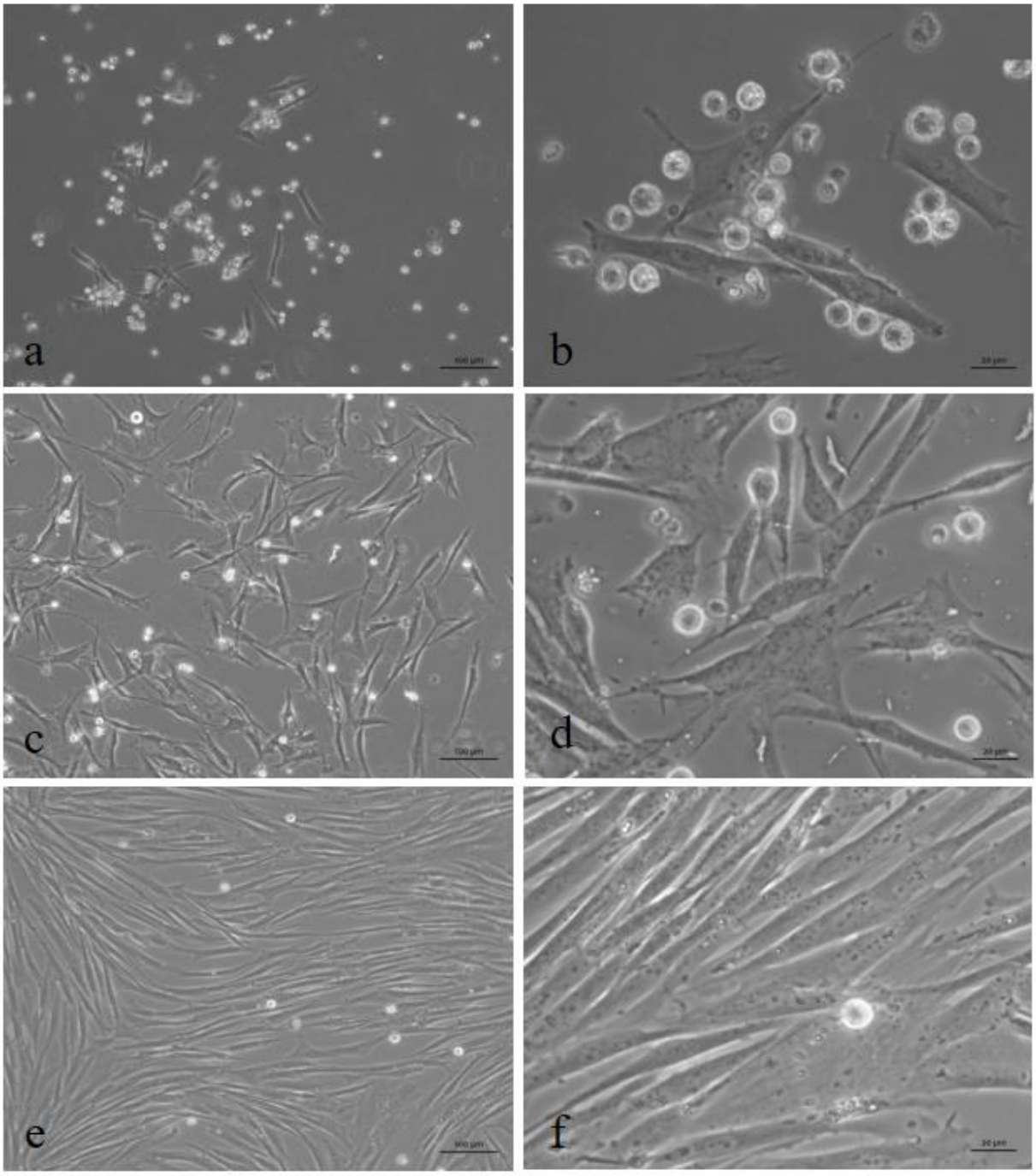

Source: Pulz, L. H., 2019

After centrifugation of the supernatant, smear and fixing on glass slide, early primary cultured mast cells contained cytoplasmic purple-positive granules seen by both the Toluidine blue and Romanowsky stains. Canine mast cells presented as uniform populations of single round cells, with round to oval uniform-sized nuclei, and abundant cytoplasm that contained variable quantities of metachromatic granules (Figure 2). Over the days of cultivation, it was noted that these cells were progressively losing their granules.

Figure 2. Mast cells 5 days after initiation of culture. (a) Romanowsky-stained preparation and (b) toluidine blue-stained preparation. Bars = 20 µm.

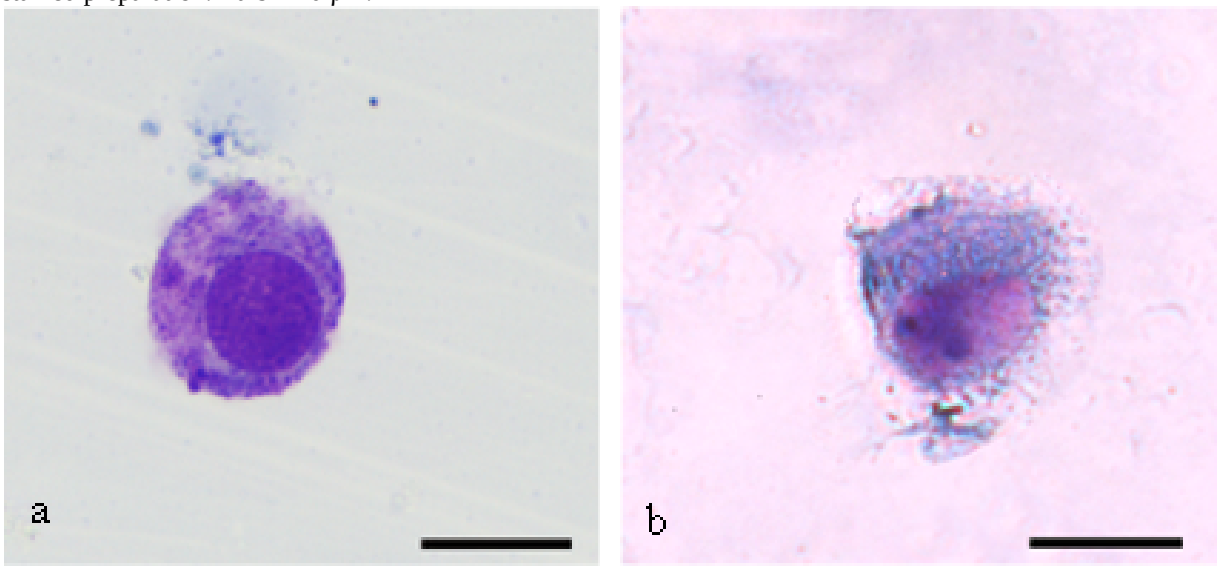

Source: Pulz, L. H., 2019

3.3.3 Cell viability

The total number of cells placed in culture ranged from 5.5 x 10^5 to 3.6 x 10^6 cells/mL (mean 1.5 x 10^6 ± 1,034,832). For primary culture (P0) we used 1 mL of volume of cells in all samples.

The Trypan blue exclusion test was used to quantify the viable mast cells in the supernatant in each passage. The number and percentage of viable mast cells obtained after digestion of skin MCT for each lesion and passage can be seen in S1-S13 Tables in Supporting Information (Appendix).

Considering the cultivation time in days, neoplastic mast cells remained viable for a period that ranged from 30 to 75 days, and the cells survived for an average time of 57.7 days. In all samples, supernatant mast cells decreased during culture passage in number (Figure 3A)

and percentage of living cells (Figure 3B), while the proliferation of adhered fibroblasts increased.

Figure 3. Neoplastic mast cell culture conditioned by fibroblasts cells versus passages. Viability was determined by the Trypan blue exclusion method. (A) MCTs cultures at different passages during the whole 5 to 11 weeks culture. Data are number of live cells in supernatant/mL of the thirteen samples. (B) Percentage of viable mast cells during the passages. The data are representative for thirteen independent cultures from individual lesions

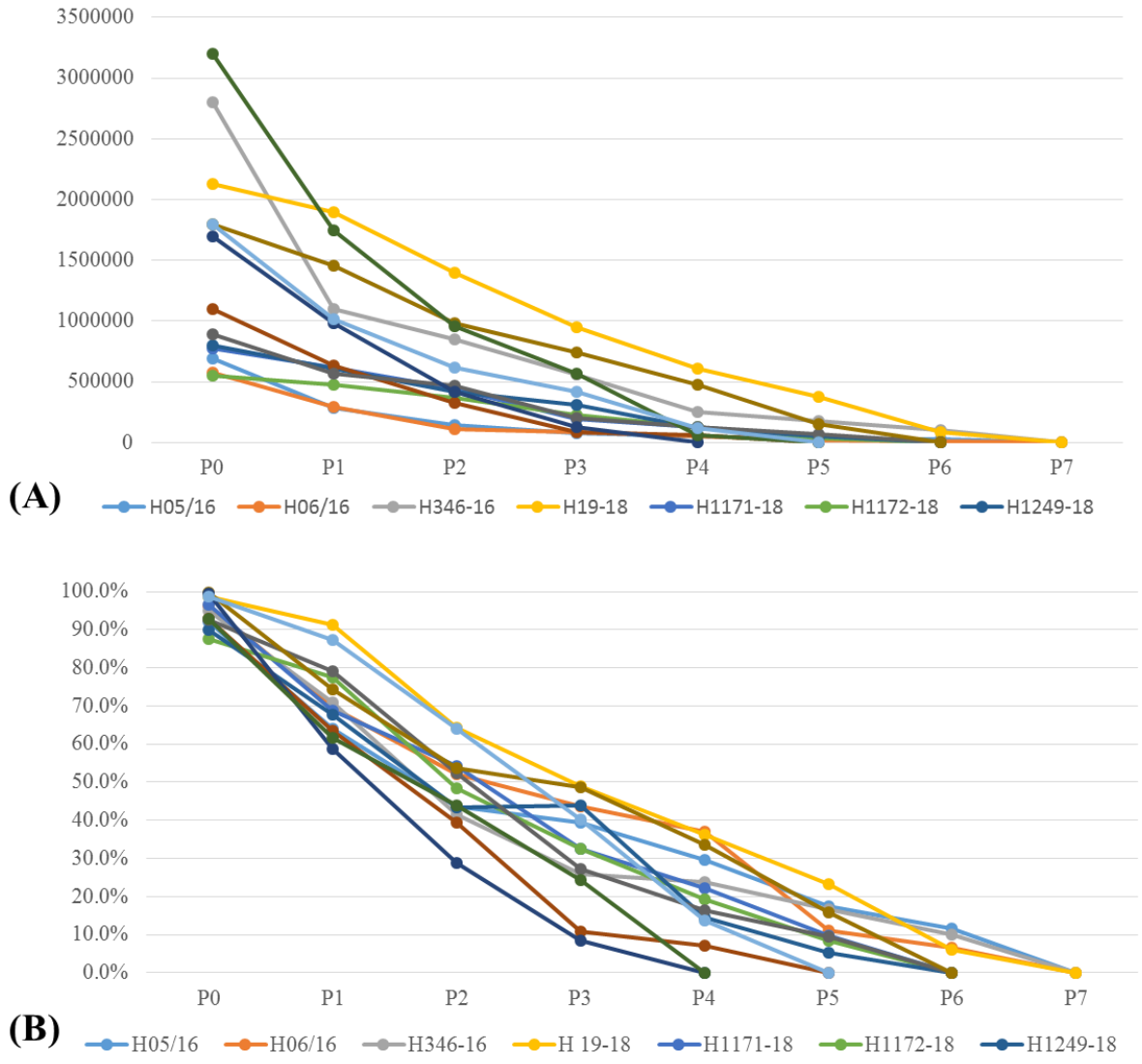

Source: Pulz, L. H., 2019

The histopathological criterion was used to divide the samples into two groups: low-grade and high-grade malignancy tumors. Mast cells from high-grade malignancy tumors were viable for a shorter period ($P=0.0442$) and less passages ($P<0.0001$) than mast cells from the low-grade samples (Figure 4).

Figure. 4. The effects of grade and passages on mast cell viability. High-grade tumor cells were viable in culture for a shorter period and less passages. All samples remained with living supernatants, for a maximum of 7 passages. The effect of grade was considered significant (P=0.0442) and the passage effect was considered extremely significant (P<0.0001)

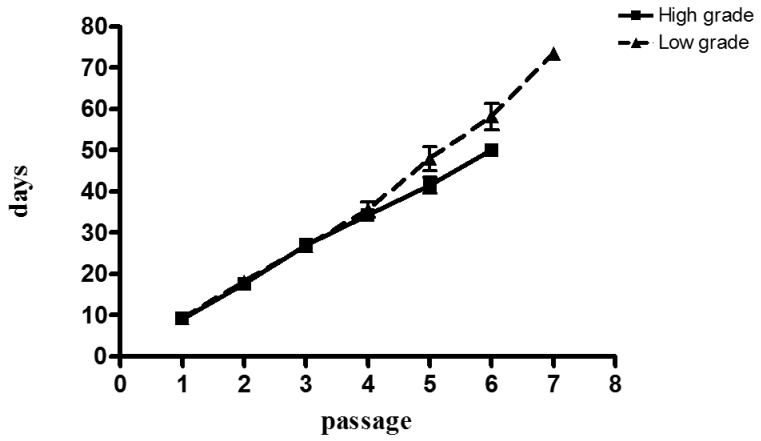

Source: Pulz, L. H., 2019

3.3.4 Quantitative real-time polymerase chain reaction analysis for Fibroblast-specific Protein 1 (FSP 1)

Some cells adhered to the flask and differentiated into spindle-shape morphology after several days *in vitro*. Neoplastic mast cells, many of which were partially degranulated, were in close proximity to these proliferating adherent cells with fibroblastic phenotype. Within 7 to 14 days, the cells had created a monolayer.

We used Fibroblast-specific Protein 1 messenger RNA (FSP1 mRNA) as a marker for fibroblasts, which was detected using reverse transcription polymerase chain reaction (PCR). Adherent cells from two tumor samples were evaluated on P0 and P1 and both displayed similar high expression of this gene (Table 2).

Table 2 – FSP1 mRNA levels measured by real-time PCR normalized to 18S ribosomal RNA (rRNA). Ct mean (*cicle threshold*) and difference between the FSP1 gene and the 18s endogenous gene for the two samples P0 and P1.

SAMPLE	FSP1 Cт Mean	18S Cт Mean	ΔCт Mean
334-16 (P0)	32,53105	27,35534	5,175709
346-16 (P1)	23,77721	20,39351	3,383701

3.3.5 *In vitro* characterization of stromal fibroblasts: immunofluorescence for α-smooth muscle-actin (SMA) and vimentin

Disaggregated cells were released in culture and, few days after cultivation, some of them adhered to the surface, assuming a spindle, flattened-spindle, or less frequently triangular shape, with frequent long terminal threadlike processes. These adherent cells were allowed to grow for 12–14 days and subsequently evaluated by immunofluorescence for the expression of vimentin and α-SMA. Normal fibroblasts are positive for vimentin and, additionaly, myofibroblasts are also α-SMA-positive. In early-passage, tumor fibroblasts (passages 1 to 3) were both highly positive for smooth muscle a-actin and vimentin (Figure 5).

Figure 5. Representative immunofluorescence images of myofibroblasts from canine MCTs culture. (a) Nuclei were stained with DAPI (4′,6-diamidino-2-phenylindole dihydrochloride; blue) (b) Adherent cells in MCT culture stained with vimentin antibody (red) and (c) anti–alpha actin (α-SMA) antibody (Phalloidin-FITC, green). (d) The merged image shows overlapping expression (Original magnification x400).

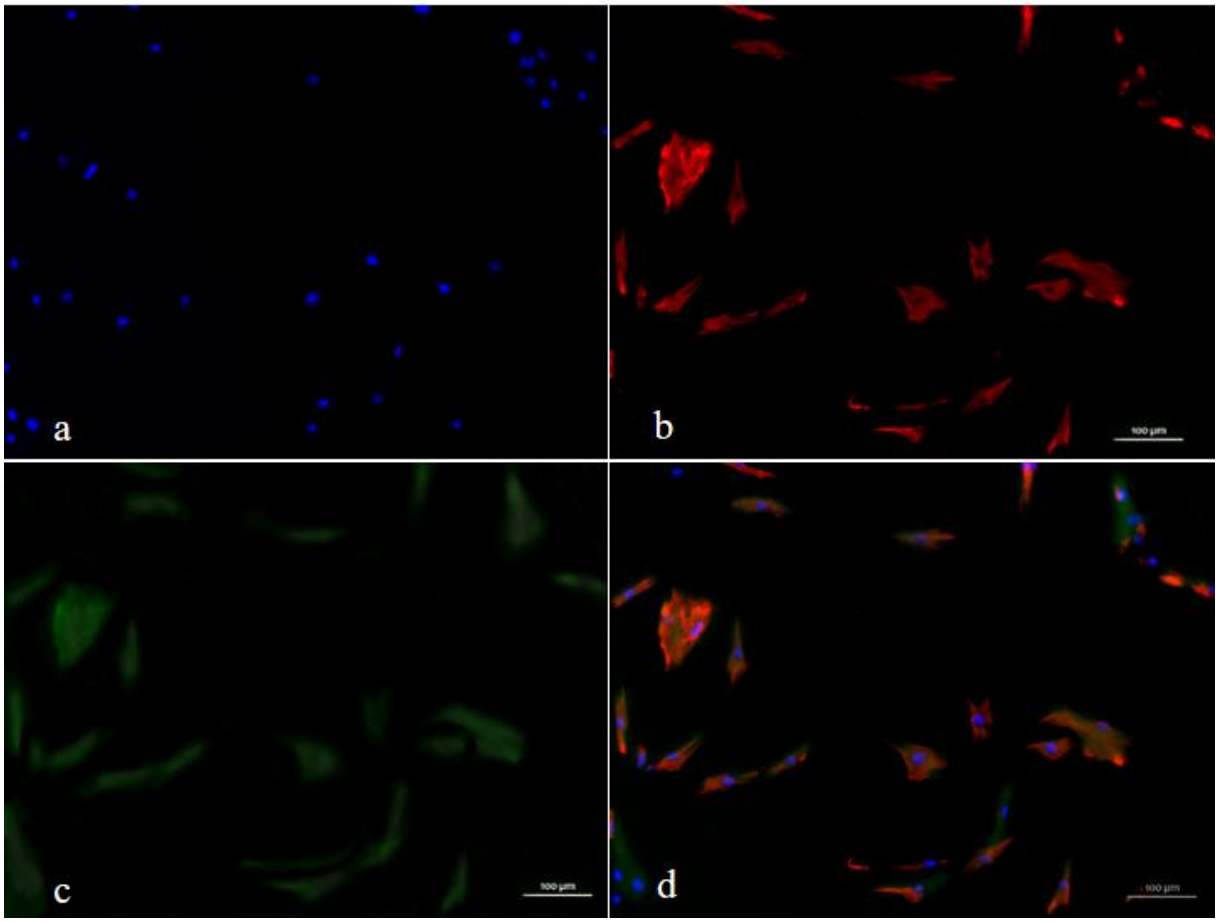

Source: Pulz, L. H., 2019

3.3.6 Fibroblasts senescence assay

In MCTs middle and late passage cultures (starting from P4), the fibroblasts ceased to be confluent and begun to change their phenotype to an enlarged cell morphology with depleted replicative potential.

Senescence-associated beta-galactosidase (SA-β-Gal) activity have been detected in fibroblasts of several samples and, by late passage, most cells were strongly positive for SA-β-Gal (Figure 6). The most intense staining was perinuclear and it was also observed that SA-β-Gal-positive cells correlated with the loss of replicative capacity, revealed by failure to reach confluence. The proportion of actively dividing cells decreases with serial passaging while increasing numbers of cells enter a state of terminal arrest.

Figure 6. Cytochemical detection of Senescence-associated β-Galactosidase (SA-β-Gal) activity in stromal fibroblasts of canine MCTs (Sample H05-16). Cells maintained in culture for 2 months (P5). (A) Positivity in most cells through the formation of blue precipitate in the cytoplasm. Bright field microscopy. (B) Fibroblasts demonstrating the most intense staining perinuclear. Phase contrast microscopy.

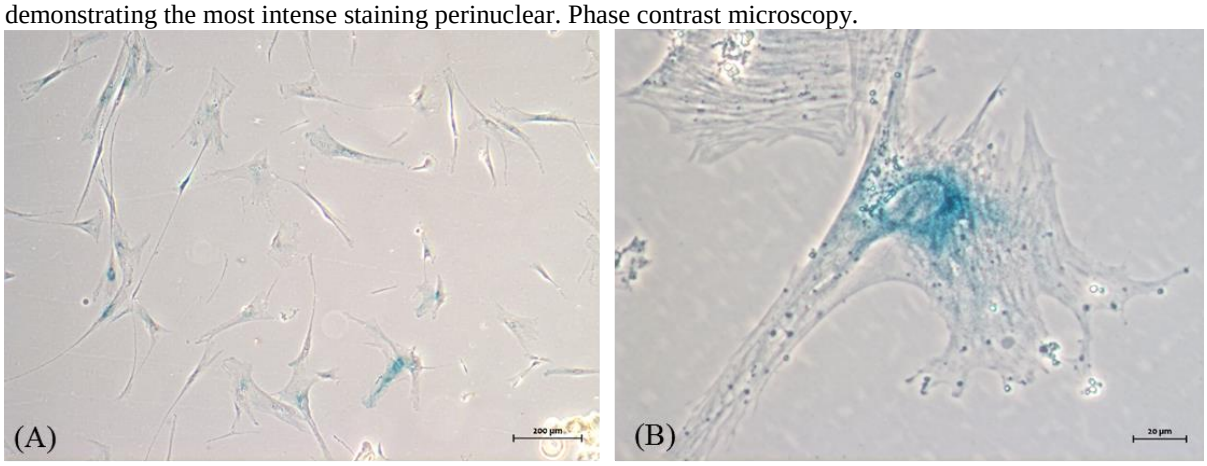

Source: Pulz, L. H., 2019

3.4 DISCUSSION

In the present study, we performed the primary culture of thirteen MCTs samples and demonstrated the incapacity of canine neoplastic mast cells to remain viable for long periods *in vitro* without the addition of growth factors or *in vivo* passages in mice, corroborating Pinello et al. (2009). Similarly, Dvorak et al. (1986) demonstrated that a population of human connective mast cells from lung could also be maintained ex vivo for a short-time (at least 13 days) when co-cultured with mouse skin-derived 3T3 fibroblasts. These human lung-derived mast cells adhered to the fibroblasts but did not multiply.

In contrast to our findings, several studies have demonstrated the establishment of mast cell lines derived from the canine MCTs without any addition of growth fators or cytokines (TAKAHASHI et al., 2001; OHASHI et al., 2006; TAKAHASHI et al., 2007; AMAGAI et al., 2008; OHMORI et al., 2008; MATSUDA et al., 2011). However, the descriptions of these cell cultures are not in enough detail to allow any definitive conclusion about their maintenance. Moreover, no cell separation methods for neoplastic mast cells were described.

Several reports indicate that long-term cultures of canine cutaneous mast cells are possible with combined *in vitro* and *in vivo* approaches (LAZARUS et al., 1986; CAUGHEY, et al., 1988; DEVINNEY, GOLD, 1990; ISHIGURO et al 2001, NAGAMINE et al., 2011). The notion that mast cell phenotype can be importantly regulated by the "microenvironment" has been the subject of much discussion and interest. There are many possible sources of variation in microenvironmental factors which might have an effect on mast cell phenotype, and each of these might potentially influence mast cell mechanisms of *in vitro* survival (DVORAK et al., 1992; DVORAK et al., 1992; ROSSI et al. 1998).

Enzymatic disaggregation of tumor nodules yielded a population of at least 90% of viable cells, as assessed by Trypan blue dye exclusion (CALONICO et al., 1985; DEMORA et al., 1996; LAZARUS et al., 1986). With respect to neoplastic mast cells, it was established by others that cells obtained from canine MCTs presented a mature mast cell phenotype, with variable amounts of cytoplasmic metachromatic granules (ISHIGURO et al., 2001; GARCIA et al., 1998; OHMORi et al., 2008). Neoplastic mast cells grew in suspension as single cells or in clusters, and this condition was similar to that observed in other canine MCT cultures (GARCÍA et al., 1998; TAKAHASHI et al., 2001; AMAGAI et al., 2008). We found that the number of metachromatic granules in cultured neoplastic mast cells was smaller than those of normal canine mast cells (LIN, RUSH, LONDON, 2006) and that there was a gradual decrease in their quantity *in vitro* (CALONICO et al., 1985). This feature has also been observed in human and munine mast cell lines (HORTON, O´BRIEN, 1983; TERTIAN et al., 1981). It should also be considered that *in vitro* mast cell aggregation through adhesion molecules can induce degranulation and histamine release (ISHIGURO et al., 2001; CONTI et al, 1995; INAMURA et al., 1998). We suggest that the progressive degranulation may be therefore caused by cell-to-cell aggregation and induced by and mechanical handling effects (DE MORA, 1993).

We believe that neoplastic mast cell survival *in vitro* depends, in part, on the interaction with the adhered fibroblasts and CAFs. Fibroblasts are known to secrete Stem Cell Factor (SCF), which is the main growth factor for mast cells (DVORAK et al., 1992; ROSSI et al.,

1998) and an essential factor for mast cell growth in rodent and human mast cells cultures (DVORAK et al., 1992; YAMADA et al., 2003; TSAI et al., 1991; LEE et al., 2010). In addition, several studies with mast cell cultures indicated the requirement of both interleukin-3 and SCF to expansion and maturation, even in the presence of stromal cells (YAMADA et al., 2003, OGAWA et al., 1983). The literature data suggest that the establishment of mast cell lines in permanent culture *in vitro* with no passages by nude mice should depend on SCF supplemented medium (ROSSI et al., 1998; LEE et al., 2010) and the presence of stromal cells may assist in the maintenance of mast cells *in vitro* (YAMADA et al., 2003; LEVI-SCHAFFER et al., 1986; RAIZMAN et al., 1990). Finally, we need to consider that the parcial decrease of mast cells in passages may in part reflect cell loss during the harvesting procedure (DEMORA et al., 1996) and because cultures were at a relatively low density.

Skin tumors used in this study provided a fibroblast population that decline *in vitro* with serial passaging, with increasing number of cells entering replicative senescence (MARTIN, SPRAGUE, EPSTEIN, 1970; SCHNEIDER, MITSUI, 1976; FUNK et al., 2000). Cellular senescence is characterized by enlarged cell size, activation of a lysosomal SA-β-Gal activity (DIMRI et al., 1995) and earlier onset of cell culture senescence with the increasing age of the cell culture donor (SCHNEIDER, MITSUI, 1976; BOWMAN, MEEK, DANIEL, 1975; KOHN, 1975). This process is thought to be caused by aging and these "aged" skin fibroblasts with limited replicative potential may be due to canine cellular aging *in vivo*, since the mean age of the dogs included in the present study was around 7.5 years.

In vivo, fibroblasts from cancer stroma undergo a myofibroblast transformation as part of the cellular response to neoplastic growth (CHIAVEGATO et al., 1995). These cells are recognised essentially, but not exclusively, based on smooth muscle α-actin expression and are called cancer-associated fibroblasts (CAFs) (VALENTI et al., 2001; KOJIMA Y et al., 2010). We have shown the presence of myofibroblasts in canine MCT cultures. This finding is in concordance with the observations of Giuliano et al. (2017), which showed that fibroblasts from canine MCT stroma have CAF phenotype and was correlated positively wtih high grade, high mitotic index and high Ki67 expression. We believe that this feature might be important to the understanding of the different clinical responses to chemotherapy, since CAFs could influence the drug-sensitivity of cancer cells (ÖSTMAN, AUGSTEN, 2009).

Besides cell loss in all samples, the histopathological grade had an effect on culture assays. The results demonstrate that histopathological grade, which is related to the degree of cell differentiation, can influence the cultivation time and number of passages. These results are interesting in the light of the different experimental approaches undertaken in literature. No

previously published work compares the *in vitro* behavior of tumors with different histopathological grades. A variability of mast cell phenotype — for example, the differences in the content of cellular proteases — reflects the action of the local microenvironment (ROSSI et al., 1998), the mechanisms underlying the relationship between the grade of malignancy and the the culture conditions remain unclear.

3.5 CONCLUSION

In conclusion, reproducible development of tumor-derived mast cells by a long-term culture may need *in vivo* passages, fibroblasts interactions and/or supplemented medium with growth factors. Cultures without artificial stimuli would be a major breakthrough to understand canine mast cell tumor biology. We also showed that stromal MCTs fibroblasts present a CAF phenotype *in vitro* when cocultured with neoplastic mast cells. Fibroblasts and CAFs transcription factors could be important for MCTs malignant phenotypes, through direct or indirect stimuli. Different stroma cells cultured together communicate to create a tumor-permissive microenvironment and thus contribute to the maintenance of cancer mast cells. Signaling mechanisms involved in these interactions may constitute attractive therapeutic targets to block canine MCT progression. Ongoing studies in our laboratory aim to investigate canine mast cells and tumoral stroma cells interactions.

3.6 REFERENCES

AMAGAI, Y.; TANAKA, A.; OHMORI, K.; MATSUDA, H. Establishment of a novel high-affinity IgE receptor-positive canine mast cell line with wild-type c-kit receptors. **Biochemical and Biophysical Research Communications**, v. 366, n. 3, p. 857-861, 2008.

AMAGAI, Y.; TANAKA, A.; MATSUDA, A.; OIDA, K.; JUNG, K.; MATSUDA, H. The phosphoinositide 3-kinase pathway is crucial for the growth of canine mast cell tumors. **Journal of Veterinary Medical Science**, v. 75, n. 6, p. 791-794, 2013.

BOWMAN, P. D.; MEEK, R. L.; DANIEL, C. W. Aging of human fibroblasts in vitro: correlations between DNA synthetic ability and cell size. **Experimental Cell Research**, v. 93, n. 1, p. 184-190, 1975.

BRAZÍS, P.; TORRES, R.; QUERALT, M.; MORA, F. D.; FERRER, L.; PUIGDEMONT, A. Evaluation of cell-surface IgE receptors on the canine mastocytoma cell line C2 maintained in continuous culture. **American Journal of Veterinary Research**, v. 63, n. 5, p. 763-766, 2002.

BUTTERFIELD, J. H.; WEILER, D.; DEWALD, G.; GLEICH, G. J. Establishment of an immature mast cell line from a patient with mast cell leukemia. **Leukemia Research**, v. 12, n. 4, p. 345-355, 1988.

CALONICO, L. D.; PHILLIPS, M. J.; MCDONALD, D. M.; GOLD, W. M. An ultrastructural analysis of dog mastocytoma cells and normal mast cells. **The Anatomical Record**, v. 212, n. 4, p. 399-407, 1985.

CAUGHEY, G. H.; LAZARUS, S. C.; VIRO, N. F.; GOLD, W. M.; NADEL, J. A. Tryptase and chymase: comparison of extraction and release in two dog mastocytoma lines. **Immunology**, v. 63, n. 2, p. 339, 1988.

CHIAVEGATO, A.; BOCHATON-PIALLAT, M. L.; D'AMORE, E.; SARTORE, S.; GABBIANI, G. Expression of myosin heavy chain isoforms in mammary epithelial cells and in myofibroblasts from different fibrotic settings during neoplasia. **Virchows Archiv**, v. 426, n. 1, p. 77-86, 1995.

CONTI, P.; BOUCHER, W.; LETOURNEAU, R.; FELICIANI, C.; REALE, M.; BARBACANE, R. C. et al. Monocyte chemotactic protein-1 provokes mast cell aggregation and [3H] 5HT release. **Immunology**, v. 86, n. 3, p. 434, 1995.

DEMORA, F.; GARCIA, G.; PUIGDEMONT, A.; ARBOIX, M.; FERRER, L. Skin mast cell releasability in dogs with atopic dermtitis. **Inflammation Research**, v. 45, n. 8, p. 424-427, 1996.

DEVINNEY, R.; GOLD, W. M. Establishment of two dog mastocytoma cell lines in continuous culture. **Studies**, v. 9, p. 10, 1990.

DIMRI, G. P.; LEE, X.; BASILE, G.; ACOSTA, M.; SCOTT, G.; ROSKELLEY, C.; MEDRANO, E. E.; LINSKENS, M.; RUBELJ, I.; PEREIRA-SMITH, O.; PEACOCKE, M.; CAMPISI, J. A biomarker that identifies senescent human cells in culture and in aging skin in vivo. **Proceedings of the National Academy of Sciences**, v. 92, n. 20, p. 9363-9367, 1995.

DVORAK, A. M.; SCHLEIMER, R. P.; SCHULMAN, E. S.; LICHTENSTEIN, L. M. Human mast cells use conservation and condensation mechanisms during recovery from degranulation. In vitro studies with mast cells purified from human lungs. **Laboratory Investigation; a journal of technical methods and pathology**, v. 54, n. 6, p. 663-678, 1986.

DVORAK, A. M.; FURITSU, T.; KISSELL-RAINVILLE, S.; ISHIZAKA, T. Ultrastructural identification of human mast cells resembling skin mast cells stimulated to develop in long-term human cord blood mononuclear cells cultured with 3T3 murine skin fibroblasts. **Journal of Leukocyte Biology**, v. 51, n. 6, p. 557-569, 1992.

FUNK, W. D.; WANG, C. K.; SHELTON, D. N.; HARLEY, C. B.; PAGON, G. D.; HOEFFLER, W. K. Telomerase expression restores dermal integrity to in vitro-aged fibroblasts in a reconstituted skin model. **Experimental Cell Research**, v. 258, n. 2, p. 270-278, 2000.

FURITSU, T.; TSUJIMURA, T.; TONO, T.; IKEDA, H.; KITAYAMA, H.; KOSHIMIZU, U.; SUGIHARA, H.; BUTTERFIELD, J. H.; ASHMAN, L. K.; KANAYAMA, Y.; MATSUZAWA, Y.; KITAMURA, Y.; KANAKURA, Y. Identification of mutations in the coding sequence of the proto-oncogene c-kit in a human mast cell leukemia cell line causing ligand-independent activation of c-kit product. **The Journal of Clinical Investigation**, v. 92, n. 4, p. 1736-1744, 1993.

GALLI, S. J. The mast cell: a versatile effector cell for a challenging world. **International archives of allergy and immunology**, v. 113, n. 1-3, p. 14-22, 1997.

GARCIA, G.; BRAZIS, P.; MAJO, N.; FERRER, L.; DE MORA, F.; PUIGDEMONT, A. Comparative morphofunctional study of dispersed mature canine cutaneous mast cells and BR cells, a poorly differentiated mast cell line from a dog subcutaneous mastocytoma. **Veterinary Immunology and Immunopathology**, v. 62, n. 4, p. 323-337, 1998.

GIULIANO, A.; DOS SANTOS HORTA, R.; CONSTANTINO-CASAS, F.; HOATHER, T.; DOBSON, J. Expression of Fibroblast Activating Protein and Correlation with Histological Grade, Mitotic Index and Ki67 Expression in Canine Mast Cell Tumours. **Journal of comparative pathology**, v. 156, n. 1, p. 14-20, 2017.

GOETZL, E. J.; PHILLIPS, M. J.; GOLD, W. M. Stimulus specificity of the generation of leukotrienes by dog mastocytoma cells. **Journal of Experimental Medicine**, v. 158, n. 3, p. 731-737, 1983.

GUECK, T.; SEIDEL, A.; FUHRMANN, H. Effects of essential fatty acids on mediators of mast cells in culture. **Prostaglandins, Leukotrienes and Essential Fatty acids**, v. 68, n. 5, p. 317-322, 2003.

HORTON, M. A.; O'BRIEN, H. A. Characterization of human mast cells in long-term culture. **Blood**, v. 62, n. 6, p. 1251-1260, 1983.

INAMURA, N.; MEKORI, Y. A.; BHATTACHARYYA, S. P.; BIANCHINE, P. J.; METCALFE, D. D. Induction and enhancement of FcεRI-dependent mast cell degranulation following coculture with activated T cells: dependency on ICAM-1-and leukocyte function-associated antigen (LFA)-1-mediated heterotypic aggregation. **The Journal of Immunology**, v. 160, n. 8, p. 4026-4033, 1998.

ISHIGURO, T.; KADOSAWA, T.; MORI, K.; TAKAGI, S.; OKUMURA, M.; FUJINAGA, T. Establishment and characterization of a new canine mast cell tumor cell line. **Journal of Veterinary Medical Science**, v. 63, n. 9, p. 1031-1034, 2001.

KIUPEL, M.; WEBSTER, J. D.; BAILEY, K. L.; BEST, S.; DELAY, J.; DETRISAC, C. J. et al. Proposal of a 2-tier histologic grading system for canine cutaneous mast cell tumors to more accurately predict biological behavior. **Veterinary Pathology**, v. 48, n. 1, p. 147-155, 2011.

KOHN, R. R. Aging and cell division. **Science**, v. 188, n. 4185, p. 203-204, 1975.

KOJIMA, Y.; ACAR, A.; EATON, E. N.; MELLODY, K. T.; SCHEEL, C.; BEN-PORATH, I. et al. Autocrine TGF-β and stromal cell-derived factor-1 (SDF-1) signaling drives the evolution of tumor-promoting mammary stromal myofibroblasts. **Proceedings of the National Academy of Sciences**, v. 107, n. 46, p. 20009-20014, 2010.

LAZARUS, S. C.; DEVINNEY, R.; MCCABE, L. J.; FINKBEINER, W. E.; ELIAS, D. J.; GOLD, W. M. Isolated canine mastocytoma cells: propagation and characterization of two cell lines. **American Journal of Physiology-Cell Physiology**, v. 251, n. 6, p. C935-C944, 1986.

LEE, H. N.; KIM, C. H.; SONG, G. G.; CHO, S. W. Effects of IL-3 and SCF on histamine production kinetics and cell phenotype in rat bone marrow-derived mast cells. **Immune Network**, v. 10, n. 1, p. 15-25, 2010.

LEVI-SCHAFFER, F.; AUSTEN, K. F.; GRAVALLESE, P. M.; STEVENS, R. L. Coculture of interleukin 3-dependent mouse mast cells with fibroblasts results in a phenotypic change of the mast cells. **Proceedings of the National Academy of Sciences**, v. 83, n. 17, p. 6485-6488, 1986.

LIN, T. Y.; RUSH, L. J.; LONDON, C. A. Generation and characterization of bone marrow-derived cultured canine mast cells. **Veterinary Immunology and Immunopathology**, v. 113, n. 1-2, p. 37-52, 2006.

LIVAK, K. J.; SCHMITTGEN, T. D. Analysis of relative gene expression data using real-time quantitative PCR and the $2^{-\Delta\Delta CT}$ method. **Methods**, v. 25, n. 4, p. 402-408, 2001.

MARTIN, G. M.; SPRAGUE, C. A.; EPSTEIN, C. J. Replicative life-span of cultivated human cells. **Lab. Invest**, v. 23, n. 1, p. 86-92, 1970.

MATSUDA, A.; TANAKA, A.; AMAGAI, Y.; OHMORI, K.; NISHIKAWA, S.; XIA, Y. et al. Glucocorticoid sensitivity depends on expression levels of glucocorticoid receptors in canine neoplastic mast cells. **Veterinary Immunology and Immunopathology**, v. 144, n. 3-4, p. 321-328, 2011.

NAGAMINE, M. K.; SANCHES, D. S.; PINELLO, K. C.; TORRES, L. N.; MENNECIER, G.; LATORRE, A. O.; FUKUMASU, H.; DAGLI, M. L. Z. In vitro inhibitory effect of trichostatin A on canine grade 3 mast cell tumor. **Veterinary Research Communications**, v. 35, n. 6, p. 391-399, 2011.

OGAWA, M.; NAKAHATA, T.; LEARY, A. G.; STERK, A. R.; ISHIZAKA, K.; ISHIZAKA, T. Suspension culture of human mast cells/basophils from umbilical cord blood mononuclear cells. **Proceedings of the National Academy of Sciences**, v. 80, n. 14, p. 4494-4498, 1983.

OHASHI, E.; MIYAJIMA, N.; NAKAGAWA, T.; TAKAHASHI, T.; KAGECHIKA, H.; MOCHIZUKI, M.; NISHIMURA, R.; SASAKI, N. Retinoids induce growth inhibition and apoptosis in mast cell tumor cell lines. **Journal of Veterinary Medical Science**, v. 68, n. 8, p. 797-802, 2006.

OHMORI, K.; KAWARAI, S.; YASUDA, N.; TANAKA, A.; MATSUDA, H.; NISHIMURA, R.; SASAKI, N.; TSUJIMOTO, H.; MASUDA, K. Identification of c-kit mutations-independent neoplastic cell proliferation of canine mast cells. **Veterinary Immunology and Immunopathology**, v. 126, n. 1-2, p. 43-53, 2008.

ÖSTMAN, A.; AUGSTEN, M. Cancer-associated fibroblasts and tumor growth–bystanders turning into key players. **Current opinion in genetics & development**, v. 19, n. 1, p. 67-73, 2009.

PATNAIK, A. K., EHLER, W. J.; MACEWEN, E. G. Canine cutaneous mast cell tumor: morphologic grading and survival time in 83 dogs. **Veterinary Pathology**, v. 21, n. 5, p. 469-474, 1984.

PINELLO, K. C.; NAGAMINE, M.; SILVA, T. C.; MATSUZAKI, P.; CAETANO, H. V.; TORRES, L. et al. In vitro chemosensitivity of canine mast cell tumors grades II and III to all-trans-retinoic acid (ATRA). **Veterinary Research Communications**, v. 33, n. 6, p. 581-588, 2009.

RAIZMAN, M. B.; AUSTEN, K. F.; KATZ, H. R. Mast cell heterogeneity. Differential synthesis and expression of glycosphingolipids by mouse serosal mast cells as compared to IL-3-dependent bone marrow culture-derived mast cells before or after coculture with 3T3 fibroblasts. **The Journal of Immunology**, v. 145, n. 5, p. 1463-1468, 1990.

ROSSI, G. L.; DI COMITE, V.; OLIVIERI, D. Mast cell cultures: bench to bedside. **Clinical & Experimental Allergy**, v. 28, n. 10, p. 1182-1190, 1998.

SCHNEIDER, E. L.; MITSUI, Y. The relationship between in vitro cellular aging and in vivo human age. **Proceedings of the National Academy of Sciences**, v. 73, n. 10, p. 3584-3588, 1976.

SOLL, A. H.; LEWIN, K.; BEAVEN, M. A. Isolation of histamine-containing cells from canine fundic mucosa. **Gastroenterology**, v. 77, n. 6, p. 1283-1290, 1979.

SOLL, A. H.; TOOMEY, M.; CULP, D.; SHANAHAN, F.; BEAVEN, M. A. Modulation of histamine release from canine fundic mucosal mast cells. **American Journal of Physiology-Gastrointestinal and Liver Physiology**, v. 254, n. 1, p. G40-G48, 1988.

STROBER, W. Trypan blue exclusion test of cell viability. **Current Protocols in Immunology**, v. 21, n. 1, p. A. 3B. 1-A. 3B. 2, 1997.

TAKAHASHI, T.; KITANI, S.; NAGASE, M.; MOCHIZUKI, M.; NISHIMURA, R.; MORITA, Y.; SASAKI, N. IgG-mediated histamine release from canine mastocytoma-derived cells. **International Archives of Allergy and Immunology**, v. 125, n. 3, p. 228-235, 2001.

TAKAHASHI, T.; OHASHI, E.; NAKAGAWA, T.; MOCHIZUKI, M.; NISHIMURA, R.; SASAKI, N. Role of β1 integrins in adhesion of canine mastocytoma cells to extracellular matrix proteins. **Journal of Veterinary Medical Science**, v. 69, n. 5, p. 495-499, 2007.

TERTIAN, G.; YUNG, Y-P.; GUY-GRAND, D.; MOORE, M. A. Long-term in vitro culture of murine mast cells. I. Description of a growth factor-dependent culture technique. **The Journal of Immunology**, v. 127, n. 2, p. 788-794, 1981.

TSAI, M.; TAKEISHI, T.; THOMPSON, H.; LANGLEY, K. E.; ZSEBO, K. M.; METCALFE, D. D., et al. Induction of mast cell proliferation, maturation, and heparin synthesis by the rat c-kit ligand, stem cell factor. **Proceedings of the National Academy of Sciences**, v. 88, n. 14, p. 6382-6386, 1991.

VAIL, D. M. Mast cell tumors. In: WITHROW S. J, MACEWEN E. G. **Small Animal Clinical Oncology**. Philadelphia: W.B. Saunders, 1996. p. 192–210.

VALENTI, M. T.; AZZARELLO, G.; BALDUCCI, E.; SARTORE, S.; SANDRI, M.; MANCONI, R. et al. Conditioned medium from MCF-7 cell line induces myofibroblast differentiation, decreased cell proliferation, and increased apoptosis in cultured normal fibroblasts but not in fibroblasts from malignant breast tissue. **The Histochemical Journal**, v. 33, n. 9-10, p. 499-509, 2001.

YAMADA, N.; MATSUSHIMA, H.; TAGAYA, Y.; SHIMADA, S.; KATZ, S. I. Generation of a large number of connective tissue type mast cells by culture of murine fetal skin cells. **Journal of Investigative Dermatology**, v. 121, n. 6, p. 1425-1432, 2003.

YE, J.; COULOURIS, G.; ZARETSKAYA, I.; CUTCUTACHE, I.; ROZEN, S.; MADDEN, T. L. Primer-BLAST: a tool to design target-specific primers for polymerase chain reaction. **BMC Bioinformatics**, v. 13, n. 1, p. 134, 2012.

APPENDIX

APPENDIX – Supporting information: Neoplastic mast cell quantification in the supernatant. Data with the description of each lesion detailing the quantification of live and death cells/mL and the respectives percentages of viable cells in each passage of canine MCT culture

Supplementary Table 1. Neoplastic mast cell quantification in the supernatant. Sample H05-16.

Date	Days of cultivation	Passage	Nº of live cells in the supernatant/ml	Nº of dead cells in the supernatant/ml	Total (live and death) cells/ml	Percentage of viable cells
20/01/2016	0	P0	690000	60000	750000	92.0%
29/01/2016	9	P1	285000	160000	445000	64.0%
04/02/2016	15	P2	140000	180000	320000	43.7%
12/02/2016	23	P3	75000	115000	190000	39.4%
19/02/2016	30	P4	56000	133000	189000	29.6%
26/02/2016	37	P5	30000	143000	173000	17.3%
06/03/2016	46	P6	25000	192000	217000	11.5%
04/04/2016	74	P7	0	*	*	0.0%

Supplementary Table 2. Neoplastic mast cell quantification in the supernatant. Sample H06-16.

Date	Days of cultivation	Passage	Nº of live cells in the supernatant/ml	Nº of dead cells in the supernatant/ml	Total (live and death) cells/ml	Percentage of viable cells
20/01/2016	0	P0	580000	30000	610000	95.1%
29/01/2016	9	P1	290000	105000	395000	73.4%
04/02/2016	15	P2	110000	155000	265000	41.5%
12/02/2016	23	P3	87000	220000	307000	28.3%
19/02/2016	30	P4	50000	255000	305000	16.4%
26/02/2016	37	P5	20000	160000	180000	11.1%
06/03/2016	46	P6	10000	140000	150000	6.7%
04/04/2016	74	P7	0	*	*	0.0%

Supplementary Table 3. Neoplastic mast cell quantification in the supernatant. Sample H346-16.

Date	Days of cultivation	Passage	Nº of live cells in the supernatant/ml	Nº of dead cells in the supernatant/ml	Total (live and death) cells/ml	Percentage of viable cells
19/07/2016	0	P0	2800000	150000	2950000	94.9%
26/07/2016	7	P1	1100000	450000	1550000	71.0%
06/08/2016	18	P2	850000	1200000	2050000	41.5%
13/08/2016	25	P3	560000	1600000	2160000	25.9%
22/08/2016	34	P4	250000	800000	1050000	23.8%
12/09/2016	55	P5	180000	900000	1080000	16.7%
21/09/2016	64	P6	100000	900000	1000000	10.0%
28/09/2016	71	P7	0	*	*	0.0%

Supplementary Table 4. Neoplastic mast cell quantification in the supernatant. Sample H19-18.

Date	Days of cultivation	Passage	Nº of live cells in the supernatant/ml	Nº of dead cells in the supernatant/ml	Total (live and death) cells/ml	Percentage of viable cells
06/02/2018	0	P0	2130000	27000	2157000	98.7%
14/02/2018	8	P1	1900000	180000	2080000	91.3%
23/02/2018	17	P2	1400000	780000	2180000	64.2%
06/03/2018	30	P3	950000	990000	1940000	49.0%
16/03/2018	40	P4	610000	1070000	1680000	36.3%
27/03/2018	51	P5	380000	1250000	1630000	23.3%
17/04/2018	61	P6	85000	1300000	1385000	6.1%
01/05/2018	75	P7	0	*	*	0.0%

Supplementary Table 5. Neoplastic mast cell quantification in the supernatant. Sample H1171-18.

Date	Days of cultivation	Passage	Nº of live cells in the supernatant/ml	Nº of dead cells in the supernatant/ml	Total (live and death) cells/ml	Percentage of viable cells
22/08/2018	0	P0	775000	26000	801000	96.7%
31/08/2018	9	P1	615000	280000	895000	68.7%
10/09/2018	19	P2	440000	370000	810000	54.3%
18/09/2018	27	P3	195000	405000	600000	32.5%
27/09/2018	36	P4	125000	435000	560000	22.3%
13/10/2018	52	P5	45000	415000	460000	9.8%
24/10/2018	63	P6	0	*	*	0.0%

Supplementary Table 6. SNeoplastic mast cell quantification in the supernatant. Sample H1172-18.

Date	Days of cultivation	Passage	Nº of live cells in the supernatant/ml	Nº of dead cells in the supernatant/ml	Total (live and death) cells/ml	Percentage of viable cells
22/08/2018	0	P0	550000	78000	628000	87.6%
31/08/2018	9	P1	480000	140000	620000	77.4%
10/09/2018	19	P2	370000	395000	765000	48.4%
18/09/2018	27	P3	230000	480000	710000	32.4%
27/09/2018	36	P4	125000	520000	645000	19.4%
13/10/2018	52	P5	40000	435000	475000	8.4%
24/10/2018	63	P6	0	*	*	0.0%

Supplementary Table 7. Neoplastic mast cell quantification in the supernatant. Sample H1249-18.

Date	Days of cultivation	Passage	Nº of live cells in the supernatant/ml	Nº of dead cells in the supernatant/ml	Total (live and death) cells/ml	Percentage of viable cells
01/09/2018	0	P0	800000	90000	890000	89.9%
14/09/2018	14	P1	610000	290000	900000	67.7%
24/09/2018	24	P2	420000	550000	970000	43.3%
03/10/2018	33	P3	310000	580000	890000	43.8%
13/10/2018	43	P4	115000	680000	795000	14.6%
22/10/2018	52	P5	50000	890000	940000	5.3%
03/11/2018	64	P6	0	*	*	0.0%

Supplementary Table 8. Neoplastic mast cell quantification in the supernatant. Sample H232-16.

Date	Days of cultivation	Passage	Nº of live cells in the supernatant/ml	Nº of dead cells in the supernatant/ml	Total (live and death) cells/ml	Percentage of viable cells
30/04/2016	0	P0	1100000	85000	1185000	92.8%
06/05/2016	6	P1	630000	360000	990000	63.6%
16/05/2016	16	P2	330000	510000	840000	39.3%
24/05/2016	24	P3	87000	720000	807000	10.8%
30/05/2016	30	P4	57500	750000	807500	7.1%
06/06/2016	36	P5	0	*	*	0.0%

Supplementary Table 9. Neoplastic mast cell quantification in the supernatant. Sample H334-16.

Date	Days of cultivation	Passage	Nº of live cells in the supernatant/ml	Nº of dead cells in the supernatant/ml	Total (live and death) cells/ml	Percentage of viable cells
24/06/2016	0	P0	890000	70000	960000	92.7%
04/07/2016	12	P1	565000	150000	715000	79.0%
09/07/2016	17	P2	470000	425000	895000	52.5%
18/07/2016	26	P3	205000	550000	755000	27.1%
26/07/2016	34	P4	125000	635000	760000	16.4%
04/08/2016	42	P5	0	*	*	0.0%

Supplementary Table 10. Neoplastic mast cell quantification in the supernatant. Sample H395-17.

Date	Days of cultivation	Passage	Nº of live cells in the supernatant/ml	Nº of dead cells in the supernatant/ml	Total (live and death) cells/ml	Percentage of viable cells
11/05/2017	0	P0	1800000	5000	1805000	99.7%
20/05/2017	9	P1	1460000	505000	1965000	74.3%
29/05/2017	18	P2	980000	840000	1820000	53.8%
09/06/2017	29	P3	746000	786000	1532000	48.7%
18/06/2017	38	P4	478000	950000	1428000	33.5%
23/06/2017	43	P5	150000	800000	950000	15.8%
30/06/2017	50	P6	0	*	*	0.0%

Supplementary Table 11. Neoplastic mast cell quantification in the supernatant. Sample H550-17.

Date	Days of cultivation	Passage	Nº of live cells in the supernatant/ml	Nº of dead cells in the supernatant/ml	Total (live and death) cells/ml	Percentage of viable cells
10/07/2017	0	P0	1700000	10500	1710500	99.4%
17/07/2017	7	P1	985000	690000	1675000	58.80%
22/07/2017	12	P2	420000	1040000	1460000	28.7%
01/08/2017	22	P3	126000	1370000	1496000	8.4%
09/08/2017	30	P4	0	*	*	0.00%

Supplementary Table 12. Neoplastic mast cell quantification in the supernatant. Sample 603-17.

Date	Days of cultivation	Passage	Nº of live cells in the supernatant/ml	Nº of dead cells in the supernatant/ml	Total (live and death) cells/ml	Percentage of viable cells
19/10/2017	0	P0	3200000	245000	3445000	92.9%
30/10/2017	11	P1	1750000	1096000	2846000	61.5%
10/11/2017	22	P2	960000	1230000	2190000	43.80%
18/11/2017	30	P3	365000	1130000	1495000	24.40%
24/11/2017	36	P4	0	*	*	0.00%

Supplementary Table 13. Neoplastic mast cell quantification in the supernatant. Sample 816-18.

Date	Days of cultivation	Passage	Nº of live cells in the supernatant/ml	Nº of dead cells in the supernatant/ml	Total (live and death) cells/ml	Percentage of viable cells
21/07/2018	0	P0	1800000	25000	1825000	98.6%
31/07/2018	10	P1	1020000	149500	1169500	87.2%
10/08/2018	21	P2	620000	350000	970000	63.9%
20/08/2018	31	P3	415000	615000	1030000	40.3%
27/08/2018	38	P4	120000	760000	880000	13.6%
03/09/2018	45	P5	0	*	*	0.0%

4 ARTICLE 3

INTERCELLULAR INTERACTIONS BETWEEN MAST CELLS AND STROMAL FIBROBLASTS OBTAINED FROM CANINE CUTANEOUS MAST CELL TUMORS

4.1 INTRODUCTION

Cutaneous mast cell tumors (MCTs) are among the most frequent cutaneous cancer types in dogs (DOBSON et al. 2002; GRÜNTZIG et al. 2016). Their clinical behavior varies from benign to highly aggressive with high metastasis rate and morbidity, which complicates accurate prediction (WELLE et al. 2008; BLACKWOOD et al. 2012). Retrospective studies conducted in large dog populations present valuable contributions to the knowledge about the clinical nature of this neoplasm. However, the study of neoplastic cells behavior *in vitro* is essential to reveal interactions between neoplastic and other cells, and to discover new therapeutic targets (HOLLE, YOUNG, SPATZ, 2016, MIKI et al., 2012). Cell culture allows cancer cells to grow and to be maintained outside of the body. This technique have been providing pivotal information as to understanding the basic biology of cancer since middle of 20th century (LANGDON, 2003).

In several tumors, but not in canine MCTs, the properties of cancer cell to cell or cell to extracellular matrix (ECM) interactions have been modeled *in vitro* in the pursuit of a more reliable mimic of the *in vivo* tumor microenvironment (BAUER et al., 2009; KIM, HAYWARD, 2012; PATHAK, KUMAR, 2012). Cell to cell interactions that occur primarily through direct contact or exchange of soluble factors play an important role in regulating the fate and function of individual cell types in many organ systems (KAJI et al., 2011). The lack these interactions is one potential reason for the loss of functional cell capabilities outside the body (BHATIA et al., 1999).

Specifically, in mast cell cultures, we must consider that the majority of the mast cell lines were established with previous subcutaneous passage in nude mice and have numerous differences compared with endogenous mast cells (DREXLER, MACLEOD, 2003). Different approaches to the canine MCT culture should include the identification of significant interactions between mast cells and different cell types, as well as the characterization of the molecular events mediating these interactions. *In vitro* assays

involving different cell types or more complex cell culture conditions could possibly generate results which may simulate more closely the *in vivo* systems.

In the present study, we examined the short-term effects of stromal fibroblasts on neoplastic mast cell *in vitro*. In order to gain a clearer understanding of the roles of fibroblasts and cancer-associated fibroblasts (CAFs) in the mast cell tumor microenvironment, we sought to investigate the type of interaction between cancer cells and adherent cells in various culture conditions. Our objective was to study and compare the effect of direct contact between mast cells and fibroblasts and the effect of soluble factors and fibroblasts mediators on mast cell viability *in vitro*. We also investigated the neoplastic mast cell behavior in single or mono-culture with different culture medium.

4.2 LITERATURE REVIEW

Tumor microenvironment, a vastly complicated network composed of various cell populations, soluble factors, signaling molecules and extracellular matrix components, orchestrates the behavior of tumor progression (CATALANO et al., 2013). Several studies highlighted the importance of the stroma in tumor development and progression (KALLURI, ZEISBERG, 2006; ORIMO, WEINBERG, 2006). Previous researches have already demonstrated that cultures from canine MCTs contained other cells than only mast cells (WILLIAMS, LARSON, PHILLIPS, 1959; PINELLO et al., 2009). The first descriptions of canine MCTs cultures with a population of cells with fibroblastic pattern and no properties characteristic of normal or neoplastic mast cells were described 60 years ago (WILLIAMS, LARSON, PHILLIPS, 1959).

Interactions between cancer cells and other constituents of the tumoral stroma have been recognized as determinant to tumor progression (PIETRAS, ÖSTMAN, 2010), in particular intratumoral fibroblasts known as CAFs (ÖSTMAN, AUGSTEN, 2009). Canine MCTs were also shown to have a subpopulation of cells with CAF-phenotype immersed in their stroma (GIULIANO et al., 2017; PULZ et al., 2019) but, to date, canine neoplastic mast cell interactions with the extracellular microenvironment has not been widely investigated.

There are several well-established indicators of fibroblast influence in cancer behavior, but none of them are exclusive to canine tumors. Numerous human studies demonstrated *in vitro* interaction between cancer cells and stromal fibroblasts using the co-culture technique (ITO et al,. 1995; SAMOSZUK, TAN, CHORN, 2005; HWANG et

al;. 2008). Co-culture is a method in which two or more cell-types are grown in one culture dish or well (MIKI et al., 2012). To explore the cancer-mediated regulation by fibroblasts, the co-culture experiments were done in indirect or direct manner. In the former, cultured cancer cells and fibroblasts are separated by a transwell chamber with micropores that allows cell to cell communication through soluble factors released by cancer cells. Several experiments confirmed significant induction of malignant progression in cancer cells co-cultured with fibroblasts in cell-cell contact compared to cultured cells in serum-supplemented medium without fibroblasts in human breast cancer cell lines (ITO et al,. 1995; SAMOSZUK, TAN, CHORN, 2005), laryngeal cancer cells (SUZUKI et al., 2004), oral squamous carcinoma (WEI et al, 2019) and human pancreatic cancer (HWANG et al., 2008; QIAN et al.,2003).

Most of the prior studies involved investigation with normal human and rodent mast cells and focused on the effect of specific mast cell secretory products on fibroblasts. These reports indicated that mast cells release potent fibrogenic substances (WALKER, HARLEY, LEROY, 1987; GRUBER, 1995; GRUBER et al., 1997). Moreover, the *in vitro* phagocytosis of biologically active discharged mast cell granules by connective tissue fibroblasts can be a way of mast cells to regulate connective tissue responses (RAO et al., 1983). Interestingly, the co-culture of mast cells with fibroblast cell lines derived from mice was accomplished to a phenotypic change in mast cells from safranin-negative to safranin-positive cells associated with heparin-producing (RENNICK et al., 1995).

Considering the effects of co-culture with fibroblasts on mast cell survival time, earlier morphologic studies have demonstrated the successful *ex vivo* maintenance of human connective tissue mast cells with skin-derived fibroblasts up to 13 days (LEVI-SCHAFFER et al., 1987). Fibroblasts can also stimulate some degree of differentiation in bone marrow mast cells (BMMC) in co-culture conditions (RAIZMAN et al., 1990) and it was reported that mast cell maturation is modulated by fibroblasts through interleukin signaling pathway (NABESHIMA et al., 2005). Additionally, mast cells in co-culture with fibroblasts released significantly more granules and increased the production of serotonin when compared to mast cell cultured alone (MARQUIS et al., 2008).

Mast cells were shown to readily attach and form intimate heterotypic cell to cell contact with fibroblast monolayers (TRAUTMANN et al., 1997). Such cell to cell interaction is important in many cellular processes including fibroblast proliferation (TRAUTMANN et al., 1998, ABE et al., 1998), collagen type I synthesis (ABE et al.,

1998; CAIRNS, WALLS, 1997), collagen gel contraction (SKOLD et al., 2001), fibroblast growth factor production (ARTUC, STECKELINGS, HENZ, 2002), fibroblast enhancement of hypoxia inducible factor-1 (HIF-1α) and vascular endothelial growth factor (VEGF) expression (ZHANG et al., 2006). Furthermore, mast cells induce Matrix Metalloproteinases (MMPs) release from fibroblasts when in cell to cell contact (ABEL, VLIAGOFTIS, 2008; MARGULIS et al., 2009).

It is rational to propose that neoplastic mast cell and stromal fibroblasts interactions could be important in the biological behavior of this still poorly understood in canine neoplasm. Since mast cells can affect growth of the feeder fibroblasts and vice versa (DAYTON et al., 1989).

4.3 MATERIALS AND METHODS

4.3.1 Tumor samples

Mast cell tumor samples were obtained from dogs that underwent surgery at the Veterinary Hospital of the School of Animal Science and Food Engineering of University of Sao Paulo, Veterinary Hospital Dr. Vicente Borelli, from the Octávio Bastos Foundation University (UNIFEOB) and private veterinary clinics, which agreed to participate in the present study. All surgical procedures were performed as part of the treatment, aiming the cure. Inclusion criteria for enrolment were histopathological diagnosis of cutaneous MCT, no previous antineoplastic treatment (radio or chemotherapy) and availability of complete medical records.

Part of surgically resected tumor tissues were placed in 10% neutral buffered formalin and all excisional sample were processed routinely and embedded in paraffin. Four-µm sections were stained with haematoxylin and eosin (HE) and MCTs graded following the criteria described by Patnaik et al. (1986) and Kiupel et al. (2011). This study was approved by the local Ethic Committee on Animal Use, University of Sao Paulo, protocol number CEUA/5637040718. Informed, written consent was obtained from the owner of each dog whose MCT biopsy was included in this study. Patient treatment was unaffected by the study.

4.3.2 Dissociation and Cell culture

Canine MCT samples were obtained immediately after excisional biopsy under sterile conditions and placed into flasks with Dulbecco's Modified Eagle Medium (DMEM-F12, Gibco®, Invitrogen) containing the antibiotics penicillin G (200 U/mL, Sigma-Aldrich) and streptomycin (100 U/mL;Sigma-Aldrich) and 15% fetal bovine serum (FBS). After subcutaneous fat tissue was removed, the tumors were minced finely into approximately 0.5–1.0 mm^3 fragments and incubated in DMEM-F12 containing an enzyme mixture: 200 U/mL collagenase type I and 100U/mL hyaluronidase supplemented with 15% FBS and 2% antibiotics penicillin/streptomycin. After 180 min in water bath at 37ºC, the disaggregated tumor was filtered through a 100-µm filter followed by filtration through a 40-µm mesh (Cell Strainer, BD Biosciences). Cells dispersed by this procedure were centrifuged at 1500 rpm for 5 min at 25°C and the sediment was re-suspended in complete DMEM-F12 (CDMEM-F12) i.e., supplemented with 15%SFB and 1% antibiotics streptomycin/ penicillin.

Mast cells were identified by metachromatic staining with toluidine blue dye and with Romanowsky stain (Diff-Quik solution, Dade Behring Inc., Düdingen, Switzerland). Cell number was assessed in a Neubauer hemocytometer and cell viability was checked with trypan blue dye.

The cells obtained from the MCT was maintained in culture at 37 C in a 5% CO_2 atmosphere in two 75mm^2 tissue culture flasks/sample in complete medium DMEM-F12**.** The medium was renewed every 5-7 days, by removing nonadherent cells and harvesting adherent cells with trypsin-EDTA. All the culture medium removed was centrifuged at 1500 rpm for 5 min and the supernatant was filtered through 100 µm cell strainers named conditioned medium. Conditioned medium was prepared from primary MCT cultures in early passages (P0 and P1).

4.3.3 Co-culture of neoplastic mast cells and stromal fibroblasts

Besides the complete DMEM-F12 medium (CDMEM-F12), in the co-culture assays we also used a medium composed by one part of complete DMEM-F12 10x concentrated and nine parts of conditioned medium designated as complete conditioned medium (CCM).

Tumoral cells cultured in P1 were used to perform the co-culture. Masts cells were obtained from the supernatant of primary cultures. To confirm the isolated supernatant cells were mast cells, a smear was prepared and stained with Toluidine Blue. In the second step, the fibroblasts that were adhered to the bottom were detached with enzymatic dissociation for 4–6 minutes at 37°C in Trypsin (TrypLE™ Express 1X, with phenol red, Thermo Fisher Scientific).

For each lesion, we obtained two bottles of primary culture at P0: one provided the neoplastic mast cells (supernatant) and the tumor stromal fibroblasts (adhered); the other was maintained for supply the "conditioned medium".

All assays were performed in duplicate, using a 12-well plate/tumor. Some wells received cell culture inserts with translucent polyester membrane (Thincert™, Greiner Bio-One, Kremsmünster, Austria). Pore sizes and density of the membrane were 0.4 µm and 2×10^6 pores/cm^2, respectively. In each well, 1 x $l0^5$ neoplastic mast cells were seeded. Stromal fibroblasts were seeded at an initial density of 1 x $l0^4$ cells/mL in a total medium volume of 1mL/well.

The experiments were conducted under the following conditions: (1) Cell to cell contact, with mast cells seeded in direct contact with fibroblasts in a complete DMEM-F12 medium (CDEMM-F12) (Fig. 1.A); (2) Transwell co-culture system using cell culture inserts (ThinCert™, Greiner Bio-One), in which two cell populations were placed in different compartments, i.e., neoplastic mast cells in the upper compartment (insert) and fibroblasts in the lower compartment (adhered to plate surface), in CDMEM-F12 medium (Fig. 1.B); (3) Mast cells in mono culture, with neoplastic mast cells cultured alone in suspension receiving CDMEM-F12 medium (Fig. 1.C) or CCM (Fig. 1.D); and (4) Fibroblasts in mono culture, seeded on the bottom of the well and maintained with CDMEM-F12 medium (Fig. 1.E) or with CCM (Fig. 1.F). Co-cultures were maintained for 8 days at 37 ºC and 5% CO_2, with daily observation using an inverted microscope (ZEISS Axio Vert.A, Germany). Mast cell viability was determined by the Trypan blue exclusion method every 48 hours with the removal of 10µL supernatant of each insert/well with previous agitation. Cell counts and viability were examined at days 2, 4, 6 and 8. Adhered cells were not quantitatively evaluated (wells: C1, C2, C3 and C4). The experiment was maintained until death of all mast cells from some of the culture conditions.

Fig 1. Co-culture schematic model for the evaluation of neoplastic mast cells and stromal fibroblasts interactions. (A) Cell to cell co-culture condition, that allows the chemical and physical interaction between neoplastic mast cells and fibroblasts. (B) Transwell co-culture system, with neoplastic mast cells and stromal fibroblasts in a condition that allows only chemical communication. Mast cells were added into the insert and fibroblasts into the well for adherence to the surface. (C) Mast cells in mono culture with complete DMEM-F12 medium and (D) with complete conditioned medium. (E) Fibroblasts in mono culture with complete DMEM-F12 medium and (F) with complete conditioned medium.

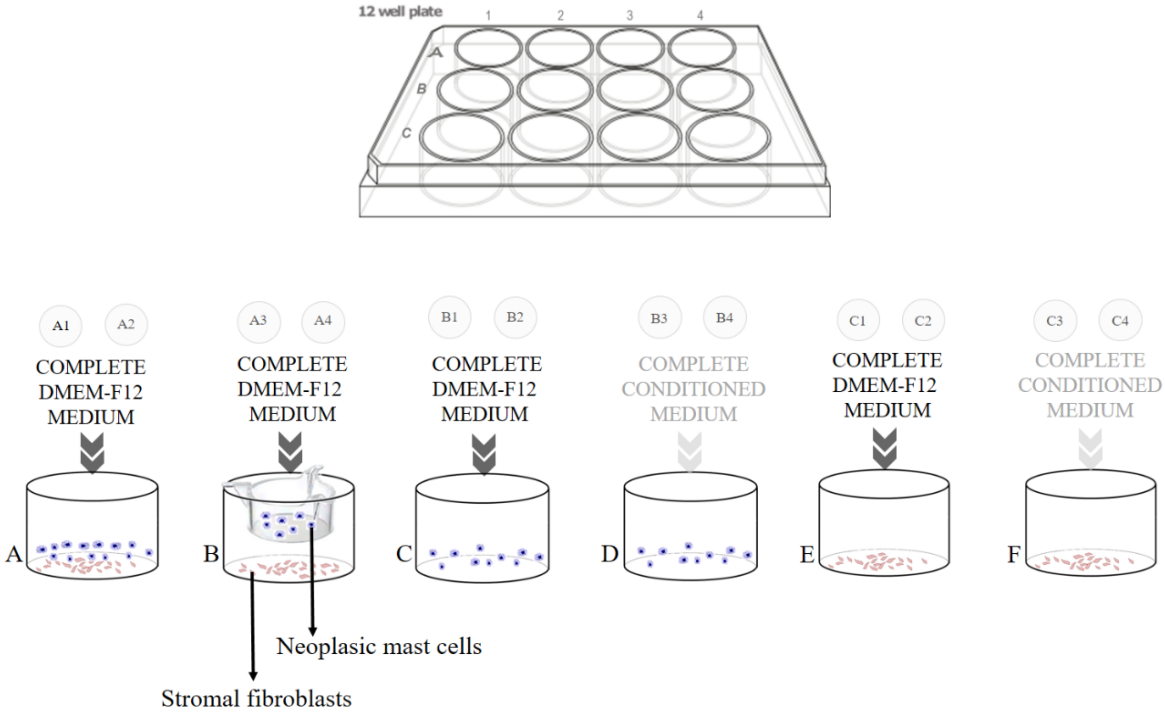

4.3.4 Statistical Analyses

Statistical analyses of different cultures conditions were performed using GraphPad Prism (GraphPad Software, California, USA). Comparisons were made using 2-Way ANOVA and significance level was defined as 0.05.

4.4 RESULTS

Four MCTs from 4 dogs were submitted to the co-culture assay (Table 1). The average age of canines included in the present study were 7.8 years and three were female (75%). MCTs were classified by two different grading systems established according to descriptive histological criteria, which is the most important prognostic factor for the disease (BLACKWOOD et al., 2012). Two of the MCTs were classified as

'high-grade of malignancy' and the other two (50%) classified as 'low-grade'. The characteristics of the dogs that bore the MCTs are detailed in Table 1.

Table 1. Dogs bearing cutaneous mast cell tumors included in co-culture analysis

N	ID	BREED	AGE (years)	GENDER	TUMOR LOCATION	PATNAIK et al. GRADING SYSTEM	TWO-TIER GRADING SYSTEM
1	550-17	Boxer	10	female	abdomen	III	High grade
2	401-18	Brazilian Terrier	9	male	limb	III	High grade
3	1171-18	Mixed breed	9	female	trunk	II	Low grade
4	1249-18	Australian Cattle Dog	3	female	head	I	Low grade

N= sample number; ID: Identification number in the pathology laboratory.

4.4.1 Primary canine MCT culture

Initially, different cell populations obtained from primary tumors were cultivated in contact. Cultures of dissociated MCTs contained neoplastic mast cells in the supernatant, often observed in clusters with variable quantity of cytoplasmic granules. The cultures also contained fibroblast-like cells as an adherent layer, with characteristic spindle shape and extensive branching processes appearing after 48 hours of *in vitro* incubation. After just 5-7 days in co-culture, the fibroblasts consistently proliferate allowing the co-cultivation assay to be performed.

4.4.2 Neoplastic mast cell and stromal fibroblasts co-cultures

Considering the four different culture conditions of neoplastic mast cells tested, the one in which we obtained the higher mast cell viability (average number of mast cells per culture condition) was the cell to cell contact. When co-cultured in direct contact with a monolayer of tumor-stromal fibroblasts, a significant higher number of neoplastic mast cells remained alive compared with all other conditions, i.e., transwell culture ($P<0.05$) and mast cells in mono cultures with CDMEM-F12 ($P<0.05$) or CCM ($P<0.05$) (Fig 2). In the transwell system, the total number of viable mast cells was significantly superior to mast cells in mono culture with CDMEM-F12 for all evaluated periods and samples.

This condition in which the two cell populations are co-cultivated in different compartments (insert and well) and stay physically separated, but may communicate via paracrine signaling through the pores of the membrane was the second best condition for

mast cell survival. However in the first days of cultivation, the transwell condition, with the tumor cells and fibroblasts in separate chambers of transwells yielded numbers of mast cells statistically identical to culture tumor cells alone with ccm in most samples (fig.2 A, C and D). Mast cells in mono culture with CDMEM-F12, survived the shortest period of time. A statistically significant difference in number of live mast cells between CDMEM-F12 medium and CCM was observed on most days analyzed (Figure 2).

The fibroblasts obtained from tumor stroma in this model system uniformly adhered to the well with characteristic morphology (Figure 3). There was no evidence of difference between the well that received CDMEM-F12 and CCM during the course of the experiment.

To determine if neoplastic mast cells *in vitro* behavior is influenced by histopathological grade we compared low grade and high grade of malignancy tumors in all 4-culture conditions, but no significant differences in mast cell viability rates were found between the two groups in cell-cell contact condition ($P>0.05$). However, in the Transwell system assay and in both mast cell mono cultures, the mast cell viability was significantly higher in high-grade than in low-grade derived cultures. Additional details are included in S1 Graphic (Appendix).

Figure. 2. Results of the co-culture assay. Each bar represents the mean and standard deviation of duplicate measurements. Canine mast cells cultured in cell to cell contact with an adherent layer of stromal fibroblasts showed the highest average number of viable cells on each day (a = P<0.05 compared with cell-cell contact condition; b = P<0.05 compared with Transwell co-culture system; c = P<0.05 compared with mast cell in mono culture with CDMEM-F12)

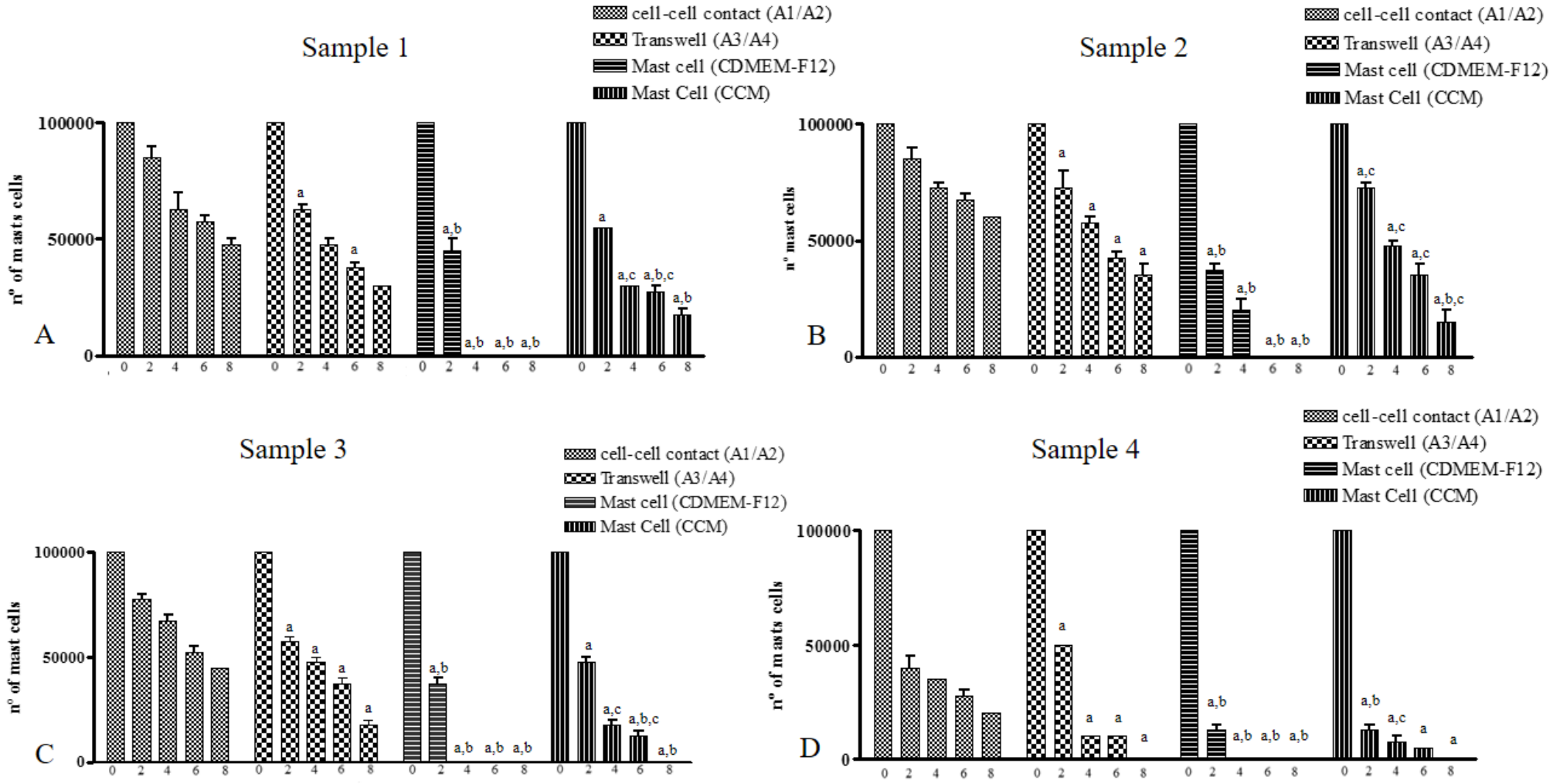

Fig 3. Neoplastic mast cells in different culture conditions after incubation for 48 h (day 2). MCT culture sample 4 (H1249-18). (A) and (B) co-culture in cell to cell contact, with round-shaped neoplastic mast cells grown on a monolayer of spindle-shaped fibroblasts; (C) and (D) Mast cells in the Transwell insert, separated from fibroblasts by a translucent membrane; (E) and (F) Mast cells in mono culture with complete DMEM-F12 medium (CDMEM-F12); (G) and (H) Mast cell in mono culture with complete conditioned medium (CCM); (F) and (H) Viable (arrows) and non-viable mast cells (arrowheads). Left: low magnification. Scale bars =100µm; Right: high magnification. Scale bars = 10µm

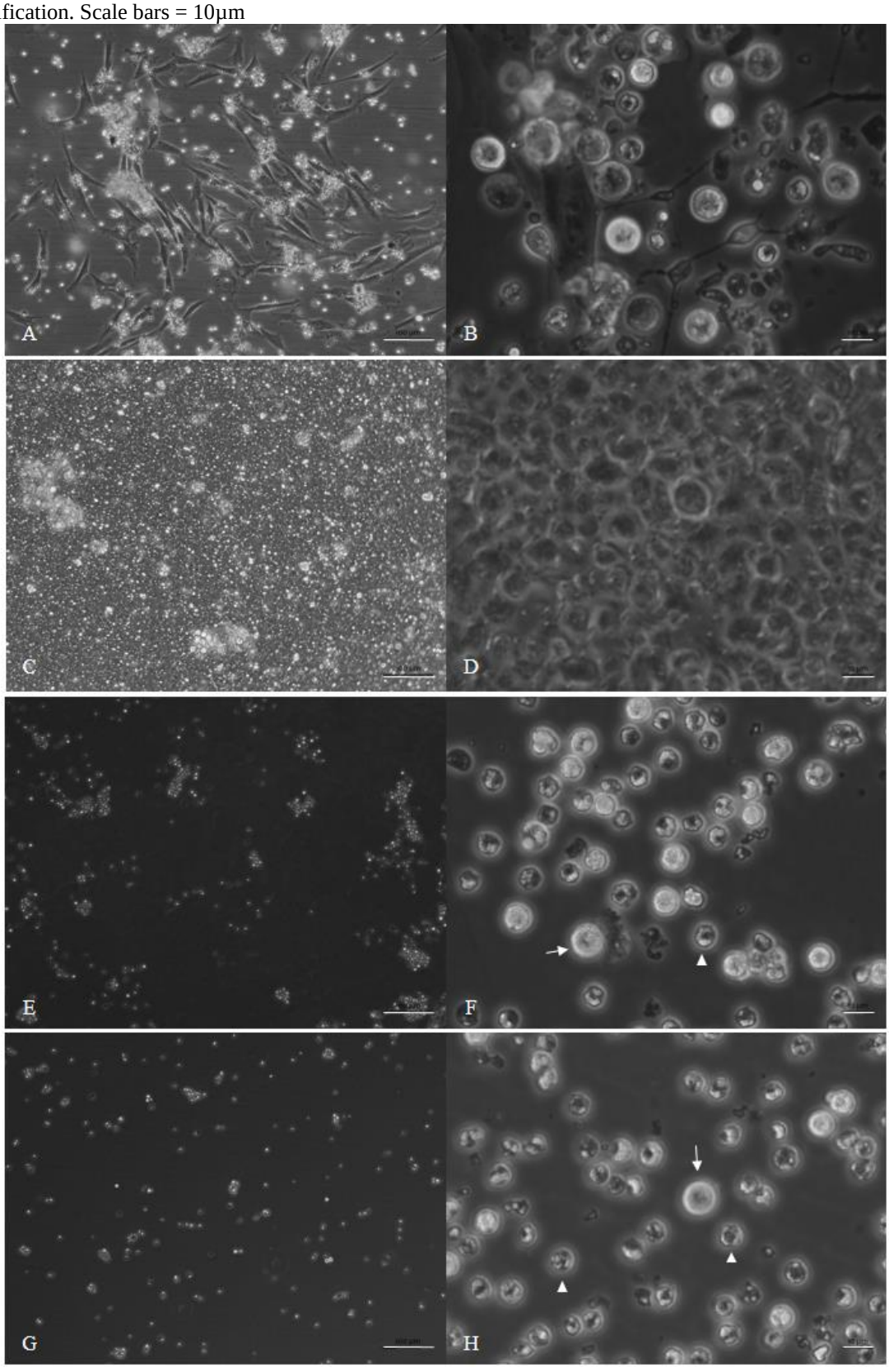

4.5 DISCUSSION

In order to verify possible biological influences in the behavior of canine cutaneous neoplastic mast cells, we tested different culture conditions. The best culture condition in which canine neoplastic mast cells remained viable in highest proportion during the experiment was obtained by maintaining canine neoplastic mast cells in direct contact with fibroblasts. In all samples, this condition increased mast cell viability rate, even when compared to the Transwell system, where the inserts permitted the diffusion any soluble growth factors but prevented direct contact between the cells.

Similarly, Montier et al. (2012) found that human intestinal mast cells survived up to 3 weeks in co-culture with fibroblasts, but when cultured with a conditioned medium from fibroblasts this period was reduced to 2 weeks and, in mono cell cultures, to only one week.

We believe that a mechanism of interaction across the cytoplasmic membrane should be considered, since we have been able to show some effect of direct contact of mast cells and fibroblasts a in tumor cell survival. In co-culture, mast cells form robust adhesions with fibroblasts (TERMEI et al., 2013) that are not mediated by known integrin or cadherin receptors (TRAUTMANN et al., 1997). Notably, mast cells normally grow in suspension and do not adhere strongly to plastic culture surfaces (BAGGIOLINI, WALZ, KUNKEL, 1989). Therefore, we considered that mast cell attachment to fibroblasts with intercellular signals may be important for *in vitro* mast cell short-term maintenance. It is probable that this cellular communication occurs through heterogeneous gap junction channels between neoplastic mast cells and fibroblasts (SALOMON, SAURAT, MEDA, 1988, AU et al., 2007; MOYER, SAGGERS, EHRLICH, 2004; FOLEY, EHRLICH 2013) promoting the enhanced interleukin release (TERMEI et al., 2013).

Many studies indicate that interleukin 8 (IL-8) and interleukin-6 (IL-6) have significant role in mutually paracrine signaling between fibroblasts and other cell types (EL GHALBZOURI, PONEC, 2004; SPIEKSTRA et al., 2007; WERNER, KRIEG, SMOLA, 2007). Previous reports suggested that the enhanced IL-8 and IL6 release were dependent on intercellular contact between intact mast cells and fibroblasts (TERMEI et al., 2013; WIGMORE et al., 1998; SCHVARTZ, SEGER, SHALTIEL, 1999).

IL-8, also known as CXCL8, was originally discovered as a leukocyte chemoattractant (MATSUSHIMA, BALDWIN, MUKAIDA, 1992) and subsequently found to play multiple roles in cancer development (THIERY et al., 2009). Fibroblasts and malignant tumor cells secrete IL-8 as a result of various environmental stress including hypoxia and chemotherapy

agents (XIE, 2001). In many human cancers, IL-8 induces angiogenesis (VÉGRAN et al., 2011) and promotes tumor progression (ROFSTAD, HALSOR, 2000; MILLAR et al., 2008; SHAHZAD et al., 2010). *In vitro* experiments demonstrated that physical separation of mast cells from fibroblasts with membranes that allow free passage of molecules between cells but prevent direct intercellular contact interrupted the fibroblasts release of IL-8 into the medium, evidencing the importance of physical contact between the cells (TERMEI et al., 2013). Gap junctions provide a conduit for intercellular calcium signaling between cells [68] and the IL-8 secretion from fibroblasts may be mediated by calcium signaling (CHARLES et al 1992, TERMEI et al., 2013).

Fibroblasts are capable of producing IL-6 when stimulated directly by mast cell via cell to cell interaction in co-culture (TRAUTMANN et al., 1998; GYOTOKU et al., 2001; FITZGERALD et al., 2004), and less efficiently by mast cell mediators such as TNF-α, IL-1, tryptase or histamine (MONTIER et al., 2012), highlighting again that the physical interaction between these cells is somehow important.

IL-6 is a pleiotropic inflammatory mediator (SCHALL et al., 1994) and is involved in several cancer-associated processes through the downstream activation of multiple signaling pathways (HEINRICH et al., 1998; SUN et al., 2014). IL-6 derived from fibroblasts suppressed apoptosis in human intestinal (MONTIER et al., 2012) and hepatic mast cells (KAMBE et al., 2001) cultured in cell to cell condition. In a model in which bone marrow derived mast cells were cultured on a fibroblast monolayer, IL-6 family cytokines (Il-6, IL-11, OSM and LIF) were demonstrated to induce proliferation of mast cells, but only when the fibroblasts were present. We previously have shown that canine MCTs present fibroblasts that were identified as CAFs by immunohistochemistry, both in tumor tissue and *in vitro* (PULZ, et al., 2019). Cell culture experiments reported that CAFs express IL-6 up to 100 fold higher than normal fibroblasts (HUGO et al., 2012).

We also found that mono cultures of neoplastic mast cells are not viable for more than 4 days in the absence of fibroblasts or their soluble factors. *In vitro* studies with human connective tissue mast cells in simple enriched medium showed that cell death was progressively increased and less of 15% of the seeded cells were still viable by day 4 of culture (DVORAK et al., 1986). Similar results were obtained *in vitro* for mast cells cultured without a stromal adherent cell layer (PINELLO et al 2009; MARQUIS et al., 2000; HORTON, O'BRIEN, 1983; YAMADA et al., 2003). Interestingly, in the present study, we did not detect differences between the two culture conditions with masts cells receiving conditioned medium, i.e., Transwell assay and mast cells in mono culture with conditioned medium obtained from

primary MCTs cultures supernatants (CCM). However, both conditions supported a superior number of viable mast cells compared to CDMEM-F12 medium. We could attribute this finding to paracrine signaling between fibroblasts and mast cells. Experiments with human and murine mast cells co-cultured with fibroblasts have implicated fibroblasts as an important source of growth factors *in vitro* by producing stem cell factor (SCF), a well-characterized mast cell growth factor (NABESHIMA et al., 2005; MONTIER et al., 2012; HUGO et al., 2012; LEVI-SCHAFFER et al. 1991, LEVI-SCHAFFER, RUBINCHIK, 1995; BISCHOFF, 2007).

Although these studies were not performed in the context of cancer, they indicate a mutual activation pathway between mast cells and fibroblasts involving bidirectional communication, which may also occur in the tumor microenvironmental setting. For example, carcinoma cell lines were stimulated and activated ascribe to direct interaction with fibroblasts, rather than via soluble factors in co-culture conditions (SUZUKI et al., 2004).

The main limitations of the present study were the lack of knowledge about the exact composition of conditioned medium and effective molecules secreted by the stromal fibroblasts in co-culture circumstances. In particular, it would have been better not to discuss the differences in high- versus low-grade tumors due to the small sample size.

4.6 CONCLUSION

This is the first study to investigate the type of interaction between mast cells and fibroblasts obtained from canine cutaneous MCTs. Our data indicate an intimate cross talk between neoplastic mast cells and stromal fibroblasts resulting in mast cell survival maintenance. Thus, neoplastic mast cells in monocultures may not serve as an excellent model for canine MCT *in vitro* studies, unless the substances for an adequate conditioned medium have been characterized.

These interactions occur through membrane channels and/or soluble molecules. Overall, the short-term direct modulatory effects of fibroblasts on neoplastic mast cells may be also important for the development of *in vivo* canine cutaneous MCTs. A more detailed understanding of the role of stromal fibroblasts, IL8 and IL6 in the development and progression of canine MCTs could lead to important improvements in the treatment of MCT. Some of these molecules that probably mediate neoplastic mast cells survival may be potential targets for future anti-MCT therapies.

4.7 REFERENCES

ABE, M.; KUROSAWA, M.; ISHIKAWA, O.; MIYACHI, Y.; KIDO, H. Mast cell tryptase stimulates both human dermal fibroblast proliferation and type I collagen production. **Clinical and experimental allergy: journal of the British Society for Allergy and Clinical Immunology**, v. 28, n. 12, p. 1509-1517, 1998.

ABEL, M.; VLIAGOFTIS, H. Mast cell-fibroblast interactions induce matrix metalloproteinase-9 release from fibroblasts: role for IgE-mediated mast cell activation. **The Journal of Immunology**, v. 180, n. 5, p. 3543-3550, 2008.

ARTUC, M.; STECKELINGS, U. M.; HENZ, B. M. Mast cell–fibroblast interactions: human mast cells as source and inducers of fibroblast and epithelial growth factors. **Journal of Investigative Dermatology**, v. 118, n. 3, p. 391-395, 2002.

AU, S. R.; AU, K.; SAGGERS, G. C.; KARNE, N.; EHRLICH, H. P. Rat mast cells communicate with fibroblasts via gap junction intercellular communications. **Journal of Cellular Biochemistry**, v. 100, n. 5, p. 1170-1177, 2007.

BAGGIOLINI, M.; WALZ, A.; KUNKEL, S. L. Neutrophil-activating peptide-1/interleukin 8, a novel cytokine that activates neutrophils. **The Journal of Clinical Investigation**, v. 84, n. 4, p. 1045-1049, 1989.

BAUER, A. L.; JACKSON, T. L.; JIANG, Y. Topography of extracellular matrix mediates vascular morphogenesis and migration speeds in angiogenesis. **PLoS Computational Biology**, v. 5, n. 7, p. e1000445, 2009.

BHATIA, S. N.; BALIS, U. J.; YARMUSH, M. L.; TONER, M. Effect of cell–cell interactions in preservation of cellular phenotype: cocultivation of hepatocytes and nonparenchymal cells. **The FASEB Journal**, v. 13, n. 14, p. 1883-1900, 1999.

BISCHOFF, S. C. Role of mast cells in allergic and non-allergic immune responses: comparison of human and murine data. **Nature Reviews Immunology**, v. 7, n. 2, p. 93, 2007.

BLACKWOOD, L.; MURPHY, S.; BURACCO, P.; DE VOS, J. P.; DE FORNEL-THIBAUD, P.; HIRSCHBERGER, J. et al. European consensus document on mast cell tumours in dogs and cats. **Veterinary and comparative oncology**, v. 10, n. 3, p. e1-e29, 2012.

CAIRNS, J. A.; WALLS, A. F. Mast cell tryptase stimulates the synthesis of type I collagen in human lung fibroblasts. **The Journal of Clinical Investigation**, v. 99, n. 6, p. 1313-1321, 1997.

CATALANO, V.; TURDO, A.; DI FRANCO, S.; DIELI, F.; TODARO, M.; STASSI, G. Tumor and its microenvironment: a synergistic interplay. **Seminars in Cancer Biology**, v. 23, p. 522-532, 2013.

CHARLES, A. C.; NAUS, C. C.; ZHU, D.; KIDDER, G. M.; DIRKSEN, E. R.; SANDERSON, M. J. Intercellular calcium signaling via gap junctions in glioma cells. **The Journal of Cell Biology**, v. 118, n. 1, p. 195-201, 1992.

DAYTON, E. T.; CAULFIELD, J. P.; HEIN, A.; AUSTEN, K. F.; STEVENS, R. L. Regulation of the growth rate of mouse fibroblasts by IL-3-activated mouse bone marrow-derived mast cells. **The Journal of Immunology**, v. 142, n. 12, p. 4307-4313, 1989.

DOBSON, J. M.; SAMUEL, S.; MILSTEIN, H.; ROGERS, K.; WOOD, J. L. N. Canine neoplasia in the UK: estimates of incidence rates from a population of insured dogs. **Journal of Small Animal Practice**, v. 43, n. 6, p. 240-246, 2002.

DREXLER, H. G.; MACLEOD, R. A. F. Editorial: Malignant hemoatopoietic cell lines: in vitro models for the study of mast cell leukemia. **Leukemia Research**, v. 27, p. 671–676, 2003.

DVORAK, A. M.; SCHLEIMER, R. P.; SCHULMAN, E. S.; LICHTENSTEIN, L. M. Human mast cells use conservation and condensation mechanisms during recovery from degranulation. In vitro studies with mast cells purified from human lungs. **Laboratory Investigation; A Journal of Technical Methods and Pathology**, v. 54, n. 6, p. 663-678, 1986.

EL GHALBZOURI, A.; PONEC, M. Diffusible factors released by fibroblasts support epidermal morphogenesis and deposition of basement membrane components. **Wound Repair and Regeneration**, v. 12, n. 3, p. 359-367, 2004.

FITZGERALD, S. M.; LEE, S. A.; HALL, H. K.; CHI, D. S.; KRISHNASWAMY, G. Human lung fibroblasts express interleukin-6 in response to signaling after mast cell contact. **American Journal of Respiratory Cell and Molecular Biology**, v. 30, n. 4, p. 585-593, 2004.

FOLEY, T. T.; EHRLICH, H. P. Through gap junction communications, co-cultured mast cells and fibroblasts generate fibroblast activities allied with hypertrophic scarring. **Plastic and reconstructive surgery**, v. 131, n. 5, p. 1036-1044, 2013.

GIULIANO, A.; DOS SANTOS HORTA, R.; CONSTANTINO-CASAS, F.; HOATHER, T.; DOBSON, J. Expression of Fibroblast Activating Protein and Correlation with Histological Grade, Mitotic Index and Ki67 Expression in Canine Mast Cell Tumours. **Journal of Comparative Pathology**, v. 156, n. 1, p. 14-20, 2017.

GRUBER, B. L. Mast cells: accessory cells which potentiate fibrosis. **International Reviews of Immunology**, v. 12, n. 2-4, p. 259-279, 1995.

GRUBER, B. L.; KEW, R. R.; JELASKA, A.; MARCHESE, M. J.; GARLICK, J.; REN S. et al. Human mast cells activate fibroblasts: tryptase is a fibrogenic factor stimulating collagen messenger ribonucleic acid synthesis and fibroblast chemotaxis. **The Journal of Immunology**, v. 158, n. 5, p. 2310-2317, 1997.

GRÜNTZIG, K.; GRAF, R.; BOO, G.; GUSCETTI, F.; HÄSSIG, M.; AXHAUSEN, K. W.; FABRIKANT, S.; WELLE M.; MEIER, D.; FOLKERS, G.; POSPISCHIL, A. Swiss Canine Cancer Registry 1955-2008: occurrence of the most common tumour diagnoses and influence of age, breed, body size, sex and neutering status on tumour development. **Journal of Comparative Pathology**, v. 155, n. 2-3, p. 156-170, 2016.

GYOTOKU, E.; MORITA, E.; KAMEYOSHI, Y.; HIRAGUN, T.; YAMAMOTO, S.; HIDE, M. The IL-6 family cytokines, interleukin-6, interleukin-11, oncostatin M, and leukemia inhibitory factor, enhance mast cell growth through fibroblast-dependent pathway in mice. **Archives of Dermatological Research**, v. 293, n. 10, p. 508-514, 2001.

HEINRICH, P. C.; BEHRMANN, I.; MULLER-NEWEN, G.; SCHAPER, F.; GRAEVE, L. Interleukin-6-type cytokine signalling through the gp130/Jak/STAT pathway. **Biochemical Journal**, v. 334, n. 2, p. 297-314, 1998.

HOLLE, A. W.; YOUNG, J. L.; SPATZ, J. P. In vitro cancer cell–ECM interactions inform in vivo cancer treatment. **Advanced drug delivery reviews**, v. 97, p. 270-279, 2016.

HORTON, M. A.; O'BRIEN, H. A. Characterization of human mast cells in long-term culture. **Blood**, v. 62, n. 6, p. 1251-1260, 1983.

HUGO, H. J.; LEBRET, S.; TOMASKOVIC-CROOK, E.; AHMED, N.; BLICK, T.; NEWGREEN, D. F. et al. Contribution of fibroblast and mast cell (afferent) and tumor (efferent) IL-6 effects within the tumor microenvironment. **Cancer Microenvironment**, v. 5, n. 1, p. 83-93, 2012.

HWANG, R. F.; MOORE, T.; ARUMUGAM, T.; RAMACHANDRAN, V.; AMOS, K. D.; RIVERA, A.; JI, B.; EVANS, D. B.; LOGSDON, C. D. Cancer-associated stromal fibroblasts promote pancreatic tumor progression. **Cancer research**, v. 68, n. 3, p. 918-926, 2008.

ITO, A.; NAKAJIMA, S.; SASAGURI, Y.; NAGASE, H.; MORI, Y. Co-culture of human breast adenocarcinoma MCF-7 cells and human dermal fibroblasts enhances the production of matrix metalloproteinases 1, 2 and 3 in fibroblasts. **British Journal of Cancer**, v. 71, n. 5, p. 1039, 1995.

KAJI, H.; CAMCI-UNAL, G.; LANGER, R.; KHADEMHOSSEINI, A. Engineering systems for the generation of patterned co-cultures for controlling cell–cell interactions. **Biochimica et Biophysica Acta (BBA)-General Subjects**, v. 1810, n. 3, p. 239-250, 2011.

KALLURI, R.; ZEISBERG, M. Fibroblasts in cancer. **Nature Reviews Cancer**, v. 6, n. 5, p. 392, 2006.

KAMBE, M.; KAMBE, N.; OSKERITZIAN, C. A.; SCHECHTER, N.; SCHWARTZ, L. B. IL-6 attenuates apoptosis, while neither IL-6 nor IL-10 affect the numbers or protease phenotype of fetal liver-derived human mast cells. **Clinical & Experimental Allergy**, v. 31, n. 7, p. 1077-1085, 2001.

KIM, J.; HAYWARD, R. C. Mimicking dynamic in vivo environments with stimuli-responsive materials for cell culture. **Trends in Biotechnology**, v. 30, n. 8, p. 426-439, 2012.

KIUPEL, M.; WEBSTER, J. D.; BAILEY, K. L.; BEST, S.; DELAY, J.; DETRISAC, C. J. et al. Proposal of a 2-tier histologic grading system for canine cutaneous mast cell tumors to more accurately predict biological behavior. **Veterinary Pathology**, v. 48, n. 1, p. 147-155, 2011.

LANGDON, S. P. Introduction to Cancer Cell Culture: basic Principles of Cancer Cell Culture. In: LANGDON, S. P. **Cancer Cell Culture:** Methods and Protocols. Volume 88. Nova York: Human Press Inc, 2003.

LEVI-SCHAFFER, F.; AUSTEN, K. F.; CAULFIELD, J. P.; HEIN, A.; GRAVALLESE, P. M.; STEVENS, R. L. Co-culture of human lung-derived mast cells with mouse 3T3 fibroblasts: morphology and IgE-mediated release of histamine, prostaglandin D2, and leukotrienes. **The Journal of Immunology**, v. 139, n. 2, p. 494-500, 1987.

LEVI-SCHAFFER, F.; RUBINCHIK E. Activated mast cells are fibrogenic for 3T3 fibroblasts. **Journal of Investigative Dermatology**, v. 104, n. 6, p. 999-1003, 1995.

LEVI-SCHAFFER, F.; SEGAL, V.; SHALIT, M. Effects of interleukins on connective tissue type mast cells co-cultured with fibroblasts. **Immunology**, v. 72, n. 2, p. 174, 1991.

MARGULIS, A.; NOCKA, K. H.; BRENNAN, A. M.; DENG, B.; FLEMING, M.; GOLDMAN, S. J.; KASAIAN, M. T. Mast cell-dependent contraction of human airway smooth muscle cell-containing collagen gels: influence of cytokines, matrix metalloproteases, and serine proteases. **The Journal of Immunology**, p. jimmunol. 0803951, 2009.

MARQUIS, B. J.; HAYNES, C. L. The effects of co-culture of fibroblasts on mast cell exocytotic release characteristics as evaluated by carbon-fiber microelectrode amperometry. **Biophysical Chemistry**, v. 137, n. 1, p. 63-69, 2008.

MATSUSHIMA, K.; BALDWIN, E. T.; MUKAIDA, N. Interleukin-8 and MCAF: novel leukocyte recruitment and activating cytokines. In: KISHIMOTO T. **Interleukins: molecular biology and immunology**. Karger Publishers, 1992. p. 236-265.

MIKI, Y.; ONO, K.; HATA, S.; SUZUKI, T.; KUMAMOTO, H.; SASANO, H. The advantages of co-culture over mono cell culture in simulating in vivo environment. **The Journal of Steroid Biochemistry and Molecular Biology**, v. 131, n. 3-5, p. 68-75, 2012.

MILLAR, H. J.; NEMETH, J. A.; MCCABE, F. L.; PIKOUNIS, B.; WICKSTROM, E. Circulating Human Interleukin-8 as an Indicator of Cancer Progression in a Nude Rat Orthotopic Human Non–Small Cell Lung Carcinoma Model. **Cancer Epidemiology and Prevention Biomarkers**, v. 17, n. 8, p. 2180-2187, 2008.

MONTIER, Y.; LORENTZ, A.; KRÄMER, S.; SELLGE, G.; SCHOCK, M.; BAUER, M. et al. Central role of IL-6 and MMP-1 for cross talk between human intestinal mast cells and human intestinal fibroblasts. **Immunobiology**, v. 217, n. 9, p. 912-919, 2012.

MOYER, K. E.; SAGGERS, G. C.; EHRLICH, H. P. Mast cells promote fibroblast populated collagen lattice contraction through gap junction intercellular communication. **Wound Repair and Regeneration**, v. 12, n. 3, p. 269-275, 2004.

NABESHIMA, Y.; HIRAGUN, T.; MORITA, E.; MIHARA, S.; KAMEYOSHI, Y.; HIDE, M. IL-4 modulates the histamine content of mast cells in a mast cell/fibroblast co-culture through a Stat6 signaling pathway in fibroblasts. **FEBS Letters**, v. 579, n. 29, p. 6653-6658, 2005.

ORIMO, A.; WEINBERG, R. A. Stromal fibroblasts in cancer: a novel tumor-promoting cell type. **Cell Cycle**, v. 5, n. 15, p. 1597-1601, 2006.

ÖSTMAN, A.; AUGSTEN, M. Cancer-associated fibroblasts and tumor growth–bystanders turning into key players. **Current Opinion in Genetics & Development**, v. 19, n. 1, p. 67-73, 2009.

PATHAK, A.; KUMAR, S. Independent regulation of tumor cell migration by matrix stiffness and confinement. **Proceedings of the National Academy of Sciences**, v. 109, n. 26, p. 10334-10339, 2012.

PATNAIK, A. K.; EHLER, W. J.; MACEWEN, E. G. Canine cutaneous mast cell tumor: morphologic grading and survival time in 83 dogs. **Veterinary Pathology**, v. 21, n. 5, p. 469-474, 1984.

PIETRAS, K.; ÖSTMAN, A. Hallmarks of cancer: interactions with the tumor stroma. **Experimental Cell Research**, v. 316, n. 8, p. 1324-1331, 2010.

PINELLO, K. C.; NAGAMINE, M.; SILVA, T. C.; MATSUZAKI, P.; CAETANO, H. V.; TORRES L. N.; FUKUMASU, H.; DAGLI, M. L. Z. In vitro chemosensitivity of canine mast cell tumors grades II and III to all-trans-retinoic acid (ATRA). **Veterinary Research Communications**, v. 33, n. 6, p. 581-588, 2009.

PULZ L. H. **Canine cutaneous Mast Cells Tumor: molecular characterization, culture and intercellular interactions between mast cells and stromal fibroblasts.** Data de depósito. Total de páginas/folhas. Tese (Doutorado em Ciências) – Faculdade de Medicina Veterinária e Zootecnia, Universidade de São Paulo, São Paulo-SP, 15 de março de 2019.

QIAN, L. W.; MIZUMOTO, K.; MAEHARA, N.; OHUCHIDA, K.; INADOME, N.; SAIMURA, M. et al. Co-cultivation of pancreatic cancer cells with orthotopic tumor-derived fibroblasts: fibroblasts stimulate tumor cell invasion via HGF secretion whereas cancer cells exert a minor regulative effect on fibroblasts HGF production. **Cancer Letters**, v. 190, n. 1, p. 105-112, 2003.

RAIZMAN, M. B.; AUSTEN, K. F.; KATZ, H. R. Mast cell heterogeneity. Differential synthesis and expression of glycosphingolipids by mouse serosal mast cells as compared to IL-3-dependent bone marrow culture-derived mast cells before or after coculture with 3T3 fibroblasts. **The Journal of Immunology**, v. 145, n. 5, p. 1463-1468, 1990.

RAO, P. S.; FRIEDMAN, M. M.; ATKINS, F. M.; METCALFE, D. D. Phagocytosis of mast cell granules by cultured fibroblasts. **The Journal of Immunology**, v. 130, n. 1, p. 341-349, 1983.

RENNICK, D.; HUNTE, B.; HOLLAND, G.; THOMPSON-SNIPES, L. Cofactors are essential for stem cell factor-dependent growth and maturation of mast cell progenitors: comparative effects of interleukin-3 (IL-3), IL-4, IL-10, and fibroblasts. **Blood**, v. 85, n. 1, p. 57-65, 1995.

ROFSTAD, E. K.; HALSØR, E. F. Vascular endothelial growth factor, interleukin 8, platelet-derived endothelial cell growth factor, and basic fibroblast growth factor promote angiogenesis and metastasis in human melanoma xenografts. **Cancer Research**, v. 60, n. 17, p. 4932-4938, 2000.

SALOMON, D.; SAURAT, J. H.; MEDA, P. Cell-to-cell communication within intact human skin. **The Journal of clinical investigation**, v. 82, n. 1, p. 248-254, 1988.

SAMOSZUK, M.; TAN, J.; CHORN, G. Clonogenic growth of human breast cancer cells co-cultured in direct contact with serum-activated fibroblasts. **Breast Cancer Research**, v. 7, n. 3, p. R274, 2005.

SCHALL, T. J.; BACON, K. B. Chemokines, leukocyte trafficking, and inflammation. **Current Opinion in Immunology**, v. 6, n. 6, p. 865-873, 1994.

SCHVARTZ, I.; SEGER, D.; SHALTIEL, S. Vitronectin. **The International Journal of Biochemistry & Cell Biology**, v. 31, n. 5, p. 539-544, 1999.

SHAHZAD, M. M.; AREVALO, J. M.; ARMAIZ-PENA, G. N.; LU, C.; STONE, R. L.; MORENO-SMITH, M.; NISHIMURA, M.; LEE, J. W.; JENNINGS, N. B.; BOTTSFORD-MILLER, J. et al. Stress effects on FOSB and interleukin-8 (IL8) driven ovarian cancer growth and metastasis. **Journal of Biological Chemistry**, p. jbc-M110. 109579, 2010.

SKÖLD, C. M.; OHKUNI, Y.; LIU, X. D.; NUMEROF, R.; RENNARD, S. I. Co-cultured human mast cells stimulate fibroblast-mediated contraction of collagen gels. **Inflammation**, v. 25, n. 1, p. 47-51, 2001.

SPIEKSTRA, S. W.; BREETVELD, M.; RUSTEMEYER, T.; SCHEPER, R. J.; GIBBS, S. Wound-healing factors secreted by epidermal keratinocytes and dermal fibroblasts in skin substitutes. **Wound Repair and Regeneration**, v. 15, n. 5, p. 708-717, 2007.

SPRAY, D. C.; BENNETT, M. V. L. Physiology and pharmacology of gap junctions. **Annual Review of Physiology**, v. 47, n. 1, p. 281-303, 1985.

SUN, X.; MAO, Y.; WANG, J.; ZU, L.; HAO, M.; CHENG, G. et al. IL-6 secreted by cancer-associated fibroblasts induces tamoxifen resistance in luminal breast cancer. **Oncogene**, 2014.

SUZUKI, S.; SATO, M.; SENOO, H.; ISHIKAWA, K. Direct cell–cell interaction enhances pro-MMP-2 production and activation in co-culture of laryngeal cancer cells and fibroblasts: involvement of EMMPRIN and MT1-MMP. **Experimental Cell Research**, v. 293, n. 2, p. 259-266, 2004.

TERMEI, R.; LASCHINGER, C.; LEE, W.; MCCULLOCH, C. A. Intercellular interactions between mast cells and fibroblasts promote pro-inflammatory signaling. **Experimental cell research**, v. 319, n. 12, p. 1839-1851, 2013.

THIERY, J. P.; ACLOQUE, H.; HUANG, R. Y.; NIETO, M. A. Epithelial-mesenchymal transitions in development and disease. **Cell**, v. 139, n. 5, p. 871-890, 2009.

TRAUTMANN, A.; FEUNERSTEIN, B.; ERNST, N.; BRÖCKER, E.B.; KLEIN, C. E. Heterotypic cell-cell adhesion of human mast cells to fibroblasts. **Archives of dermatological research**, v. 289, n. 4, p. 194-203, 1997.

TRAUTMANN, A.; KROHNE, G.; BRÖCKER, E. B.; KLEIN, C. E. Human mast cells augment fibroblast proliferation by heterotypic cell-cell adhesion and action of IL-4. **The Journal of Immunology**, v. 160, n. 10, p. 5053-5057, 1998.

VÉGRAN, F.; BOIDOT, R.; MICHIELS, C.; SONVEAUX, P.; FERON, O. Lactate influx through the endothelial cell monocarboxylate transporter MCT1 supports an NF-kappaB/IL-8 pathway that drives tumor angiogenesis. **Cancer Research**, p.2828, 2011.

WALKER, M. A.; HARLEY, R. A.; LEROY, E. C. Inhibition of fibrosis in TSK mice by blocking mast cell degranulation. **The Journal of Rheumatology**, v. 14, n. 2, p. 299-301, 1987.

WEI L, Y.; LEE, J. J.; YEH, C. Y.; YANG, C. J.; KOK, S. H.; KO, J. Y. et al. Reciprocal activation of cancer-associated fibroblasts and oral squamous carcinoma cells through CXCL1. **Oral Oncology**, v. 88, p. 115-123, 2019.

WELLE, M. M.; BLEY, C. R.; HOWARD, J.; RÜFENACHT, S. Canine mast cell tumours: a review of the pathogenesis, clinical features, pathology and treatment. **Veterinary Dermatology**, v. 19, n. 6, p. 321-339, 2008.

WERNER, S.; KRIEG, T.; SMOLA, H. Keratinocyte–fibroblast interactions in wound healing. **Journal of Investigative Dermatology**, v. 127, n. 5, p. 998-1008, 2007.

WIGMORE, S. J.; WALSH, T. S.; LEE, A.; ROSS, J. A. Pro-inflammatory cytokine release and mediation of the acute phase protein response in fulminant hepatic failure. **Intensive Care Medicine**, v. 24, n. 3, p. 224-229, 1998.

WILLIAMS, W. J.; LARSON, E.; PHILLIPS, T. L. A neoplastic connective tissue mast cell capable of continuous growth in tissue culture. **The Journal of Cell Biology**, v. 6, n. 3, p. 361-368, 1959.

XIE, K.Interleukin-8 and human cancer biology. **Cytokine & Growth Factor Reviews**, v. 12, n. 4, p. 375-391, 2001.

YAMADA, N.; MATSUSHIMA, H.; TAGAYA, Y.; SHIMADA, S.; KATZ, S. I. Generation of a large number of connective tissue type mast cells by culture of murine fetal skin cells. **Journal of Investigative Dermatology**, v. 121, n. 6, p. 1425-1432, 2003.

ZHANG, Q.; OH, C. K.; MESSADI, D. V.; DUONG, H. S.; KELLY, A. P.; SOO, C. et al. Hypoxia-induced HIF-1 α accumulation is augmented in a co-culture of keloid fibroblasts and human mast cells: involvement of ERK1/2 and PI-3K/Akt. **Experimental Cell Research**, v. 312, n. 2, p. 145-155, 2006.

APPENDIX

S1 Figure. Comparison of viable mast cells values in the studied high and low grade of malignancy MCTs in each culture condition. Graph shows median of live mast cells values in low grade tumors and high-grade tumors on each day evaluated with its respective standard deviation. (A) Cell-cell contact: in vitro viable mast cells values were not significantly different between low grade and high grade tumors (P=0.0555). (B) The transwell condition shows the statistical significance in viable mast cell values of high and low grade MCTs (P=0.0304). (C) Mast cell mono cultures with complete DMEM-F12 medium and (D) Mast cell mono cultures with complete conditioned medium (CCM): the overall live cell count were significantly higher in high grade tumors than those in low-grades tumors (P=P=0.0266 and P=0.0021, respectively).

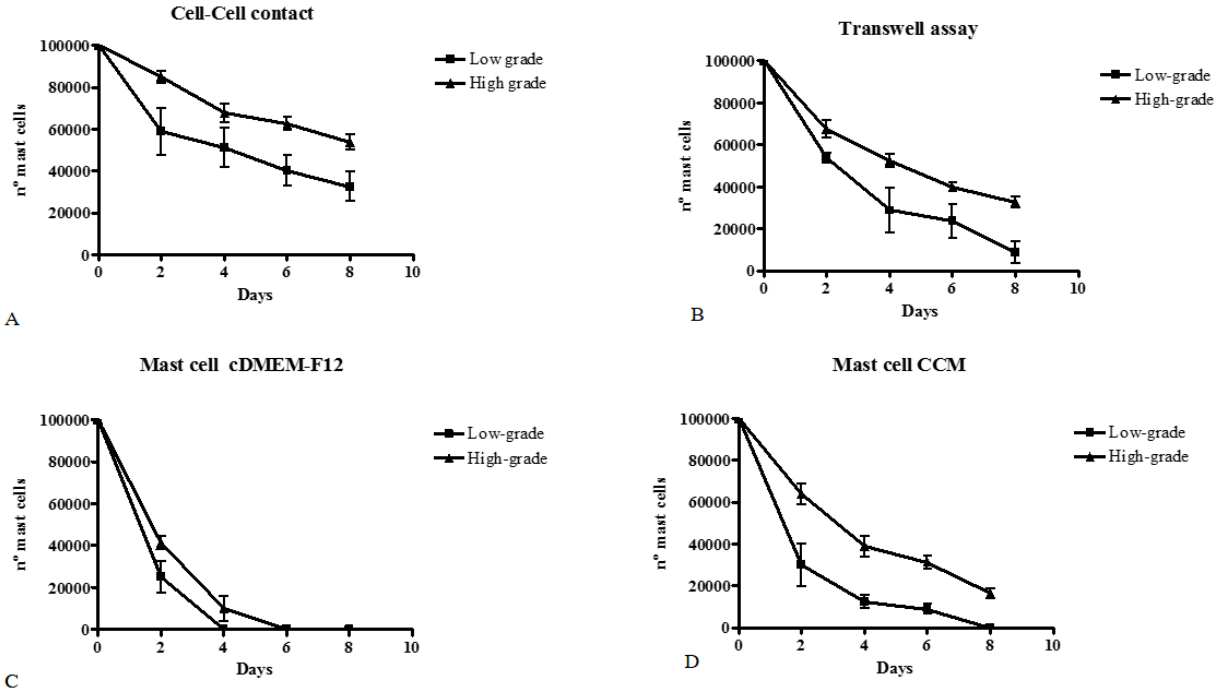

5. GENERAL CONCLUSION

The aim of this study was to investigate mechanisms to understand the canine MCT malignant behavior beyond morphological characteristics. First, we found differentially expressed genes in high risk tumors related to the extracellular matrix. Changes in gene expression that mediate invasion and metastasis may not reflect histopathological alterations that could be evaluated in the microscopic examination. The differences in gene expression displayed by the cutaneous MCTs that had high grade of malignancy, high proliferation and short survival time appear to reflect the requirements of the extracelular stimuli. The avaiable literature particularly documents the connection between stromal cells as CAFs and poor prognoses, and this was also verified in the presente study. In addition, to highlight the importance of this tumoral compartment, we identified selected emerging genes affecting the malignant MCTs phenotype.

Then, we demonstrated the interaction between tumor cells and stromal fibroblasts *in vitro*. It seems clear that stromal fibroblasts and CAFs can influence neoplastic mast cell activity in culture condition. Future studies, are necessary to investigate several stroma-specific factors associated with canine mast cell tumor and elucidate the specific mechanisms of action of these molecules.

Cell migration is facilitated by reduced cell-cell and cell-ECM adhesion and cell softening achieved through cytoskeletal reorganisation. Some of these altered features mediate canine cutaneous MCT invasion and metastasis and may be potential targets for novel therapies directed toward the microenvironment. Furthermore, controlled studies are necessary to assess the real effect of chemotherapy protocols. Thus, *in vitro* experimental investigations will be required to demonstrate the effects of antineoplastic drugs and/or to clarify the role of strmoal cells derived molecules (e.g. on cell adhesion, deformability and motility) on neoplastic canine mast cells. The need for an improved understanding of the progression and treatment responses of MCTs has pushed for increased relevance of canine MCT *in vitro* tumor models.

Finally, we believe that further studies are necessary to identity stromal cell derived factors and their mechanisms of action to provide new tools for the establishment of more accurate prognosis or to predict tumor response to chemotherapy.